Aus dem

Lübecker Institut für Experimentelle Dermatologie

Direktor: Prof. Dr. Ralf Ludwig

# Molecular Pathogenesis in the Initiation and Progression of Colorectal Cancer

Inauguraldissertation

Zum Erwerb des Doktorgrades

der Universität zu Lübeck

-Aus der Sektion Medizin-

vorgelegt von

**Faisal Hassan Alhosani**

Dubai, UAE

Lübeck 2025

1. Berichterstatter*in: Prof. Dr. rer. nat. Hauke Busch

Ko-Betreuer*in: Prof. Dr. med. Cyrus Khandanpour

2. Berichterstatter*in: PD Dr. rer. nat. Yves Laumonnier

Tag der mündlichen Prüfung: 10.07.2025

Zum Druck genehmigt. Lübeck, den 11.07.2025

-Promotionskommission der Sektion Medizin-

# Abstract

## Molecular Pathogenesis in the Initiation and Progression of Colorectal Cancer

Faisal Alhosani

Colorectal cancer (CRC) cases are among the third most common malignancies worldwide and a leading cause of cancer-related mortality. CRC is typically classified into precursor lesions such as adenomas, high-grade dysplasia, or carcinoma in situ, and malignant forms like adenocarcinomas, reflecting the progressive nature of colorectal tumorigenesis.. The incidence and mortality rates are reflected at the national level, with CRC being the deadliest cancer among males in the United Arab Emirates (UAE). The specific etiology of CRC is still largely unclear. However, Researchers generally agree that the primary contributors to colorectal cancer include genetic predisposition, dietary patterns, particularly those high in processed or red meats, and underlying non-cancerous conditions such as inflammatory bowel disease, as well as lifestyle factors like smoking, excessive alcohol consumption, physical inactivity, and obesity.. In particular, dysregulation of the nuclear factor- κB (NF-κB) pathway is thought to play a highly complex role in CRC. The CARD11-BCL10- MALT1 (CBM) signalosome complex is critical for NF-κB activation in lymphocytes, particularly T and B cells. The *CARD11* gene is a crucial part of this complex and is also speculated to be involved in CRC onset and development. However, the specific *CARD11* effects in CRC are poorly researched compared to other cancers. Thus, this study aimed to elucidate how *CARD11* overexpression exacerbates the prognosis of CRC. To identify the cellular pathways influenced by *CARD11*, transcriptomic analysis was carried out on *CARD11*– overexpressed HCT-116 and HT-29 CRC cell lines alongside empty vector-transfected cell lines. Furthermore, transcriptomic data was compared from adenoma and carcinoma CRC patients with low- *CARD11* (*CARD11-)* and high- *CARD11* (*CARD11*+)

expression. The results indicated that *CARD11* plays a key role in CRC progression. Absolute GSEA (absGSEA) on HCT-116 transcriptomics data revealed that *CARD11* overexpression promotes cell growth and tissue remodeling and enhances immune response. Key genes co-expressed with *CARD11*, such as *EP300*, *KDM5A*, *HIF1A*, *NFKBIZ*, and *DUSP1*, were identified as mediators of these processes. In the HT-29 cell line, *CARD11* overexpression activated pathways involved in chemotaxis and extracellular matrix (ECM) organization, marked by *IL1RN*, *MDK*, *SPP1*, and chemokines like *CXCL1*, *CXCL3*, and *CCL22*, which were shown to contribute to the more invasive stage of CRC. In patient samples, adenoma patients exhibited increased expression of genes associated with the tumor immune microenvironment, such as *IL6ST*, collagen family members, and CRC transition markers like *GLI3* and *PIEZO2* *Transcriptomics analysis indicated distinct expression profiles in both cell lines with CARD11 overexpression. The analysis showed there were relatively more genes upregulated in HCT-116 compared to the HT-29 cell line, indicating that CARD11 overexpression has a more pronounced effect on the HCT-116. While HT-29 maintained a more stable expression pattern, HCT-116 showed significant activation of pathways related to immune responses.*in *CARD11*+ adenoma patients. Carcinoma patients showed a dramatic increase in the expression of *MAPK8IP2* in *CARD11*+ carcinoma patients alongside other cancer-related genes, including *EMB*, *EPHB6*, and *CPEB4*. For the various stages of CRC study, the transcriptional co-regulatory mechanisms pathway exhibited differentially expressed genes (DEGs) in the adenocarcinoma cohorts. These included *CEBPZ*, *MED10*, and *PAWR*. In contrast, *SIRT6, ARRB1, TADA2A, CTBP1*, and *CTBP2* were upregulated genes in adenoma samples. The protein kinase functional pathways exhibited downregulation of *OBSCN*, *ERN1, ERN2*, and *CAM2KG* genes in the adenocarcinoma cohorts. In conclusion, this study reveals *CARD11* as a key regulator in colorectal cancer progression, influencing diverse pathways tied to immune modulation, ECM remodeling, and tumor invasiveness. Besides stage-specific transcriptomic profiling, these findings highlight distinct molecular patterns between

adenoma and carcinoma, providing a deeper understanding of CRC pathogenesis and affirming the value of *CARD11* as both a biomarker and a potential therapeutic target.

**Zusammenfassung**

## Molekulare Pathogenese bei der Entstehung und dem Fortschreiten von Darmkrebs

Faisal Alhosani

Fälle von kolorektalem Karzinom (CRC) gehören weltweit zu den dritthäufigsten bösartigen Erkrankungen und sind eine führende Ursache für krebsbedingte Sterblichkeit. CRC wird typischerweise in Vorläuferläsionen wie Adenome, hochgradige Dysplasien oder Karzinome in situ sowie in maligne Formen wie Adenokarzinome eingeteilt, was die progressive Natur der kolorektalen Tumorentwicklung widerspiegelt. Die Inzidenz- und Sterblichkeitsraten zeigen sich auch auf nationaler Ebene, wobei CRC in den Vereinigten Arabischen Emiraten (VAE) die tödlichste Krebsart bei Männern darstellt. Die spezifische Ätiologie von CRC ist weiterhin weitgehend unklar. Forscher sind sich jedoch einig, dass die Hauptursachen für kolorektalen Krebs genetische Veranlagung, Ernährungsgewohnheiten – insbesondere eine Ernährung mit hohem Anteil an verarbeiteten oder roten Fleischsorten –, zugrundeliegende nicht-kanzeröse Erkrankungen wie chronisch entzündliche Darmerkrankungen sowie Lebensstilfaktoren wie Rauchen, übermäßiger Alkoholkonsum, Bewegungsmangel und Fettleibigkeit umfassen.

Insbesondere wird angenommen, dass die Fehlregulation des nuklearen Faktors κB (NF-κB) eine hochkomplexe Rolle bei CRC spielt. Der CARD11-BCL10-MALT1-(CBM-)Signalosom-Komplex ist entscheidend für die Aktivierung von NF-κB in Lymphozyten, insbesondere T- und B-Zellen. Das CARD11-Gen ist ein wichtiger Bestandteil dieses Komplexes und wird auch als potenziell an der Entstehung und Entwicklung von CRC beteiligt angesehen. Die genauen Wirkungen von CARD11 bei CRC sind jedoch im Vergleich zu anderen Krebsarten wenig erforscht. Ziel dieser Studie war es daher, aufzuklären, wie eine CARD11-Überexpression die Prognose von CRC verschlechtert.

Um die von CARD11 beeinflussten zellulären Signalwege zu identifizieren, wurde eine Transkriptomanalyse an HCT-116- und HT-29-CRC-Zelllinien mit CARD11-Überexpression sowie an mit Leer-Vektor transfizierten Zelllinien durchgeführt. Darüber hinaus wurden Transkriptomdaten von CRC-Patienten mit Adenomen und Karzinomen mit niedriger (CARD11−) bzw. hoher (CARD11+) CARD11-Expression verglichen. Die Ergebnisse zeigten, dass CARD11 eine zentrale Rolle im Fortschreiten von CRC spielt. Eine Absolute GSEA (absGSEA) der HCT-116-Transkriptomdaten ergab, dass die CARD11-Überexpression Zellwachstum und Gewebeumbau fördert und die Immunantwort verstärkt. Schlüsselgene, die mit CARD11 ko-exprimiert wurden, wie EP300, KDM5A, HIF1A, NFKBIZ und DUSP1, wurden als Vermittler dieser Prozesse identifiziert.

In der HT-29-Zelllinie aktivierte die CARD11-Überexpression Signalwege, die mit Chemotaxis und Organisation der extrazellulären Matrix (ECM) verbunden sind, erkennbar an IL1RN, MDK, SPP1 und Chemokinen wie CXCL1, CXCL3 und CCL22, die zur invasiveren CRC-Phase beitragen. Bei

Patientenproben zeigten Adenom-Patienten eine erhöhte Expression von Genen, die mit dem tumorimmunologischen Mikromilieu verbunden sind, wie IL6ST, Kollagen-Familienmitglieder und Übergangsmarker von CRC wie GLI3 und PIEZO2.

Die Transkriptomanalyse zeigte unterschiedliche Expressionsprofile in beiden Zelllinien mit CARD11-Überexpression. Die Analyse ergab, dass in HCT-116 relativ mehr Gene hochreguliert waren als in HT-29, was darauf hindeutet, dass die CARD11-Überexpression in HCT-116 einen stärkeren Effekt hat. Während HT-29 ein stabileres Expressionsmuster beibehielt, zeigte HCT-116 eine signifikante Aktivierung von Immunantwort-Signalwegen bei CARD11+-Adenompatienten.

Bei Karzinompatienten wurde ein dramatischer Anstieg der Expression von MAPK8IP2 bei CARD11+-Patienten festgestellt, zusammen mit anderen krebsbezogenen Genen wie EMB, EPHB6 und CPEB4. Für die verschiedenen Stadien der CRC-Erkrankung zeigte der transkriptionale Ko-Regulationsmechanismus unterschiedlich exprimierte Gene (DEGs) in den Adenokarzinom-Kohorten, darunter CEBPZ, MED10 und PAWR. Im Gegensatz dazu waren SIRT6, ARRB1, TADA2A, CTBP1 und CTBP2 in Adenomproben hochreguliert. Die funktionalen Signalwege der Proteinkinase zeigten eine Herunterregulierung von OBSCN, ERN1, ERN2 und CAM2KG in den Adenokarzinom-Kohorten.

Zusammenfassend zeigt diese Studie, dass CARD11 ein zentraler Regulator im Fortschreiten des kolorektalen Karzinoms ist und verschiedene Signalwege beeinflusst, die mit Immunmodulation, ECM-Remodelling und Tumorinvasivität verbunden sind. Neben stadienbezogenen Transkriptomprofilen verdeutlichen diese Ergebnisse die unterschiedlichen molekularen Muster zwischen Adenomen und Karzinomen, was zu einem tieferen Verständnis der CRC-Pathogenese beiträgt und den Wert von CARD11 sowohl als Biomarker als auch als potenzielles therapeutisches Ziel unterstreicht..

# Acknowledgements

I would like to express my deepest gratitude to my supervisors at the University of Lubeck, Professors Hauke Busche and Cyrus Khandanpur, and to my supervisors at the University of Sharjah, Professors Rifat Hamoudi and Riyadh Bendardaf, for their unwavering support throughout my academic journey at the University of Lubeck and at the University of Sharjah, College of Medicine. I would like to express my heartfelt gratitude to Dr. Jennifer Hundt, Dr. Marieke Hohen, and Mrs. Connie Jackson for their unwavering support throughout my PhD journey. I also extend my sincere appreciation to my academic mentors: Dr. Axel Kuenstner, Dr. Sven, Mr. Sen Guo, Dr. Burcu, Dr. Reem, Dr. Poorna, and Mrs. Rochi, and the faculty and staff of the University of Lubeck, Medical Biology Systems Group and to the Research Institute for Medical and Health Sciences, University of Sharjah. Their commitment to advancing scientific research and their willingness to share their knowledge have significantly contributed to the project's success. I am deeply grateful for their support and the opportunity to work under their guidance. My gratitude also extends to my colleagues and friends for their invaluable advice and support. I would also like to express my appreciation to the Dubai Scientific Research Ethics Committee (DSREC), the Dubai Health Authority (DSREC-SR-02/2023_07), and the Research and Ethics Committee (REC) of the University Hospital Sharjah (UHS-HERC-055-25022019) for providing ethical approval for this study. Special thanks to all patients who provided informed consent to participate in the study.

Finally, my heartfelt gratitude goes to my parents for their unwavering encouragement and support, whose patience, understanding, and belief in me have been a constant source of strength. Thank you for being by my side throughout this journey.

# Publications Associated with this Research

Alhosani, F., Ilce, B. Y., Alhamidi, R. S., Bhamidimarri, P. M., Hamad, A. M., Alkhayyal, N., Künstner, A., Khandanpour, C., Busch, H., Sayed, K., AlFazari, A., Bendardaf, R., & Hamoudi, R. (2024). Transcriptome Profiling Associated with *CARD11* Overexpression in Colorectal Cancer Implicates a Potential Role for Tumor Immune Microenvironment and Cancer Pathways Modulation via NF-κB. International Journal of Molecular Sciences, 25(19), 10367. https://doi.org/10.3390/ijms251910367

Alhosani, F., Alhamidi, R. S., Ilce, B. Y., Altaie, A. M., Ali, N., Hamad, A. M., Künstner, A., Khandanpour, C., Busch, H., Harati, R., Sayed, K., AlFazari, A., Bendardaf, R., & Hamoudi, R. (2024). Transcriptome-Wide Analysis and Experimental Validation from FFPE Tissue Identifies Stage-Specific Gene Expression Profiles Differentiating Adenoma, Carcinoma In-Situ and Adenocarcinoma in Colorectal Cancer Progression. International Journal of Molecular Sciences, 26(9), 4194. https://doi.org/10.3390/ijms26094194

# Table of Contents

# LIST OF ABBREVIATIONS

| | |
|---|---|
| absGSEA | absolute GSEA |
| AJs | adherens junctions |
| APC | adenomatous polyposis coli |
| *BRAF* | B-Raf proto oncogene |
| *CARD11* | caspase recruitment domain family member 11 |
| CEA | carcinoembryonic antigen |
| CIBERSORTX | cell-type identification by estimating relative subsets of RNA transcripts |
| ccRCC | clear cell renal cell carcinoma |
| CIMP | CpG island methylator phenotype |
| CIN | chromosomal instability |
| CIS | carcinoma *in situ* |
| CRC | colorectal cancer |
| CT | computed tomography |
| CTC | circulating tumor cell |
| DEGs | differentially expressed genes |
| DLBCL | large B cell lymphoma |
| DSREC | Dubai Scientific Research Ethics Committee |
| DLA | dual luciferase assay |
| ECM | extracellular matrix |

| | |
|---|---|
| EGFR | Epidermal Growth Factor Receptor |
| FAP | familial adenomatous polyposis |
| FPKM | fragments per kilobase million |
| GSEA | gene set enrichment analysis |
| gFOBT | guaiac-based fecal occult blood tests |
| GMRB | gut microbe-related biomarker |
| HGD | high-grade dysplasia |
| HNPCC | hereditary non-polyposis colorectal cancer |
| iFOBT | immunochemical fecal occult blood tests |
| IKK | Inhibitor of nuclear kappa factor B kinase |
| LGD | Low-Grade Dysplasia |
| LOH | Loss Of Heterozygosity |
| LS | Lynch Syndrome |
| MALT1 | mucosa-associated lymphoid tissue lymphoma translocation protein 1 |
| miRNA | microribonucleic acid |
| MMR | Mismatch Repair |
| MSI | Microsatellite Instability |
| NF-κB | Nuclear Factor-kappa light chain enhancer of activated B cells |
| NMR | Nuclear Magnetic Resonance |
| OS | Overall Survival |

| | |
|---|---|
| PCA | Principal Component Analysis |
| QoL | Quality of Life |
| SEPT9 | Septin 9 |
| TGFβR2 | Transforming Growth Factor B Receptor 2 gene |
| TSA | Traditional Serrated Adenomas |
| TME | Tumor Microenvironment |
| UAE | United Arab Emirates |
| UVM | Uveal Melanoma |
| VEGF | Vascular Endothelial Growth Factor |

# List of Figures

# List of Tables

# Chapter I.

# Introduction

## 1.1 Background and Aims

CRC is considered the third most common type of cancer, accounting for a significant proportion of cancer-related mortalities. The condition has become more prevalent in recent decades, with the advancing age of the population (Siegel *et al.*, 2023). The CRC burden among Arab young adults is also increasing at unprecedented rates. Specifically, CRC diagnoses among individuals aged below 50 are rising annually by around 3%. The 5-year CRC survival is contingent on the stage of the disease: 70% for stage IV and 95% for stage I (Alzaabi, 2022). However, most CRC cases are usually diagnosed in later stages, resulting in a generally low survival rate.

Colorectal cancer (CRC) classified by histological type, anatomical location, and stage of progression. The most common histological subtype is adenocarcinoma, which typically arises from adenomatous polyps through a well-established adenoma-carcinoma sequence. Early lesions may present as carcinoma in situ (stage 0), confined to the mucosal layer. They can progress through stages I to IV based on the depth of invasion, lymph node involvement, and distant metastasis, as defined by the TNM staging system endorsed by the American Joint Committee on Cancer (AJCC) and used by the ACS(Society 2024, UK 2024). Cancer Research UK similarly categorizes CRC by type, grade, and stage, noting that adenomas are benign precursors. High-grade dysplasia and carcinoma in situ are transitional forms that occur before invasive cancer develops(UK 2024). These classifications are essential for guiding treatment decisions and assessing prognosis.. Colorectal adenomas are extended protrusions of the intestinal mucosa and are usually benign. However, they are precancerous and can develop into malignant structures. Notably, >95% of colorectal adenocarcinomas originate from intestinal benign polyps, and less than 10% of adenomas develop into malignant lesions in about ten years(Lang, Kuipers et al. 2020, Bortz and

Friedrich-Nel 2023) (Taherian et al., 2023). ). Carcinomas usually develop from colorectal adenomas displaying carcinoma *in situ* (CIS) or high-grade dysplasia (HGD). These later CRC stages typically feature infiltration, ulceration, and uplift. CRC is also highly heterogeneous, with many variations between similar tumors in different patients and between cancer cells in a tumor.

Regardless of the CRC type and patient variables, such as gender, the signs and symptoms are generally common. For example, all young CRC patients exhibit the four common signs of early onset, such as diarrhea, rectal bleeding, abdominal pain, and iron deficiency (Weinberg*et al.*, 2019; Wang *et al.*, 2023). The genetic instability and the mutation burden in tumor cells necessitate the development of therapeutic strategies that address the heterogeneity and dynamics within tumors. The identification of novel biomarkers is a necessity for facilitating personalized treatment strategies, including prevention, diagnosis, prognosis, and therapeutic targeting.. At the cellular level, cell cycle dysregulation and immune cell infiltration of the colonic epithelium could contribute to CRC in terms of the predisposition to carcinoma and sustained inflammation (Chen *et al.*, 2024; Lewandowska *et al.*, 2022). The tumorigenic microenvironment may arise from chronic inflammation. Conditions like inflammatory bowel disease (IBD) that involve continuous inflammation are associated with an increased risk of CRC. (Burgos-Molina et al., 2024). One key mediator of inflammatory responses is the nuclear factor kappa- light-chain-enhancer of activated B cells (NF-κB). When inflammatory stimuli like cytokines and microbial products are encountered, NF-κB is activated and translocated to the nucleus, where the expression of the inflammatory and immune response genes takes place (Barnabei et al., 2021). ThNF-κB of activated B cells has a central role in mediating the central organization of inflammatory responses, immune responses, cell survival, and apoptosis. These functions are achieved by regulating numerous transcription factors, inflammatory cytokines, and molecules related to the intestines. Upon response to various triggers, such as pathogens and abnormal cell growth, NF-κB signaling

initiates and orchestrates inflammation processes (Dorrington & Fraser, 2019). Since it has been documented that the NF-κB signaling pathway is constitutively activated in various tumor tissues, few studies have focused on the NF-κB pathway to target cancer as a therapy (Staudt, 2010; Davis *et al.*, 2001).

One of the features of CRC is the dysregulation of the NF-κB pathway, which engages in colonic inflammation (Martin *et al.*, 2021). Studies have shown that 66% of CRC cell lines and 40% of human CRC tissues exhibit constitutive activation of NF-κB (Hassanzadeh, 2011). Many stimuli activate NF-κB by phosphorylating and ubiquitinating, degrading the inhibitory molecules that keep NF-κB subunits in the cytoplasm. For example, the IκB-kinase (IKK) complex is responsible for signal-induced phosphorylation of the inhibitor of κBs (IκBs) (Christian *et al.*, 2016). The IKK complex is activated by various stimuli that require the formation of the *CARD11*-BCL10-MALT1 (CBM) complex in the cytoplasm triggered by stimulation through the T- and B-cell receptors (TCR/BCR) (Turvey *et al.*, 2014).

The Caspase Recruitment Domain Family Member 11 (*CARD11*) gene, one of the members of CBM complex, is among the genes involved in transducing NF-κB signaling via B- and T-cell receptors. This gene, illustrated in Figure 1, is a multi-domain scaffold protein with a characteristic caspase-associated recruitment domain (Dorjbal *et al.*, 2019). It is a crucial signal transducer between antigen recognition and the activation of downstream NF-κB in lymphocytes and is an essential signaling molecule in adaptive immune response (Bedsaul *et al.*, 2018). The Kaplan–Meier survival curve from microarray-based gene expression data, illustrated in Figure 1, shows a significant decrease ($p < 0.001$) in survival for CRC patients with higher expression of *CARD11*.


*Figure 1: Schematic representation of the domain architecture of the human CARD11 protein. CARD11 is a multi-domain scaffold protein composed of several conserved signaling domains essential for NF-κB activation. The N-terminal region contains the CARD domain (Caspase-associated recruitment domain, light purple), which mediates protein–protein interactions critical*

*for initiating downstream signaling. Adjacent to it is the L domain (linker, green), followed by the coiled-coil (CC) domain (blue), which facilitates oligomerization and assembly of the CBM complex. The central region includes an inhibitory domain (ID, beige) and four repressive elements (RE1–RE4, dark red) that maintain CARD11 in an inactive conformation in resting cells. The C-terminal MAGUK region consists of PDZ, SH3, and GUK domains (grey and yellow), which contribute to membrane localization and interaction with other signaling proteins. Upon activation through antigen receptor signaling, conformational changes relieve autoinhibition, allowing CARD11 to form the active CBM complex and propagate NF-κB signaling.*

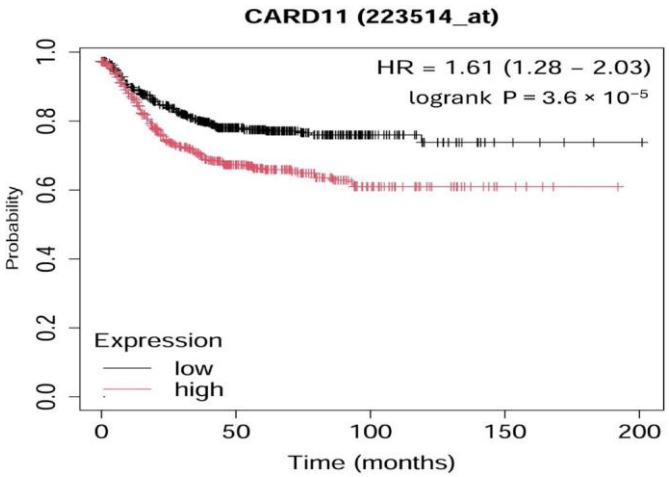


*Figure 2: Kaplan–Meier overall survival plot for CRC patients based on CARD11 expression. The analysis ran on 1167 patients; 598 patients had high expression, and 569 patients had low expression of CARD11 (https://kmplot.com)*

To the best of our knowledge, there have been no attempts to investigate the role of *CARD11* overexpression on the modulation of NF-κB activation in CRC. It is particularly unclear whether *CARD11* overexpression affects the transcriptomic profiles in CRC cell lines. To gain a better understanding of the role of *CARD11* in CRC pathogenesis and, more specifically, how over-expression of *CARD11* can affect the downstream signaling pathways in the pathogenesis of CRC, this project aimed to characterize whole transcriptomic changes associated with the effect of *CARD11* overexpression in CRC cell lines as well as the effect of *CARD11* overexpression in colorectal adenoma and carcinoma patients. Understanding the role of *CARD11* in CRC may help identify novel diagnostic and therapeutic targets and elucidate novel mechanisms involved in CRC progression via NF-κB dysregulation. Additionally, the study aimed to identify candidate biomarkers associated with distinct stages of CRC

development—from adenoma to carcinoma in situ and ultimately to adenocarcinoma—to support precision medicine approaches and enhance early detection and stratified treatment strategies.

### 1.2 Statement of the Problem Hypothesis

Several screening methods for CRC and precursor sessile serrated lesions and adenomatous polyps have been developed over the years. According to Bresalier *et al.* (2020), optical colonoscopy is the most commonly used approach. However, this technique typically necessitates sedation, involves pre-test bowel cleansing, and introduces a risk of adverse events. Furthermore, such methods are insensitive to CRC heterogeneity, resulting in up to one-third of guideline-eligible patients not accessing screening as recommended (Bresalier *et al.*, 2020). Moreover, CRC screening in many countries, including the United Arab Emirates (UAE), is typically a two-step procedure where an initial positive screening assessment is followed by a colonoscopy for further diagnosis (Bresalier *et al.*, 2020). Furthermore, biopsy-based approaches for detecting CRC cannot offer clinically useful predictive and prognostic information specific to each patient (Marcuello *et al.*, 2019). These limitations have motivated extensive research on developing non-invasive screening methods using biomarkers, including blood, stool, and molecular markers.

Effective biomarkers must meet several requirements for clinical applicability. For example, they should be patient-friendly and have high specificity and sensitivity for various CRC stages and high-risk precursor lesions. Furthermore, the use of biomarkers should be cost-effective to increase overall acceptance. Currently available biomarkers have several limitations that contravene these requirements, especially regarding the capacity for early CRC detection. For instance, fecal hemoglobin, the biomarker used in fecal occult blood tests, exhibits relatively low sensitivity in detecting early-stage lesions. Specifically, the sensitivity

is 40-85% of CRCs and ~10% of adenomas, and the tests are reported to reduce CRC mortality by only 30% (Tanaka *et al.*, 2010). Blood-based biomarkers are also similarly problematic. For example, methylated Septin 9 (SEPT9) detects CRC with 92% specificity and 48% sensitivity, which further reduces to 35% for stage 1 CRC (Bresalier *et al.*, 2020). These issues translate to a general absence of reliable biomarkers for early CRC detection.

Emerging molecular insights offer promising avenues for addressing this gap. Among them, the NF-κB is known to play a significant role in several cancers, including renal carcinoma, where it is linked with poor prognosis. The canonical pathway activation has been shown to hold immunomodulatory and antiapoptotic functions as a reaction to the tumor microenvironment, while the non-canonical pathway is associated with tumor reinitiation and cancer cell maintenance (Dobre *et al.*, 2022). NF-κB has a particularly key role in CRCs, which significantly depend on inflammation. For instance, sporadic CRC features increased expression of pro-inflammatory cytokines, such as IL-6, INFγ, IL-17a, IL-1b, and Il-8. Thus, because of the aberrant NF-κB activity, pharmacological NF-κB inhibitors against cancer progression and initiation are being considered for novel therapeutic interventions. miRNAs also contribute to cancer progression, with notable roles in tumor suppression and oncogenesis (Dobre *et al.*, 2022). Furthermore, miRNAs control the NF-κB signaling pathway in cancer primarily by governing protein expression. Therefore, miRNAs are also implicated in inflammation and innate response modulation. These examples demonstrate the highly complex role of NF-κB in CRC, which warrants additional research to acquire more insights and infer novel solutions to detect and manage CRC.

The *CARD11* gene is also involved in the development of different cancers. Its depletion has demonstrated anti-tumor effects, partly through the suppression of systemic autoimmunity, suggesting a dual role in oncogenesis and immune regulation (Shi et al., 2021). In large B-cell lymphoma, CARD11 has been shown to drive tumorigenesis;

specifically, mutations in its coiled-coil domain lead to constitutive NF-κB activation, which is further amplified upon antigen receptor stimulation (Lenz et al., 2008). Additionally, CARD11 has been associated with uveal melanoma (UVM), where its elevated expression correlates with worse clinicopathological features and reduced overall survival (Shi et al., 2021). High CARD11 levels were linked to the upregulation of key oncogenic hub genes. Slattery *et al.* (2018) suggest similar correlations may be present in CRCs, reporting that the gene is significantly downregulated during CRC initiation and progression. However, the sole effect of *CARD11* in CRC are poorly researched compared to other cancers, resulting in extensive knowledge gaps. Therefore, additional research is required to determine the feasibility of *CARD11* as a biomarker for clinical CRC diagnosis and a novel therapeutic target for clinical interventions.

This study is guided by two central hypotheses:

1- CARD11 is implicated in the initiation and progression of CRC through the activation of NF-κB signaling pathway.

2- Identification of putative molecular biomarkers that differentiate between various stages of CRC development including adenoma, carcinoma in situ, and adenocarcinoma.

## 1.3 Thesis Structure

The thesis is structured into six chapters, each addressing distinct aspects of the study on *CARD11* overexpression in CRC. The scope of each chapter is as follows:

- **Chapter I:** introduces the research problem, objectives, and the role of *CARD11* and NF-κB in CRC pathogenesis.
- **Chapter II:** reviews relevant literature, discussing CRC pathways, NF-κB signaling, and gaps in current knowledge.
- **Chapter III:** outlines the methodology, including cell line experiments, RNA sequencing, and data analysis techniques used in the project.
- 
- **Chapter IV:** presents the results, highlighting *CARD11*-induced changes in transcriptomic profiles, pathway activations, and immune microenvironment modulation.
- **Chapter V:** interprets the obtained findings, emphasizing their implications in CRC biology and potential clinical applications.
- **Chapter VI:** concludes the study, summarizing key insights, acknowledging limitations, and proposing directions for future research.

## Chapter II.

## Literature Review

### 2.1 Initiation of Disease

CRC is a leading cause of cancer-related mortality globally and the third most prevalent malignancy. While hereditary factors strongly impact CRC, disease initiation is mostly sporadic and slowly develops over multiple years through the adenoma-carcinoma sequence (La Vecchia & Sebastián, 2020). Adenomas originate from the alteration of the standard mechanisms regulating DNA repair and cell proliferation. Continuous epithelial renewal is needed because of the incessant loss of intestinal mucosa surface cells, and proliferation only manifests at the crypt base. The advancement of mutant cells toward the colonic lumen disrupts the normal terminal differentiation and apoptosis processes, resulting in discrete adenomas. The adenomatous polyps grow with time and gain invasive potential. The progress from normal to hyperproliferative epithelium features stepwise changes in crucial growth regulatory genes. Notably, mutations in the B-Raf proto (BRAF) oncogene result in serrated polyps, while adenomatous polyposis coli (APC) gene mutations foster the development of typical adenomas (Nguyen *et al.*, 2020). The ensuing events are specific to the engaged pathways, summarized in Figure 3.

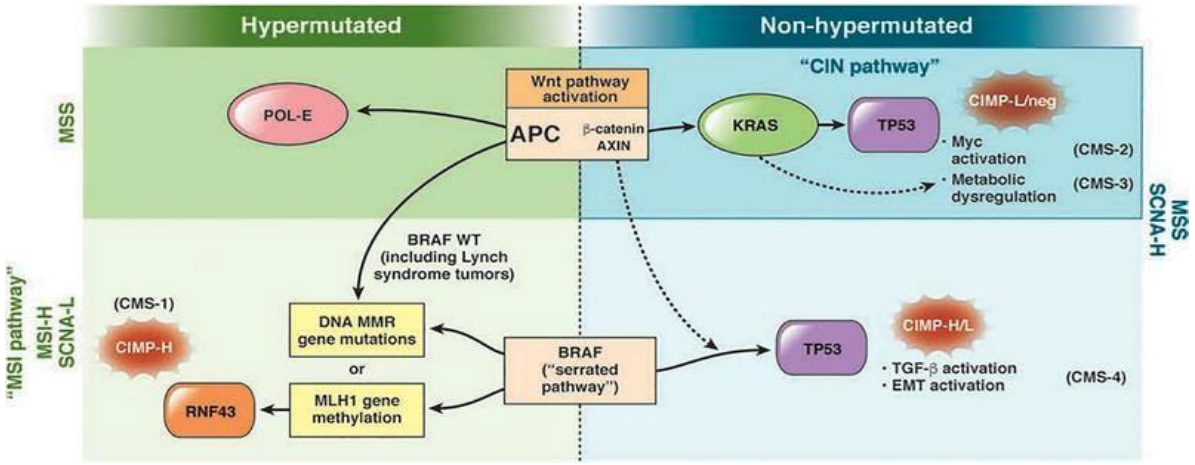


*Figure 3: The pathways of colorectal carcinogenesis (Source: Nguyen et al., 2020)*

### 2.2 Chromosomal Instability (CIN) Pathway

The CIN pathway is present in up to 70% of sporadic colorectal tumors (Pino & Chung, 2010). Loss of heterozygosity (LOH) and extensive imbalances in chromosome number (aneuploidy) characterize malignancies that develop through this pathway. Furthermore, defects in telomere stability, chromosomal segregation, and the DNA damage response typically activate CIN. Besides the typical karyotypic abnormalities, CIN tumors feature a buildup of mutations in specific oncogenes and tumor suppressor genes. For example, APC and TP53 mutations are common, with the former being the earliest genetic event (Nguyen *et al.*, 2020). However, there is no scientific consensus on whether CIN initiates the relevant milieu for the development of these mutations or if the mutations activate the CIN pathway.

### 2.3 Microsatellite instability (MSI) Pathway

The MSI pathway can be regarded as a form of genomic instability, accounting for the initiation of about 15% of sporadic CRC cases (Colussi *et al.*, 2013). Despite being relatively infrequent than the CIN pathway, the MSI pathway represents more than 95% of Hereditary Non-Polyposis CRC (HNPCC) cases (Colussi *et al.*, 2013). The epigenetic silencing of the MLH1 gene is arguably the leading cause of the MSI phenotype in sporadic cases. Moreover, colorectal tumors initiated through the MSI pathway often feature high methylation levels in regulatory areas. MSI mutations also involve the Transforming Growth Factor B Receptor 2 gene (TGFβR2) gene, which is mutated in over 90% of MSI CRC (Nguyen *et al.*, 2020). The causative events for tumorigenesis vary, but APC mutations are most common. Therefore, the initiating events for adenoma genesis may be similar for CIN and MSI pathways.

### 2.4 Serrated Neoplasia Pathway

The serrated neoplasia pathway involves the development of CRC from serrated polyps and is thought to account for approximately 15% of CRCs (IJspeert *et al.*, 2015). The main types of serrated polyps include precancerous sessile serrated adenomas, hyperplastic polyps,

and traditional serrated adenomas (TSAs). Hyperplastic polyps are the most common, accounting for up to 90% of the reported cases of serrated lesions (Bauer & Papaconstantinou, 2008). The serrated neoplasia pathway is fundamentally dissimilar from the CIN and MSI pathways. For example, the V600E mutation in BRAF is typically instigated. Moreover, most hyperplastic polyps feature BRAF mutations, constitutively causing unrestrained cell division and activating the MAPK-ERK pathway (Gibney *et al.*, 2013). Serrated tumors grow through two main routes after BRAF mutation: DNA mismatch repair (MMR) gene mutations and MLH1 gene methylation (Nguyen *et al.*, 2020).

### 2.5 Other Relevant Pathways

Recent studies have indicated the possibility of multiple additional pathways for CRC initiation. For instance, Nguyen *et al.* (2020) report frequent mutations in FAM123B, SOX9, ARID1A, and POLE genes. POLE mutations produce a hypermutated phenotype featuring single nucleotide variance with MSI or aneuploidy. APC mutations may be the starting point in this pathway. However, the ensuing downstream mutations are mostly unknown. Researchers have also described colorectal tumors lacking notable hypermutation or aneuploidy. These tumors also start with APC mutations and acquire PCBP1, SOX9, PIK3CA, and KRAS mutations (Liu *et al.*, 2018). The uncertainty of the specificities of all CRC initiation pathways suggests that significant research is still required to fully characterize the condition and facilitate accurate prevention measures and diagnostics.

### 2.6 Epidemiology

#### *2.6.1 Incidence*

CRC is the third most common malignancy globally. Based on data from the Global Cancer Observatory (Estimated number of deaths from 2022 to 2045, Both sexes, age [0-85+]: Colorectum, 2024), the estimated number of new CRC cases globally in 2022 was 19,976,499. As seen in Figure 4 Asia had the highest number of new cases at 9,826,539. Furthermore, the

estimated number of new cases in the United Arab Emirates (UAE) in 2022 was 5,526. From a large-scale perspective, CRC is more incident in males than females. For example, the new male CRC cases in Asia in 2022 were 5,093,995, while the female cases were 4,732,544. However, CRC was slightly more incident among females than males in the UAE. Specifically, the estimated number of female cases was 2,919, while the number of male cases was 2,607. Nonetheless, CRC is the most diagnosed cancer among men in the UAE (Rawla *et al.*, 2019). Developed nations like the UAE are also at the highest risk of CRC compared to developing countries (Rawla *et al.*, 2019).

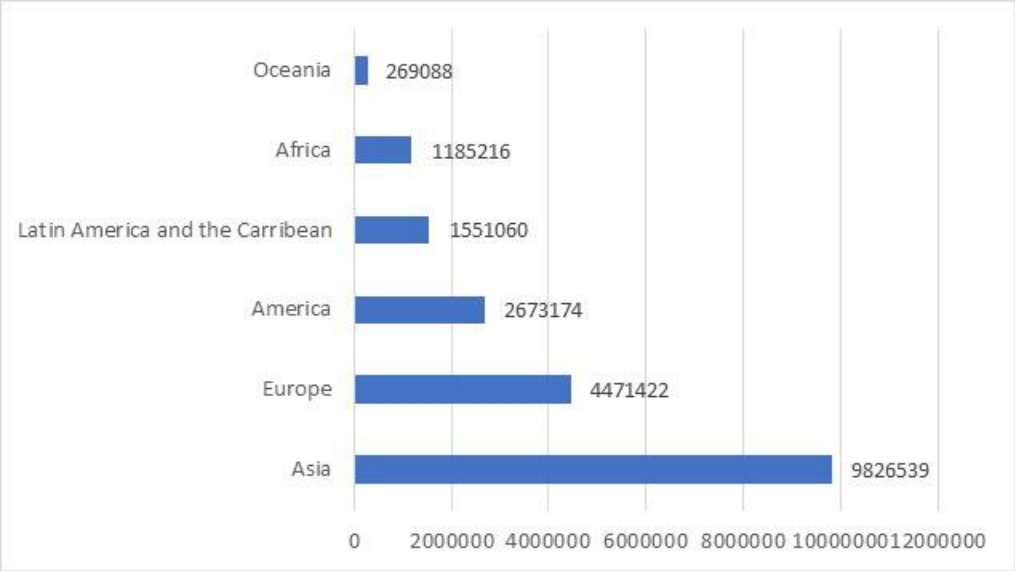


*Figure 4: The CRC incidence globally (Data sourced from WHO Cancer Tomorrow)*

### *2.6.2 Mortality*

CRC has a relatively high mortality rate. The estimated number of deaths globally in 2022 was 904,019, translating to a mortality rate of 4.53%. Notably, there were 9,743,832 cancer deaths in 2022. Therefore, CRC accounted for 9.28% of all cancer deaths. Furthermore, more males (499,775) died from CRC than females (404,244). The number of deaths in 2022 was highest in Asia (462,252), indicating the high disease burden in the region. In the UAE, the number of deaths was 236, translating to a 4.27% mortality rate. The number of deaths was higher in males (149) than in females (87), confirming the relatively high severity among males.

CRC is also the deadliest cancer among males in the UAE (Rawla *et al.*, 2019).

### *2.6.3 Trends*

As illustrated in Figure 5, the estimated number of new CRC cases globally is expected to increase annually. Global cases should reach 30,971,263 by 2045, marking a 64.5% upsurge. The situation is particularly concerning in Asia, where the number of new cases should reach 16,162,830, translating to a 60.79% increase from 2022. The estimated number of new CRC cases in the UAE in 2045 is 1,740, representing a 216.4% growth. The mortality rate is also expected to increase with the number of new CRC cases. In Asia, the number of deaths by 2045 is projected to reach 901,210, marking a 95% increase from 2022. In the UAE, the number of deaths by 2045 should be 822, representing a 248.3% increase from 2022. These statistics indicate that the UAE's CRC burden is growing faster than the continental and global averages.

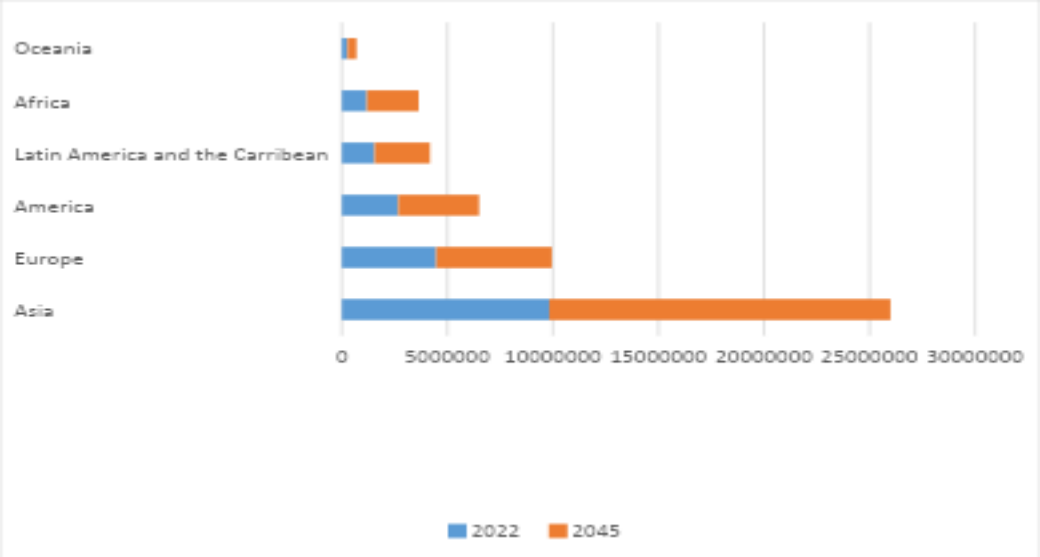


*Figure 5: The global trend in new CRC cases (Data sourced from WHO Cancer Tomorrow)*

### *2.6.4 Survival*

Despite the increasing CRC incidence, recent treatment improvements have decreased mortality in the second and third categories of countries. According to recent research, clinical solutions to remove polyps along with early detection strategies, including fecal occult blood testing, flexible sigmoidoscopies, fecal immunochemistry, and colonoscopies, have been the main drivers of improved survival (Rawla *et al.*, 2019). Furthermore, the increasing incidence

in recent years may be due to the introduction of advanced screening methods, resulting in the detection of previously undiagnosed cases. However, survival in Arab countries like the UAE is lower than in Western nations (Alzaabi, 2022). Poor awareness of symptoms and inadequate screening means that most CRC cases are detected in advanced stages, limiting treatment outcomes. The 5-year CRC survival is contingent on the stage of the disease: 70% for stage IV and 95% for stage I (Alzaabi, 2022). This disease severity in later stages explains the comparatively low CRC survival rate in the Arab world.

## 2.7 Etiology

The specific etiology of CRC is still largely unclear. However, researchers generally agree that the leading causes are related to genetic factors, dietary factors, and non-cancerous diseases (Baojun et al., 2022, Rawla *et al.*, 2019).

### *2.7.1 Genetic Factors*

Genetic factors account for approximately 20% of CRC cases (Baojun, 2022). Specifically, the first-generation relatives of CRC patients have a three-fold increased susceptibility to the disease. Lynch syndrome (LS), an inherited disorder instigated by germline epimutations in a DNA MMR gene, has been shown to particularly predispose individuals to CRC (Valle, 2014). Notably, MMR genes act like tumor suppressors, and cancer occurs when a second hit CpG island methylation, deletion, or mutation somatically deactivates the target cell's wild-type allele, such as a colonic epithelium cell. Familial adenomatous polyposis (FAP), an inherited syndrome involving the development of thousands of colorectal adenomatous polyps, is the second most common genetic cause of CRC (Valle, 2014). Other impactful syndromes include MUTYH-associated polyposis, polymerase proofreading-associated polyposis, hereditary mixed polyposis syndrome, and hamartomatous polyposis syndromes.

### *2.7.2 Dietary and Lifestyle Factors*

CRC incidence is also associated with several dietary factors, including a high intake of animal proteins and processed meats (Baojun et al., 2022). Murphy *et al.* (2019) reports

a 12% increased predisposition to CRC for each 100g/day consumption of processed meats. This effect may be due to processed meat's carcinogenic exposures from common preservation techniques, such as curing and smoking. For example, chemicals and compounds like polycyclic aromatic hydrocarbons, heterocyclic amines, and N-nitroso may initiate the main CRC pathways. Lifestyle factors, such as smoking and alcohol intake, also contribute to a high predisposition to the sickness. For example, each daily consumption of 10g of alcohol/ ethanol increases CRC risk by approximately 7% (Murphy *et al.*, 2019). Similarly, researchers have estimated a 15% increased CRC risk among regular smokers. In particular, cigarette smoke is thought to instigate the development of serrated polyps and may reduce the preventive effects of drugs like aspirin (Murphy *et al.*, 2019). The significance of lifestyle factors in CRC initiation may explain the relatively high prevalence in developed countries.

### *2.7.3 Non-Cancerous Diseases*

The development of colorectal cancer (CRC) is linked to several non-cancerous conditions, including Crohn's disease, ulcerative colitis, colorectal adenomas (arising from glandular), and colorectal polyps (abnormal growth from mucus membrane). Among these, adenomatous polyps are arguably the most significant contributors to CRC., accounting for up to 40% of cases (Baojun et al., 2022). These growths can develop gradually for up to 20 years before becoming cancerous (Rawla et al., 2019). Polyps growing from granular cells dedicated to mucus production in the large intestines are particularly dangerous. Furthermore, up to 5% of individuals with ulcerative colitis develop CRC, and this percentage increases to 10% in individuals experiencing ulcerative colitis for over two decades (Baojun et al., 2022). Colorectal adenomas bigger than 3 cm also have a 40% chance of progressing to cancer (Baojun et al., 2022). The CRC risk dramatically reduces for adenomas smaller than 1cm, with a <2% risk of progression to cancer (Baojun et al., 2022). Therefore, individuals with reported non-cancerous diseases should receive regular medical checks to facilitate early

CRC detection.Clinical Symptoms.

The initial stages of CRC are often asymptomatic. Most CRCs begin with a benign polyp that can take up to 20 years to become malignant and cause noticeable symptoms. However, as the disease progresses, individuals often exhibit intestinal obstruction, hematochezia, abdominal mass, and other systemic symptoms.

**Hematochezia:** Patients often experience a chronic, sporadic passage of small amounts of bright red or maroon blood through the anus. The rectal bleeding typically originates from cancerous polyps in the rectum or colon. Baojun et al., 2022 also reports that patients may exhibit jam-like stool, mucus blood stool, or blood stool due to excessive rectal bleeding(Baojun Duan 2022).

**Intestinal obstruction:** Low bowel obstruction is the most common CRC symptom, manifesting in about 20% of reported cases (Grigorean *et al.*, 2023). This symptom can occur abruptly or be preceded by separate premonitory signs that generally appear to be non-specific, such as anemia(Nakagawa, Tachibana et al. 2015). Moreover, sudden onset obstructions may be associated with intussusceptions at the colic level, volvuluses in supratumoral mobile sections, enteral ischemic phenomena, and peritoneal carcinomatosis. Notably, the hypermobility and increased weight of endoluminal content instigate colic volvulus. Furthermore, the extent of constriction of the involved mesenteries rather than the rotation number contributes to necrosis in intestinal volvuluses(Fo, Kang et al. 2023).

**Abdominal mass and abscesses:** Abdominal masses typically occur in right colon cancer and are characterized by mass enlargement due to tumor development in the lining of the colon or rectum. Up to 22% of CRCs invade proximal organs without distant metastases. Such CRCs spread along tissue planes and may cause the development of masses and abscesses in uncommon locations like the abdominal wall (Attar *et al.*, 2018). Tumors developing from the intraperitoneal section of the colon have the highest likelihood of invading the abdominal

wall. While abdominal masses are relatively more frequent in CRCs, abscesses are rare and only affect 0.3-4% of patients (Attar *et al.*, 2018).

**Systemic symptoms:** As mentioned before, CRC has no obvious signs in its early stages. The disease progression also lasts many years, resulting in several systemic symptoms like tumor proliferation, emaciation, anemia, and cachexia. Anemia, indicated by iron deficiency, is the most prevalent extraintestinal symptom (Chardalias *et al.*, 2023). Specifically, malignancy causes inflammation, resulting in functional iron deficiency through the hepcidin pathway. Furthermore, chronic blood loss due to hematochezia leads to the depletion of iron stores and absolute iron deficiency. Most patients also exhibit cachexia, a syndrome characterized by systemic inflammation, catabolic activity, and weight loss. While the underlying causes are poorly understood, researchers speculate that systemic and local immune responses to tumors may instigate cachexia (Kasprzak, 2021).

### 2.8 Diagnosis and Treatment

Many CRCs are detected in advanced stages since patients do not exhibit obvious clinical symptoms in early disease progression phases, constraining treatment efficacy and increasing the mortality rate. Thus, researchers recommend investigation for individuals above 20 if they possess any of the following symptoms: abdominal mass, progressive weight loss, unexplained anemia, blood in stool, alterations in stool shape and defection habits, and incessant abdominal discomfort (Baojun et al., 2022).

Patients with suspected CRC are generally diagnosed through digital rectal examinations. Additional tests include:

1. **Positron emission computed tomography**: This test offers information on a tumor's metabolic attributes and anatomical site. The obtained results typically help diagnose, assess recurrence, and stage CRC(Mostafa, Mousa et al. 2021).
2. **Computed tomography (CT) and nuclear magnetic resonance (NMR):** CT is commonly used for CRC staging by displaying the underlying conditions, such as

the abdominal lymph nodes, lesion sizes, and impact of lesions on proximal organs and tissues. NMR imaging achieves similar outcomes but at higher resolution than CT scans(Jimenez, Mirnezami et al. 2013).

3. **Ultrasound:** Used to detect abdominal lymph nodes and intestinal masses(Maconi 2014).
4. **X-ray:** X-ray tests after barium enema are used to investigate mucosal destruction and filling defects at tumor sites. However, this approach is not feasible for patients with intestinal obstruction(Kawasaki, Torisu et al. 2021).
5. **Colorectal endoscopy:** Used to observe lesion shape, size, and position directly(Gao, Zhou et al. 2023).
6. **Tumor markers:** Carbohydrate Antigen 19–9 and carcinoembryonic antigen markers are typically used to characterize tumors and check for reoccurrence(Ilhan, Balcik et al. 2025).
7. **Fecal occult blood tests:** Used to check for hidden blood in stool, with positive results for approximately 5ml of colorectal bleeding (Baojun et al., 2022).

Surgery is the most common treatment for CRC, and it is often combined with other therapeutic approaches, including immunotherapy, molecular targeted therapy, radiotherapy, and chemotherapy. The main surgical methods include palliative and radical surgery. While radical surgery is used to stop disease progression, palliative surgery is employed to improve the quality of life (QoL) and survival time of patients with advanced CRC. According to Baojun et al., 2022, the 5-year survival rate of early-CRC patients receiving surgery treatment is over 90%. However, the treatment outcomes are contingent on the quality of surgery and the preoperative staging quality. Thus, researchers recommend that all dissections follow the embryological anatomical planes to guarantee that the targeted tumor and its primary lymphatic spread zone are removed (Kuipers *et al.*, 2015).

Furthermore, surgery feasibility for patients with metastasis and other inoperable conditions should be checked after neoadjuvant therapy to assess surgical treatment opportunities.

The primary forms of chemotherapy for CRC include palliative chemotherapy, adjuvant chemotherapy following radical surgery, and neoadjuvant chemotherapy. Baojun (2022) reports that neoadjuvant chemotherapy is commonly combined with radiotherapy to reverse disease progression, create opportunities for surgery, minimize postoperative reoccurrence, and enhance patients' QoL. Conversely, adjuvant chemotherapy is employed to destroy the remaining cancerous cells after radical surgery. The most common chemotherapy drugs are raltitrexed, oxaliplatin, irinotecan, and fluorouracil. Recently, molecularly targeted drugs have been developed and are typically combined with chemotherapeutic drugs. Two molecularly targeted drug types are currently available: anti-epidermal growth factor and anti-angiogenesis agents (Baojun et al., 2022). While chemotherapy applies to both colon and rectal cancer, radiotherapy is most feasible for rectal cancer. The main radiotherapy regimes include postoperative concurrent chemoradiotherapy and preoperative concurrent chemoradiotherapy, all of which can prolong survival, improve QoL, and enhance the local control rate. Other treatments to prolong survival include immunotherapy, radiofrequency therapy, local cryotherapy, biotherapy, and hyperthermia amalgamated with radiotherapy and chemotherapy.

### 2.9 Pathology and Different Tumor Types

CRC is usually limited to intestinal mucosa and submucosa in its early phases. Furthermore, lymphatic metastasis usually does not manifest in these initial stages, but it occurs in approximately 10% of patients after the tumor expands out of the submucosa(Song, Li et al. 2024) (Baojun et al., 2022). The major forms of CRC also mostly feature infiltration, ulceration, and uplift. Moreover, CRC is highly heterogeneous, with many variations between

similar tumors in different patients and between cancer cells in a tumor. Genetic and non-genetic factors at the transcriptomic, epigenomic, and genomic levels cause heterogeneity.

CRC classifications have changed over the years. Multiple histologic variants are possible based on the World Health Organization (WHO) classification. However, medullary carcinoma, signet cell adenocarcinoma, and mucinous adenocarcinoma are the main histological types (Gulinac, Mileva et al. 2024). Moreover, like many cancers, CRC can be staged based on the Duke's system. While this classification has mostly been superseded, it may still be applied in some medical contexts for additional staging detail. The main stages are Duke A (limited beneath the muscularis propria), Duke B (proliferation through the muscularis propria), Duke C (inclusion of regional lymph nodes), and Duke D (distant metastasis) (Banias, Jung et al. 2022). CRCs can also be graded as well, moderately, or poorly differentiated based on the characteristics of tissues and cells observed under a microscope. Well-differentiated cells appear more normal with mature structures, while poorly differentiated cells seem less normal and are unusually arranged. Moderately differentiated cells are somewhat normal, with a comparable number of normal and abnormal structures (Kobayashi, Ishida et al. 2024).

### *2.9.1 Adenoma*

Colorectal adenomas are extended protrusions of intestinal mucosa (polyps originating from glandular tissue). These tumors are typically benign, but they are usually regarded as precancerous and can develop into malignant structures. Colorectal adenomas can be classified based on the growth pattern as villous, tubular, or tubulovillous. A villous adenoma comprises over 75% villous features and extended leaf- or finger-like surface projections (Taherian et al., 2023). Conversely, tubular adenomas mainly consist of tubular glands and comprise<25% of villous structures (Taherian et al., 2023). Tubulovillous adenomas include tubular glands and villous structures in significant proportions. While multiple cases of all three adenomas have

been reported, tubular tumors are the most common, accounting for 80% of CRC incidence (Taherian et al., 2023). However, villous adenomas are most likely to become cancerous mainly because they occupy the largest surface area. Nonetheless, after adjusting for surface area, all adenomas have a similar potential to progress to cancer.

### *2.9.2 Adenocarcinoma*

Colorectal adenocarcinoma is a cancerous stage of tumor development and accounts for over 90% of colorectal carcinomas (Fleming *et al.*, 2012). Conventional adenocarcinoma features glandular formation, the premise of histologic tumor classification. According to Fleming *et al.* 2012, >95% of the tumor is gland forming in well-differentiated adenocarcinoma. Contrarily, the gland formation is 50-95% for moderate differentiation and <50% for poor differentiation (Fleming *et al.*, 2012). Moderately differentiated colorectal adenocarcinomas, illustrated in Figure 6, are most prevalent in practice, accounting for ~70% of cases (Fleming *et al.*, 2012). Conversely, the prevalence is 10% for well-differentiated adenocarcinomas and 20% for poorly differentiated varieties (Fleming *et al.*, 2012). Moreover, >95% of colorectal adenocarcinomas originate from intestinal polyps, and up to 9.4% of adenomas develop into malignant lesions in about ten years (Taherian et al., 2023). However, the adenoma-adenocarcinoma interval is contingent on the adenoma's pathological type, morphological attributes, and size.

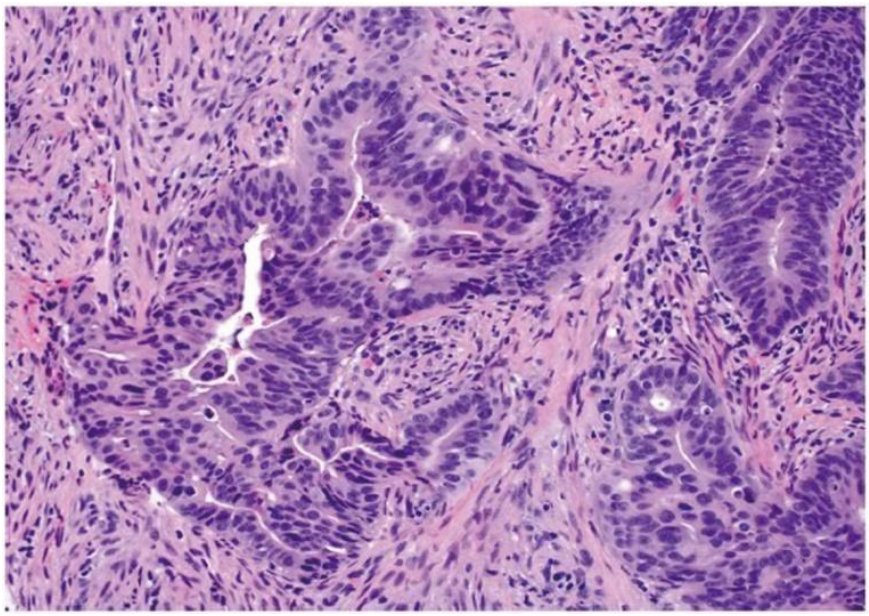

*Figure 6: An example of moderately differentiated colorectal adenocarcinoma (H&E stain, magnification ×200).Source: Fleming et al., 2012*

### *2.9.3 Colorectal Carcinoma in situ*

Carcinomas often develop in colorectal adenomas displaying carcinoma in situ (CIS) or high-grade dysplasia (HGD). This possibility led to the Vienna classification, which categorizes colorectal adenomas as low-grade dysplasia (LGD), HGD, and CIS.

**LGD:** These adenomas exhibit mild to moderate dysplasia. Moreover, the affected epithelium is covered with spindle-shaped, relatively uniform hyperchromatic nuclei with regular membranes (Rubio & Delinassios, 2010). The layered nuclei do not develop beyond the inner half of the epithelium, and the chromatic particles are quite minute.

**HGD:** These adenomas feature severe dysplasia, whereby the epithelium is covered with moderately pleomorphic, hyperchromatic, spindle-shaped nuclei (Rubio & Delinassios, 2010). Furthermore, the nuclear membrane is regular, while the chromatin particles are irregular. Unlike LGD, the layered nuclei also develop beyond the epithelium's superficial half and can affect the luminal epithelial boundary.

**CIS:** These adenomas exhibit marked pleomorphic cells with swollen round- or oval-shaped nuclei. Moreover, the nuclei feature bridges of angular chromatic components that reach the nucleolus-associated chromatin. The nucleus also has a ≥2.5 μm diameter, a notched

nuclear membrane, and an irregular shape (Rubio & Delinassios, 2010). Atypical mitosis is also present, and nuclear polarity is typically disrupted (Rubio & Delinassios, 2010). Furthermore, the adenomas feature glandular changes comprising branching or budding crypts and tubules. The glands are also normally obliquely arrayed to the basement membrane.

**2.10 Role of NF-κB in Cancer**

As illustrated in Figure 7, NF-κB is a transcription factor comprising five subunits: p100/p52 (NF-κB2), p105/p50 (NF-κB1), RelB, p65 (RelA, NF-κB3), and Rel (cRel). The NF-κB fundamentally regulates cell activity via marginal differences in binding NF-κB dimers to specific sequences. Research suggests that the NF-κB pathway

typically changes in hematopoietic and solid malignancies, fostering tumor-cell proliferation and survival (Xia *et al.*, 2018). More recent evidence also suggests that the NF-κB has a tumor-suppressive function in various cancers, primarily by transcriptionally activating the Fas ligand (Xia *et al.*, 2018). While the underlying processes are diverse and complex, they can be generalized based on whether they involve inflammation.

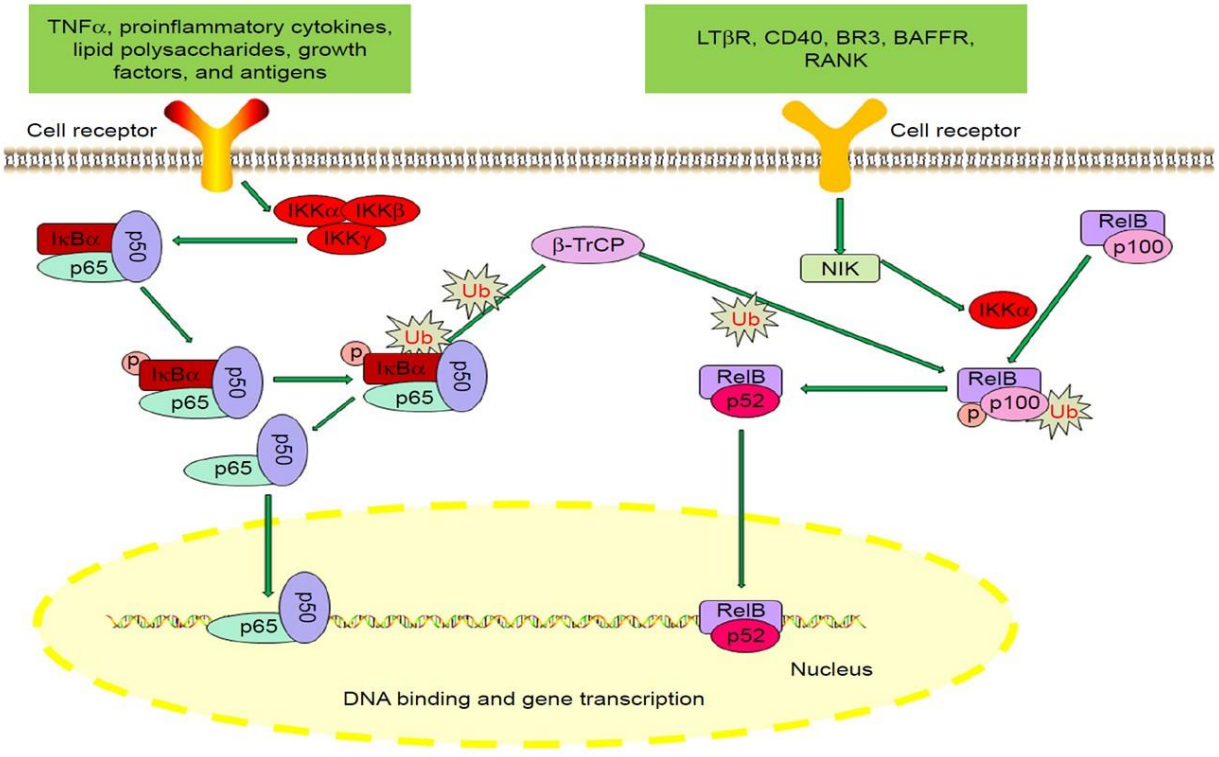


*Figure 7: The structure of NF-κB members (Source: Xia et al., 2018)*

### *2.10.1 The Anti- and Pro-inflammatory Effects of NF-κB*

NF-κB mediates the linkage between inflammation and cancer in several instances. In malignant tissues with excessive NF-κB activity, pro-inflammatory cytokine accumulation at a tumor site results in a pro-tumorigenic microenvironment (Xia *et al.*, 2014). For instance, the immune cells permeating gastrointestinal mucosa in individuals with inflammatory bowel disease secrete pro-tumorigenic cytokines like Il-17 and IL-1 (Xia *et al.*, 2014). These effects result in amplified NF-κB activity and an elevated risk of colon cancer. Moreover, such inflammatory signals may activate epigenetic processes that adjust let-7 tumor suppressor microRNAs (miRNAs) (Xia *et al.*, 2018). The IL-6/STAT3 may also be controlled, resulting in a positive feedback loop that initiates cancer and instigates uninhibited cell proliferation (Xia *et al.*, 2014). Many more possible relationships between NF-κB, inflammation, and cancer have also been reported. For example, in the study conducted by Xia et al. (2014), NF-κB activation triggers cytidine deaminase expression, resulting in mutations to cellular genes like p53. This mechanism was observed in multiple human cell lines, including breast cancer (MCF-7, T47D), cervical cancer (HeLa), and embryonic kidney (HEK293) cells, where NF-κB signaling was directly shown to upregulate APOBEC3B transcription. The elevated enzymatic activity was associated with an increased mutational burden in tumor suppressor genes, such as TP53. (Xia *et al.*, 2014). Therefore, there is a direct connection between increased NF-κB activity, and the chronic inflammation associated with the onset and progression of different cancers.

### *2.10.2 Additional Effects of NF-κB*

NF-κB influences the development of cancer through additional factors other than inflammation. For example, NF-κB instigates cell proliferation and inhibits apoptosis by stimulating anti-apoptotic gene expression, such as the Bcl2 group of apoptosis regulators (Xia *et al.*, 2014). Furthermore, NF-κB facilitates tumor metastasis at various levels, such as by strongly controlling cell adhesion molecules like integrins and the associated ligands. These

molecules foster cancer cell extravasation and progression to distant tissues and organs (Xia et al., 2014). Lastly, NF-κB reshapes tumor metabolism to ensure adequate energy supply to cancerous cells. To prove this premise, researchers have demonstrated that NF-κB activation in p53−/− mouse embryonic fibroblasts amplify glucose uptake (Xia *et al.*, 2014). These effects confirm the significant role of the NF-κB in the onset and development of different cancers, including CRC.

### *2.10.3 Role of the CARD11 Gene*

The Caspase Recruitment Domain Family Member 11 (*CARD11*) gene is a critical bridge between antigen detection and the downstream NF-κB activation in lymphocytes. Gain-of-function mutations in this gene can instigate constitutive NF-κB activity and the proliferation of invasive B-cell lymphocytes (Shi *et al.*, 2021). This process can result in lymphatic lymphomas, such as large B-cell lymphoma. Positive *CARD11* expression is also strongly linked with inferior event-free survival. Conversely, *CARD11* depletion often causes an anti-tumor effect through systemic autoimmunity inhibition (Shi *et al.*, 2021Specifically, its overexpression in renal cell carcinoma is associated with reduced patient survival (Tian *et al.*'s (2024)). The methylation of the CARD11 gene body directly increases its expression, as observed in kidney renal cell carcinoma (KIRC) and lung adenocarcinoma (LUAD) (McGuire *et al.*, 2021). Although it directly activates the canonical NF-κB pathway, it also stimulates the mTOR pathway, leading to decreased autophagy and increased tumorigenesis (McGuire *et al.*, 2021). These relationships indicate that methylation typically increases oncogene expression during tumorigenesis and tumor progression in epithelial cancers like CRC. Therefore, investigations targeting *CARD11* could provide early insights into possible CRC development in patients.

## 2.11 Proposed Strategies to Detect CRC

CRC is still an active research area, with extensive scientific interest in the solutions for early detection and increasing survival rates. Biomarkers for CRC detection are among the

main points of interest in building highly sensitive and specific non-invasive CRC diagnosis methods. These markers can be generalized as stool, blood, and molecular types. Furthermore, several CRC cell lines have been characterized, and their feasibility for scientific assays targeting different biomarkers has been investigated extensively. This section reports some of the main findings obtained in recent years.

### *2.11.1 Stool Biomarkers*

Stool-based molecular diagnostics are based on the secretion, exfoliation, or leakage of CRC biomarkers into stool. The leakage is typically due to the tumor growth's disturbance of vessels and blood along the digestive tract. The possibility of having significant proportions of tumor markers in stool has motivated the development of several standard and innovative assays.

Researchers have developed multiple innovative stool-based tests to replace fecal occult blood assays. In their review of literature, Gonzalez-Pons and Cruz-Correa (2015) generalize the main proposals as DNA-, RNA-, and stool protein-based assays(Gonzalez-Pons and Cruz-Correa 2015). Fecal occult blood tests are among the most used diagnostic methods for CRC. Fecal occult blood tests are generally classified as guaiac-based (gFOBT) and immunochemical (iFOBT). Meklin *et al.* (2020) investigated the comparative performance of iFOBT and gFOBT, finding iFOBT superior to gFOBT. Specifically, iFOBT can achieve 86% sensitivity and 85% specificity, while gFOBT attains 68% sensitivity and 88% specificity (Meklin *et al.*, 2020). However, both assays are limited in that colorectal bleeding is often intermittent. Furthermore, blood tests are not specific for human pseudoperoxidase and may detect blood from different gastrointestinal sites (Gonzalez-Pons & Cruz-Correa, 2015).

### *2.11.2 Blood Biomarkers*

CRC-specific antigens in blood have received extensive research attention over the years. Despite the vast studies spanning decades, only two notable blood-based biomarkers are available for clinical use: carcinoembryonic antigen (CEA) and carbohydrate antigen 19-9

(CA19-9) (Gonzalez-Pons & Cruz-Correa, 2015). The sensitivity and specificity of these biomarkers for CRC detection are also relatively low compared to other maladies like pancreaticobiliary malignancies (Gonzalez-Pons & Cruz-Correa, 2015; Thomsen *et al.,* 2018). Thus, researchers are actively investigating innovative blood-based biomarkers, including cell-free nucleic acids, genetic and epigenetic alterations, proteins, and tumor cells. According to Loktionov (2020), SEPT9 methylation detection offers the best CRC detection performance among all DNA-based approaches. However, its application is limited to opportunistic diagnoses, and the requisite DNA methylation is highly laborious. Moreover, the sensitivity and specificity are low, limiting the diagnostic potential. miRNAs have been proposed as potential substitutes for DNA biomarkers, with promising results(Loktionov 2020). For example, Ng *et al.* (2017) report 97.8% specificity and 96.6% sensitivity for miR-19-3p, which is downregulated in CRC(Ng, Wan et al. 2017). However, Loktionov (2020) argues that these findings and their clinical relevance are yet to be confirmed.

### *2.11.3 Tumor Biomarkers*

Several molecular tests targeting different biomarkers have been implemented in clinical practice over the years. According to Gonzalez-Pons and Cruz-Correa (2015), the main conventional biomarkers include MSI, KRAS mutations, and BRAF mutations. Evrard *et al.* (2019) compiled evidence of the diagnostic performance of MSI testing, finding 67-100% sensitivity and 61-92% specificity for the Bethesda panel and 89-100% sensitivity and 79%-100% for the pentaplex panel(Evrard, Tachon et al. 2019). Conversely, KRAS mutational assays attain an average of 77% sensitivity and 87% specificity (Ye *et al.*, 2021). Conversely, the BRAF gene is the KRAS' immediate downstream effector in the Ras/Raf/MAPK signaling pathway (Gonzalez-Pons & Cruz-Correa, 2015). Colling *et al.* (2016) also illustrate that the Idylla BRAF test achieves 96% specificity and 100% sensitivity(Colling, Wang et al. 2016). These findings confirm the argument for the superior performance of tests targeting tumor biomarkers. Molecular approaches to classify tumors are rapidly evolving with the

improving knowledge of the processes and mechanisms instigating colorectal carcinogenesis. Some relatively well-researched markers include the CpG island methylator phenotype (CIMP) and RNA expression. These biomarkers achieve 96% specificity and 59.63% sensitivity (Ghatak *et al.*, 2022).

### *2.11.4 CARD11 as a Biomarker*

*CARD11* is considered a potential predictive marker for early CRC, although conforming studies are limited. Liu *et al.* (2024) suggest that the gene is involved in the role of gut microbes in CRC development. BCL10, a gut microbe-related biomarker (GMRB) and part of the CARD family, is strongly involved in inflammatory response mediation. Specifically, it interacts with the mucosa-associated lymphoid tissue lymphoma translocation protein 1 (*MALT1*) and *CARD11* to create the *CARD11-BCL10-MALT1* complex, generally referred to as the CBM complex (Liu *et al.*, 2024). This complex is activated downstream of TCR and BCR signaling in T and B cell cells, triggering the MAPK and NF-κB pathways. This chain of events results in a strong phenotypic response. For example, NF-κB hyperactivation enables the chemokine microenvironment's tumor-specific reprogramming, which initiates the production of anti-CRC effects. Roseburia intestinalis in the gut also generates butyrate, which may directly bind the surface receptors on T cells, resulting in the CBM complex-based initiation of the NF-κB signaling. This outcome may result in CD8 T cell activation. These findings suggest that the aberrant CBM activity derived from *BCL10* mutations is a crucial factor in several maladies, including CRC. However, the specific applicability to CRC has not yet been studied in detail, and the sensitivity and specificity are only speculative.

Lu *et al.* (2021) examined the biological implications of *CARD11* deficiency to infer the potential roles in disease and carcinogenesis. They studied two patients with similar pathogenic biallelic loss-of-function *CARD11* variants that instigated undetectable protein expression. The findings indicate that this variant inhibits CBM complex formation, extensively constraining MALT1, c-Jun N-terminal kinase, and NF-κB activity in T and B cells.

These adverse effects directly result in suboptimal circulating T follicular helper cell development and B cell development constraints at the type 1 transitional and naïve B cell phase. Consequently, antibody responses are impaired, and germinal center units on lymph node histology become missing. Collectively, these findings illustrate that *CARD11*¬-dependent signaling is integral for the immune signaling pathways associated with B and T cell development(Lu, Sharma et al. 2021). While these insights are not specific to CRC, they provide background information on the potential roles of *CARD11* and the CBM complex in carcinogenesis. Additional studies specific to CRC could transform the gene into a reliable predictive biomarker for early CRC and treatment response.

Lenz, Davis et al. 2008 investigated the role of *CARD11* in diffuse large B cell lymphoma (DLBCL). This study is relevant to CRC since B cell lymphoma of the colon is among the most prevalent forms of colon cancer. After sequencing the gene's coiled-coil domain exon in DLBCL samples, the authors found missense substitutions impacting amino acids in 9.6% of the cases. The findings also indicate that *CARD11* amplification has a 23% prevalence rate and is associated with substantially low overall survival. This conclusion demonstrates the potential part of *CARD11* gene amplification in carcinogenesis. Furthermore, the researchers found that while *CARD11* mutations do not strongly correlate with NF-κB activity, there is a significant association between NF-κB activation and *CARD11* amplifications. Moreover, *CARD11* protein expression is strongly associated with AKT activation. These findings can be leveraged to develop predictive diagnostics and targeted cancer therapy to modulate NF-κB activity(Lenz, Davis et al. 2008).

Dong *et al.* (2011) present results supporting these conclusions. They find significant recurrent somatic mutations in ABIN-1, ABIN-2, A20, and *CARD11*, with *CARD11* having the highest mutation level. However, while *CARD11* mutants are potent in vitro activators of the NF-κB pathway, only ABIN-1, ABIN-2, and A20 impair normal functions. These results suggest that *CARD11* mutations may not be as detrimental as *CARD11* amplifications,

reiterating the findings of Bu *et al.* (2012). Nonetheless, more research is required to determine the specific applicability of *CARD11* and similar genes to diagnosing and treating early CRC.

Wei *et al.* (2019) also assesses the association between *CARD11* mutations and immunodeficiencies associated with abnormal NF-κB and the underlying role in the development of diseases like CRC. The authors used three genetic mouse models to meet this objective: *CARD11* E134G point mutation depicting BENTA disease, *CARD11* knockout representing immunodeficiency, and a model holding an oncogenic K215M mutation. Comparisons of the models indicated that *CARD11* retains a noncanonical role in negatively regulating the SKT-FOX01 signal axis. However, this function is separate and independent from NF-κB activation. The results also illustrate that E134G mutant mice phenotypically mimic *CARD11* knockout individuals. Specifically, the E134G mutation increases SKT activation and disrupts FOXO1 proteins in B cells. Conversely, the K215M mutation has relatively more robust inhibitory implications on AKT activation and a more stable FOXO1. Similarly, K215M and E134G mutants have converse implications on B cell differentiation and development. These results indicate that *CARD11* impacts not only the NF-κB pathway but also the FOXO1 and AKT signaling pathways(Wei, Zhang et al. 2019). Thus, the gene can be a feasible predictive biomarker for several maladies, including CRC.

Researchers have presented the feasibility of *CARD11* as a marker for different cancers, illustrating the possible extension to CRC. For example, Tian *et al.* (2024) demonstrate that the gene can act as a therapeutic biomarker for clear cell renal cell carcinoma (ccRCC) drug therapies. Specifically, the authors show that *CARD11* is upregulated in ccRCC mainly because of body methylation. Furthermore, *CARD11* expression in the tumor microenvironment is positively associated with elevated T lymphocyte infiltration and high inhibitory immune checkpoint expression. These effects suggest that *CARD11* knockdown suppresses the invasion, migration, and proliferation of cancer cells and increases the cells' apoptosis(TIAN, CHEN et

al. 2024).

Si, Lin et al. 2021 also reports that *CARD11* changes can be used as a biomarker of skin cutaneous melanoma under immune checkpoint blockade. The authors report that *CARD11*- mutant (MT) tumors feature elevated immunogenicity and significantly downregulated immunosuppression-related gene expression. Furthermore, immune activation-associated pathways are upregulated, while immunosuppression-associated pathways are downregulated. The tumors also feature extensive damage response and repair pathway mutations and DNA damage response(Si, Lin et al. 2021). These findings suggest that *CARD11* can be targeted as a predictive marker for immune checkpoint inhibitor efficacy in cancer patients.

#### *2.11.5 Summary*

The reviewed literature provides an in-depth examination of the multifaceted nature of colorectal cancer (CRC), with a particular focus on its epidemiology, pathogenesis, and progression. CRC represents a significant global health concern, with sporadic cases comprising the majority compared to hereditary instances. The adenoma-carcinoma sequence remains central to disease development, highlighting pivotal molecular pathways, including chromosomal instability (CIN), microsatellite instability (MSI), and serrated neoplasia. Mutations in key genes, including APC and BRAF, initiate tumorigenesis, while emerging evidence implicates additional genes such as FAM123B, SOX9, ARID1A, and POLE, underscoring the complexity of CRC pathophysiology.

Epidemiological trends indicate an increasing incidence and mortality rates of CRC globally, with particularly pronounced growth projected in regions such as Asia and the United Arab Emirates. Established risk factors encompass genetic syndromes, dietary patterns—such as high intake of processed meats and alcohol—lifestyle choices including tobacco use, and pre-existing conditions like adenomatous polyps and inflammatory bowel

disease. Early-stage CRC is often asymptomatic, which contributes to delayed diagnoses and suboptimal survival outcomes in specific populations. Recent advancements in screening, imaging, and molecular diagnostics have markedly improved early detection and patient prognoses. The current therapeutic paradigm integrates surgical intervention, chemotherapy, radiotherapy, immunotherapy, and targeted molecular agents. Furthermore, the literature details the distinct histological classifications and grading systems for CRC, ranging from benign adenomas to invasive adenocarcinomas. It emphasizes the considerable heterogeneity observed in disease presentation and progression.Importantly, molecular mechanisms, notably the NF-κB signaling pathway and CARD11 gene expression, are identified as critical contributors to CRC initiation and progression. These mechanisms establish key connections among inflammation, immune regulation, and genetic alterations influencing tumor behavior. CRC can be diagnosed non-invasively using either stool, blood, or molecular (tumor) biomarkers. Stool-based tests are based on the premise of the leakage of biomarkers into the colon lumen after the disturbance of blood vessels by tumor growth. However, this process is often not continuous and manifests in neoplastic lesions, resulting in the leaked markers' low sensitivity and specificity. Secreted and exfoliated markers from colonocytes, such as proteins, RNA, and DNA, can improve CRC prediction performance. However, available research is still inconsistent, limiting translation into evidence-based practices. Blood biomarkers are considered more reliable than stool biomarkers, but extensive large-scale studies are still needed to translate current knowledge into effective clinical strategies. Furthermore, most candidate blood biomarkers proposed in literature are only detectable in advanced CRC stages. Researchers present molecular biomarkers as potential predictive markers for CRC, with sensitivity and specificity close to 100%. However, many potential molecular markers are poorly understood and are the subject of ongoing research.

Of the proposed biomarkers, the *CARD11* gene appears to be particularly promising. Existing evidence indicates various *CARD11* roles in carcinogenesis. For example, *BCL10*

mutations instigate aberrant CBM complex activity that may instigate CRC. Furthermore, *CARD11*-dependent signaling impacts the immune signaling pathways associated with B and T cell development. *CARD11* amplifications and mutations also cause notable changes in the NF-κB, FOXO1, and AKT signaling pathways, potentially resulting in carcinogenesis. Therefore, *CARD11* is a feasible target for additional research on developing predictive biomarkers for early CRC. Future studies should investigate the comparative role of *CARD11* mutations and amplifications on carcinogenesis. Collectively, these insights underscore the need for ongoing research to refine CRC prevention, diagnostic modalities, and therapeutic strategies.

### 2.12 Colorectal Cancer Cell Lines

Tumors that are well differentiated tend to be less aggressive and grow more slowly. Undifferentiated or poorly differentiated cancer cells look and behave very differently from normal cells in the tissue and tend to be more aggressive (Jogi et al, 2012). As part of this study, we used two colorectal carcinoma cell lines to identify the cellular pathways modulated by the dysregulation of *CARD11*. HCT116 is an aggressive cell line with the KRAS mutation that does not differentiate, whereas HT29 with p53 mutation shows an intermediate ability to differentiate, making it less aggressive than HCT116 (Yeung et al., 2010).

### 2.13 Theoretical Framework

This thesis is grounded on the hallmarks of cancer proposed by Hanahan and Weinberg (2011), which refer to the biological capabilities acquired during tumorigenesis. These hallmarks, including sustained proliferative signaling, evasion of growth suppressors, resistance to cell death, and tumor-promoting inflammation, provide a comprehensive lens to examine *CARD11*'s role in CRC. In particular, the study leverages the tumor microenvironment (TME) framework and its interplay with inflammatory pathways, particularly the NF-κB signaling pathway, which is critical in modulating immune responses, promoting chronic inflammation, and driving cancer progression (Xia *et al.*, 2018). *CARD11*,

a key mediator in NF-κB activation, represents a molecular link between immune modulation and tumor development. Furthermore, the thesis applies systems biology principles to analyze transcriptomic changes induced by *CARD11* overexpression. Whole transcriptome profiling and bioinformatics analysis are used to identify affected cellular pathways, such as chromatin remodeling, chemotaxis, and immune signaling, aligning with the dynamic nature of cancer as a disease of genetic and epigenetic alterations. The TME framework contextualizes the study of *CARD11*'s role in CRC and provides a foundation for identifying novel biomarkers and therapeutic targets.

### 2.14 Gaps in the Literature

Biomarkers for early CRC detection and therapeutic interventions define a currently open search area. While several blood and stool-based tests are available, assays targeting molecular biomarkers should establish the future state-of-the-art CRC diagnosis. *CARD11* is an ideal predictive marker, owing to its association with the immune signaling pathways associated with B and T cell development, CBM complex activity, and NF-κB, FOXO1, and AKT signaling pathways. However, current understanding of *CARD11 in CRC progression* is limited, and few studies have explored its diagnostic and therapeutic potential.This deficiency creates a significant gap in CRC diagnosis research. Moreover, while many CRC cell lines are available for studying potential biomarkers, HCT116 and HT-29 appear particularly reliable. However, the specific role of CARD11 in these cell lines remains largely unexplored. This thesis aims to address these gaps by investigating the role of *CARD11* as a predictive marker for early CRC detection and progression.

### 2.15 The Research Questions

The overarching aim of the study was to elucidate how *CARD11* overexpression influences CRC progression, particularly through its modulation of the NF-κB pathway and its impact on the tumor immune microenvironment. Nine research questions were formulated to guide the research and meet this goal:

1. How does *CARD11* overexpression impact mRNA and protein levels in CRC cell lines (HCT-116 and HT-29)?
2. Does overexpression of *CARD11* induce NF-κB activation in CRC cell lines?
3. What are the transcriptomic changes associated with *CARD11* overexpression in CRC cell lines?
4. Which cellular pathways are activated or suppressed due to *CARD11* overexpression, as revealed by gene set enrichment analysis?
5. How do transcriptomic profiles differ between adenoma and carcinoma patients with high and low *CARD11* expression?
6. Which key genes are associated with *CARD11* overexpression, and how can they be validated for their roles in CRC?
7. How does *CARD11* overexpression influence the immune cell characteristics in CRC cell lines and patient samples?
8. How do the distinct stages of CRC impact the characteristics of immune cells?
9. Which key genes are associated with distinct stages of CRC?

**2.16 Opportunities for Contributions to Knowledge**

The compiled insights from the literature review indicate that despite the extensive research on CRC pathogenesis, limited studies explore the transcriptomic effects of *CARD11* overexpression or its specific contributions to NF-κB signaling in CRC. Thus, this thesis should contribute to existing knowledge by confirming the importance of NF-κB in cancer-related inflammation, particularly elucidating the mechanistic role of *CARD11*'s in activating downstream pathways and reshaping the tumor immune microenvironment. More specifically, the study should identify the cellular pathways and key gene networks influenced by *CARD11* overexpression and offer insights into the dynamic transition between early and advanced CRC stages, revealing potential stage-specific biomarkers. These contributions should expand existing knowledge by elucidating novel molecular mechanisms

underpinning *CARD11*'s involvement in CRC, identifying actionable biomarkers for early detection, and highlighting potential therapeutic targets to modulate NF-κB signaling.

# Chapter III:

# Methodology

## 3.1 Introduction

The study employed a comprehensive methodological framework to investigate the role of *CARD11* in CRC cell lines, aiming to elucidate its impact on gene expression and pathway activation. Using HCT-116 and HT-29 cell lines, the research integrated cellular and molecular biology techniques, including transfection, RNA extraction, quantitative RT-PCR, and Western blot analysis, to examine *CARD11* overexpression and its influence on NF-κB activation via dual luciferase assays. Advanced RNA sequencing and bioinformatics tools, such as DESeq2 and Gene Set Enrichment Analysis (GSEA), were leveraged to identify differentially expressed genes (DEGs) and enriched pathways. Functional insights were further validated through Metascape clustering, Kaplan-Meier survival analysis, and immune cell profiling using CIBERSORTX. Additionally, archival CRC tissue samples were analyzed using IHC staining to explore *CARD11*-associated molecular signatures, contributing to a robust understanding of its biological and clinical significance in CRC progression and immune regulation.

## 3.2 Cell Culture

Two CRC cell lines, HT29 and HCT116, were obtained from Bio Medical Scientific Services (BiOMSS, Al Ain, UAE) and cultured in RPMI 1640, supplemented with 10% fetal bovine serum (Sigma Aldrich, St. Louis, USA) and 1% Penicillin/Streptomycin (Sigma). The cultures were maintained at 37°C in a 5% CO2 atmosphere. Table 1 provides the detailed characteristics of HCT116 (Staging "TNM"= T3N1M1) and HT29 (Staging "TNM"= T2- 3N1M0) cells. For

subculturing, the cells were rinsed twice and then incubated with Dulbecco's phosphate-buffered saline (PBS) (Sigma; D8537). They were treated with Trypsin/EDTA solution (Sigma; T4299) for 3-5 minutes at 37°C. After this incubation, trypsin activity was neutralized by adding one volume of trypsin inhibitor (Sigma; T6522) and three volumes of complete cell culture medium. The cells were then collected and centrifuged at 1,200 rpm for 5 minutes at 4°C. Finally, the supernatant was discarded, and the cells were re-suspended in a fresh, complete medium before being seeded at the required density.

Table *1: The characteristics of the HT29 and HCT116 cell lines*

| Cell line | HCT116 | HT29 |
|---|---|---|
| Age | 48 yrs | 44 yrs |
| Origin | Colon ascending | Colon |
| Disease | Colorectal adenocarcinoma | Colorectal adenocarcinoma |
| Stage | Duke's D | Duke's C |
| MSI status | MSI | MSS |
| QMP Panel 11 | + | + |
| QMP Panel 12 | + | + |
| QN | - | + |
| KRAS | G13D | wt |
| BRAF | Wt | V600E |
| PK3CA | H1047R | P4491 |
| PTEN | Wt | wt |
| TP53 | Wt | R273H |
| ERBB2 | Wt | wt |

*Sourced: from ATCC and Mutations in several genes; KRAS, BRAF, PIK3CA, PTEN, TP53 (Ahmed, Eide et al. 2013), and ERBB2 (Jang, Jung et al. 2019).*

### 3.3 FFPE Tissue Specimens from Endoscopic Biopsies of CRC Patients

This study included ten patients with tubular adenoma and, 24 patients with primary CRC (adenocarcinoma), and 8 with carcinoma in situ from the American Hospital Dubai and the University Hospital Sharjah. Table 4 illustrates the participants' key characteristics. The ethical approval for the study was obtained from the Dubai Scientific Research Ethics Committee (DSREC), Dubai Health Authority (DSREC-SR-02/2023_07), and the Research and Ethics Committee of the University Hospital Sharjah (UHS-HERC-055-25022019). The research methods and experiments were conducted based on the respected guidelines of the

Declaration of Helsinki and the Belmont Report. The primary diagnosis was performed to determine and score tumors, lymph nodes, and metastasis under the supervision of two pathologists (K.S. and R.H).

*Table 2: Patient characteristics for the 42 biopsies collected from adenoma ,and adenocarcinoma and carcinoma in situ patients in the UAE*

| No. | Gender | Age | Nationality | Subtype |
|---|---|---|---|---|
| 1 | Male | 61 | Italian | Tubular Adenoma |
| 2 | Male | 61 | Qatari | Tubular Adenoma |
| 3 | Male | 54 | Emirati | Tubular Adenoma |
| 4 | Male | 61 | Emirati | Tubular Adenoma |
| 5 | Female | 39 | Italian | Tubular Adenoma |
| 6 | Male | 75 | Indian | Tubular Adenoma |
| 7 | Female | 64 | British | Tubular Adenoma |
| 8 | Male | 48 | Portuguese | Tubular Adenoma |
| 9 | Female | 51 | Emirati | Tubular Adenoma |
| 10 | Male | 50 | South African | Tubular Adenoma |
| 11 | Female | 77 | Emirati | Adenocarcinoma |
| 12 | Female | 83 | Syrian | Adenocarcinoma |
| 13 | Female | 45 | Emirati | Adenocarcinoma |
| 14 | Male | 92 | Emirati | Adenocarcinoma |
| 15 | NA | 80 | Iraqi | Adenocarcinoma |
| 16 | Female | 53 | Slovakia | Adenocarcinoma |
| 17 | Female | 52 | Emirati | Adenocarcinoma |
| 18 | Male | 69 | Emirati | Adenocarcinoma |
| 19 | Male | 75 | Sudanese | Adenocarcinoma |
| 20 | Female | 68 | Emirati | Adenocarcinoma |
| 21 | Male | 76 | Emirati | Adenocarcinoma |
| 22 | Female | 70 | Emirati | Adenocarcinoma |
| 23 | Female | 80 | Lebanese | Adenocarcinoma |
| 24 | Female | 59 | French | Adenocarcinoma |
| 25 | Female | 43 | Filipino | Adenocarcinoma |
| 26 | Male | 56 | Swiss | Adenocarcinoma |
| 27 | Female | 64 | Emirati | Adenocarcinoma |
| 28 | Female | 38 | Iraqi | Adenocarcinoma |
| 29 | Female | 44 | Sudanese | Adenocarcinoma |
| 30 | Female | 32 | Emirati | Adenocarcinoma |
| 31 | Female | 65 | Egyptian | Adenocarcinoma |
| 32 | Male | 77 | Indian | Adenocarcinoma |
| 33 | Male | 84 | Syrian | Adenocarcinoma |
| 34 | Female | 65 | Egyptian | Adenocarcinoma |
| 35 | Male | 70 | Romanian | Carcinoma in situ |
| 36 | Female | 80 | Emirati | Carcinoma in situ |
| 37 | NA | NA | NA | Carcinoma in situ |
| 38 | Male | | Filipino | Carcinoma in situ |
| 39 | Female | | Emirati | Carcinoma in situ |
| 40 | Male | | Emirati | Carcinoma in situ |
| 41 | Female | | Egyptian | Carcinoma in situ |
| 42 | | | record does not exists? | Carcinoma in situ |

### 3.4 LB agar plates and LB broth preparation

A 35g/L (Sigma; L2897) concentration of LB Agar mixture was produced and autoclaved to dissolve. After that, 100 g/mL of ampicillin was dissolved in the LB agar solution, and the LB agar solution was then added to sterile tissue culture plates and left to form a gel. Once fully gelled, the LB agar plates were parafilm-sealed and kept upside-down at 4°C for two weeks. Before usage, the plates were warmed up in an incubator at 37°C. LB broth was generated by mixing 25g/L of LB broth powder (Sigma; L3522) with water and autoclaving it to dissolve. Finally, 100g/mL of ampicillin was dissolved in the LB agar solution. The LB broth was kept at 4°C before usage.

### 3.5 Bacterial Transformation

The pcDNA3 plasmid was used in the study. It was amplified using One ShotTM TOP10 Chemically Competent *E. coli* (Invitrogen; C404010) (Addgene plasmid # 89130; http://n2t.net/addgene:89130; RRID: Addgene 89130). By gently tapping, 100ng of plasmid DNA was gently mixed with the competent bacteria in a bottle. The plasmid-bacteria mixture was incubated under ice for 20 minutes, then exposed to a 30-second heat shock at 42°C, followed by another 20 minutes of ice-based incubation. After re-suspension in 250µL of SOC medium (Invitrogen; 15544034), the transformed bacteria were incubated at 37°C in an orbital shaker for 1 hour at 225rpm. 100µL from the vial was streaked over preheated LB agar plates and incubated at 37°C overnight. Five distinct colonies were injected into 5mL of the ampicillin-LB broth and grown overnight at 37°C in an orbital shaker.

A 200µL sample was aliquoted from each tube to determine whether the bacterial transformation was successful. Centrifugation was used to isolate the bacterial material, which was then resuspended in 30µl of PBS. The cells were heated at 100°C for 5 minutes in a heat block, followed by 5 minutes of centrifugation at 7500xg to lyse and collect the plasmid DNA. Consequently, the plasmid DNA extracted into the supernatant was analyzed by qRT-PCR to

verify the transformation. A successful transformation was carried out on one of the bacteria, which was grown in 50mL of ampicillin-LB broth and incubated at 37°C overnight in an orbital shaker.

### 3.6 Plasmid Extraction

Plasmid DNA was extracted from cells using the Plasmid Maxiprep System (Qiagen). A 2mL sample of cells was transferred into 500mL of LB medium containing ampicillin for selection. The cells were then pelleted by centrifugation at 6,000g for 15 minutes. Then, 10mL of Buffer P1 and 10mL of Buffer P2 were added to the pellet. The mixture was incubated at room temperature for 5 minutes. Next, 10mL of prechilled Buffer P3 was added and gently mixed until the solution became colorless. After incubating for 30 minutes, the mixture was centrifuged at 20,000g. The resulting supernatant was placed onto a QIAGEN tip. The QIAGEN-tip was washed with 60mL of Buffer QC. Finally, 15mL of MilliQ water was used to elute the DNA into a 50mL Falcon tube.

### 3.7 Transfection of CRC Cell Lines with *CARD11*

Overexpression was performed using *CARD11* cloned in pcDNA3.1 vector (OHu21225D) (GenScript, Piscataway, NJ, USA). Cells were seeded at $2 \times 10^5$ cells per well in 6-well plates the day before transfection. The DNA concentrations and the incubation time for optimal transfection were optimized for each cell line before the experiments. The HCT-116 and HT-29 cell lines were transfected with 1µg and 2µg of *CARD11* plasmid construct, respectively, using the advanced ViaFect transfection reagent (Thermo Fisher Scientific, Waltham, MA, USA). The transfection ratio was 3:1 (Viafect Transfection reagent: DNA). To compare the transfection efficiency, the cells of a 6-well plate were kept non-treated as a control, and the cells of a 6-well plate were treated only with ViaFect transfection reagent without adding the DNA as a mock. Cells transfected with the empty pcDNA3.1 vector were used as the experimental control. The *CARD11* expression level was checked at the 24$^{th}$ and 48$^{th}$-hour

post-transfection at the mRNA and protein levels using RT-qPCR and a Western blot, respectively.

### 3.8 RNA Isolation from Cell Lines

Cells, pelleted at $12\times10^3$g for 5 minutes and washed three times with ice-cold 1X sterile PBS, were used to extract RNA from cell lines. RNA was extracted from cell pellets using the PureLink RNA Mini kit (Invitrogen; 12183018A). For each sample, 600µl of the Lysis buffer, with freshly added 2-mercaptoethanol, was added and mixed well to spread the cell pellet. The cell pellet was then dissolved in 900µl of 100% ethanol, carefully mixed, and then transferred, 700µl at a time, to the provided Spin Cartridge. The samples were transferred to the column after a 15-second centrifugation at 12,000xg at room temperature. The columns were washed twice with 700µl of Wash Buffer I and 500µl of Wash Buffer II, and the RNA was eluted in 30µL of nuclease-free water. The NanoDrop 2000 spectrophotometer (Thermo Scientific, United States) was used to measure the amount of RNA.

### 3.9 Cell line RNA clean-up with Turbo DNAse

The TURBO DNA-free TM Kit (Invitrogen; AM1907) was used to remove any potential DNA contamination from cell line-derived RNA. Each RNA sample received 1µL of 10X Turbo DNAse Buffer and 0.1µL of Turbo DNAse. Following 20 minutes of incubation at 37°C, 1 volume of the DNAse Inactivation Reagent was added to the sample-DNAse mixture. After incubation for two minutes at room temperature, the samples were centrifuged at 10,000xg for 1.5 minutes. After that, the supernatant was gathered and kept at -80°C.

### 3.10 cDNA synthesis for samples extracted from cell lines

The High-Capacity cDNA Reverse Transcription Kit for RT-PCR (Applied Biosystems; 4374966) was used to create cDNA. The reverse transcription master mix for cDNA synthesis was formulated using 2µL of RT buffer, 0.8µL of dNTP mix, 3µL of RT random primers, 1µL of reverse transcriptase, and 4.2µL of nuclease-free water per sample. A Veriti 96 thermal

cycler (Applied Biosystems) was then used to reverse transcribe 100ng of template RNA with 10µl of the master mix. Specifically, the template was incubated at 25°C for 10 minutes and 37°C for 120 minutes, followed by inactivation through the heat at 85°C for 5 minutes. The samples were frozen at -20°C.

### 3.11 RNA Isolation from FFPE Samples

Three consecutive 3µm sections of the same FFPE block were used to extract RNA from tissue samples. A needle microdissection was done to increase the tumor content. Specifically, a sterile needle was used to carefully select and label the tumor areas from the slides, after which the marked areas were collected for molecular analysis.

RNA was extracted using the RNA RecoverAll kit (ThermoFisher Scientific, Cambridge, Massachusetts, USA). Using 100µL of the digestion buffer in the kit, the micro-dissected tumor area was retrieved from the PCR tube cap, and 4µL of protease was added, followed by gently swirling. The samples were then incubated for 15 minutes at 50°C and 10 minutes at 80°C, with gentle spinning every five minutes. Consequently, 275µL of 100% ethanol and 120µl of the Isolation Additive were added, and the resultant mixture was put into the Filter Cartridge. Using an Eppendorf® Centrifuge 5804/5804R, the mixture was centrifuged for 30 seconds at 10,000 rpm to pass through the filter. The filter was washed with 500µL of Wash solution 2/3 and 700µL of Wash solution 1. The RNA on the filter cartridge was treated with a DNAse master mix containing 6µL of 10X DNAse Buffer, 4µL of DNAse (provided by the kit), and 50µL of nuclease-free water for 30 minutes at room temperature to digest the DNA. Afterward, the filter was washed with 700µl of Wash 1 and 500µL of Wash 2/3. Nuclease-free water was applied to the filter cartridge, and after 5 minutes, the RNA was released from the filter by centrifugation. The amount of produced RNA was measured using a NanoDrop 2000 spectrophotometer (Thermo Scientific, United States).

### 3.12 FFPE RNA Clean-up with Zymo RNA Clean and ConcentratorTM-5 kit

The RNA samples were concentrated using the RNA Clean and ConcentratorTM-5 kit (Zymo Research; R1013). The samples were diluted to 50µL and mixed with 100µL of RNA binding buffer. After thoroughly mixing the RNA with 150µL of 100% ethanol (Honeywell; 24103), the samples were transferred to Zymo-Spin IC Columns and centrifuged at 13,000g for 30 seconds. After removal of the flow-through, 400µl of RNA Prep Buffer was added to the column and washed with the RNA Wash Buffer. The RNA samples were eluted with 6-12µl of nuclease-free water (Applied Biosystems; 901578) and stored at -80°C. The amount of RNA was measured using a NanoDrop 2000 spectrophotometer (Thermo Scientific, United States).

### 3.13 Immunohistochemistry staining of FFPE samples

Six samples each of adenoma, carcinoma in situ, and adenocarcinoma were sectioned to a thickness of 3 µm and placed on positively charged slides, which were then baked on a hot plate at 62°C for 30 minutes. The sections were deparaffinized by immersing them sequentially in Xylene-1 and Xylene-2 for five minutes each. Rehydration was performed by dipping the slides in a graded series of ethanol concentrations of 100%, 90%, 70%, and 50% for two minutes each. Antigen retrieval was completed using Tri-sodium citrate buffer (pH 6.0), heated in a microwave oven at 95°C for 15-20 minutes. After retrieval, the samples were cooled at room temperature for 20 minutes. The slides were then washed under running tap water for 10 minutes, rinsed with distilled water, and treated with 3% hydrogen peroxide for 30 minutes at room temperature. After washing with distilled water and performing three sequential PBS buffer washes of three minutes each, protein blocking was applied for 20 minutes. The blocking solution was drained, and 100µl of diluted *CARD11* primary antibody was added, incubating the slides overnight in a humidified slide tray. Following three additional PBS buffer washes of three minutes each, 100 µl of biotinylated secondary antibody from the HRP kit was added,

and the slides were incubated at room temperature for 30 minutes. After three more PBS buffer washes, 100µl of streptavidin peroxidase was applied, followed by a 20-minute incubation in a humidified slide tray. The slides were rewashed with PBS buffer three times, treated with DAB for four minutes, and washed under running tap water for five minutes. Counterstaining was performed with pre-diluted hematoxylin stain for two minutes, followed by rinsing under running tap water for five minutes and a distilled water rinse. The slides were then dehydrated by being immersed in a graded ethanol series (70%, 80%, 90%, and absolute ethanol) for five minutes each. Consequently, the slides were cleared in two changes of xylene for five minutes each and mounted with DPX. Finally, the slides were air-dried before microscopic examination.

### 3.14 *CARD11* Quantitative Reverse Transcriptase-PCR (qRT-PCR)

Complementary DNA (cDNA) was synthesized from total RNA using a High-Capacity Reverse Transcription Kit (Applied Biosystems, Waltham, MA, USA) that uses a random hexamer and oligo Dt mixture. Gene expression was determined by quantitative PCR (qPCR) using Maxima SYBR Green/ROX qPCR MasterMix (2×) (Thermo Fisher Scientific) on QuantStudio3 Real-Time PCR thermal cycler (Applied Biosystems). qPCR runs were performed using the primer sets presented in Table 2. The housekeeping gene (18S) was used to normalize the *CARD11* gene expression levels, and the fold change, which measures relative expression, was calculated using the Comparative Ct ($2^{-\Delta\Delta Ct}$) method(Livak and Schmittgen 2001). Following Thermo Fisher Scientific recommendations, the qRT-PCR cycling conditions were optimized using Maxima SYBR Green/ROX qPCR MasterMix (2×) and performed on a QuantStudio 3 Real-Time PCR thermal cycler. The reaction began with an enzyme activation and denaturation step at 95°C for 10 minutes. This was followed by 40 cycles of amplification, each consisting of a denaturation phase at 95°C for 15 seconds, following by an annealing/extension phase with 60°C for 30 seconds, during which fluorescence data were collected. After that, the samples were heated to 95°C for 15 seconds

and cooled to 60°C for 1 minute. Then the temperature increased to 95°C at a rate of 0.1°C per second, while continuously monitoring fluorescence to assess the specificity of the amplicons.

*Table 3: Sequence of primer pairs used in the qPCR*

| Gene ID | Forward Primer Sequence | Reverse Primer Sequence |
|---|---|---|
| *CARD11* | AGCGGGACAGCTACAATGAC | TGACCGCCATGTTCTC |
| 18S | TGACTCAACACGGGAAACC | TCGCTCCACCAACTAAGAAC |

### 3.15 Rapid Protein extraction assay for Western Blot

The HCT116 and HT29 cells were collected by removing the culture medium from the adherent cells. This was followed by trypsinization and then centrifugation at 1,100 rpm for 5 minutes, followed by two times of washing with phosphate buffer saline solution (PBS). Consequently, 50 µL of Triton X lysis buffer (50 mM Tris, 150 mM EGTA, 1% Triton-x100), 5 µL of protease inhibitor, and 30 seconds of pulse-and-hold sonication were used to lyse the cells. The samples were centrifuged for 10 minutes at 14,000 rpm at 4°C, and the supernatant was transferred into a fresh tube and stored at -20 °C until use.

### 3.16 Determination of Protein Concentration

Bovine Serum Albumin (BSA) from Thermo Scientific, along with the BCA assay kit for protein quantitation (also from Thermo Scientific), was used to determine the concentration of the isolated proteins. A total of nine BSA standards were prepared with concentrations of 0, 25, 125, 250, 500, 750, 1000, 1500, and 2000 µg/mL. Equal amounts of 1:20 dilutions of protein lysates were added in triplicate to a 96-well plate. To create the working reagent, a mixture with a ratio of 50:1 (Reagent A to Reagent B) was prepared by combining 50 parts of BCA Reagent A with 1 part of BCA Reagent B. This working reagent was added in volumes of 200 µL to each well. After a 30-minute incubation at 37 °C, the optical density was measured at a wavelength of 595 nm using spectrophotometry. The protein concentration was determined by fitting the absorbance data to the standard curve

generated from the BSA standards.

### 3.17 Gel Electrophoresis and Western transfer

A Lamilli buffer and 10% b-mercaptoethanol were used to dilute a 50µg lysate concentration, which was afterward incubated at 95° C for 5 minutes. Proteins were separated on a 10% sodium dodecyl sulphate polyacrylamide gel (SDS-PAGE) using the Bio-rad gel electrophoresis system. Protein samples and a pre-stained protein ladder were electrophoresed at 110 volts for 1.5 hours in a Tris-Base/Glycine/SDS running buffer. A transfer buffer was used to wash the gels, and a methanol-containing transfer buffer was used to soak the membrane. This process helped transfer the samples onto the nitrocellulose membrane (Bio-Rad). Three pieces of filter paper, gel, membrane, and three more pieces of filter paper were then combined into a transfer "sandwich" and put into the Bio-Rad Transblot Cell. Protein transfer was completed at 25 volts 1A for 30 minutes.

### 3.18 Immunoblotting

The gel was transferred to a 0.45 µm nitrocellulose membrane (Thermo Fisher Scientific) and blocked with 5% skimmed milk and 5% BSA from Sigma-Aldrich for 1 hour at room temperature. The membrane was then incubated overnight at 4°C with agitation using Anti-CARD11 (CARMA1) (Rabbit monoclonal, dilution 1:1000, ab124730, Abcam, Cambridge, UK). The β-actin antibody served as an internal control. After incubation, the blots were washed three times with 1x TBST washing buffer to remove any unbound antibodies. Following the washes, the blots were incubated with anti-rabbit IgG secondary antibody, diluted in the same blocking solution, for 1 hour at room temperature with agitation. After another set of three washes with 1x TBST, the blots were exposed to a Pierce ECL kit (Thermo Fisher Scientific) for 1 minute. Chemiluminescence was measured using a Gel Doc system (Bio-Rad), with β-actin used as the loading control.

### 3.19 Investigating the Effect of CARD11 Overexpression on NF-κB Activation Using Dual Luciferase Assay

The potential role of NF-κB activation via CARD11 was analyzed in vitro using a Luciferase Reporter Assay System (Promega, Southampton, UK) in HCT-116 and HT-29 cell lines. Briefly, cells were seeded at 5 × 104 cells per well in 24-well plates. Four different groups were used: an untransfected cell line as control and samples transfected with CARD11 expression vector, pNF-κB-luc (a Firefly luciferase re-porter for NF-κB activity-p65), and both CARD11 and pNF-κB-luc (p65) vectors. All groups were structured and transfected with pRL-TK (a Renilla luciferase reporter) which served as the internal control. The cells were harvested, washed with PBS, lysed, and assayed for luciferase activities using a GloMax Plate Reader(Promega).

### 3.20 Transcriptome Sequencing

A targeted Ampliseq Transcriptome panel on the Ion S5 XL System (ThermoFisher Scientific) was used for RNA sequencing. About 30 ng of Turbo DNase-treated RNA extracted from the both cell lines, and as well as the patient's samples were used for cDNA synthesis using the SuperScript VILO cDNA Synthesis kit (ThermoFisher Scientific). The Ion AmpliSeq gene expression core panel primers were used for amplification. Enzymatic shearing was performed using the FuPa reagent to obtain amplicons of ~200 bp, and the sheared amplicons were ligated with the adapter and unique barcodes. The prepared library was purified using Agencourt AMPure XP Beads (Beckman Coulter) and quantified using the Ion Library TaqMan™ Quantitation Kit (Applied Biosystems). The libraries were further diluted to 100pM and pooled equally. The pooled libraries were amplified using emulsion PCR on the Ion OneTouch™ 2 instrument (OT2), and the enrichment was performed on the Ion OneTouch™ ES. Finally, the prepared template libraries were sequenced with the Ion S5 XL Semiconductor sequencer using the Ion 540™ Chip.

### 3.21 RNA-Seq Data Analysis

RNA-seq data analysis was performed using the Ion Torrent Software Suite version 5.4. To align the raw sequencing reads generated by Ion Torrent sequencing against the reference sequence from the hg19 (GRCh37) assembly.. The Torrent Mapping Alignment Program (TMAP) was utilized, and the specificity and sensitivity were maintained by implementing a two-stage mapping approach by employing BWA-short, BWA-long, SSAHA (Ning *et al.*, 2001), Super- Maximal Exact Matching (Li, 2012), and the Smith-Waterman algorithm (Smith *et al.*, 1981) for optimal mapping. The raw read counts of the targeted genes were normalized using the Fragments Per Kilobase Million (FPKM) normalization method.

Principal component analysis (PCA) was applied to the samples using the R statistical software (version 4.2.0). DEG analysis was performed using the DESeq2 R/Bioconductor package with raw read counts from the RNA sequencing data to identify the DEGs in each comparison of cell lines with *CARD11*-transfected against cell lines with empty vector-transfected (Ritchie *et al.*, 2015; Love *et al.*, 2014). This process was also applied in the study of adenoma versus carcinoma. Genes with fewer than ten read counts were excluded from further analyses. A $p < 0.05$ significance level was used to select DEGs close to noise, prioritizing sensitivity in detecting probable biological signals, focusing mainly on genes associated with the inflammation and immune response . An unadjusted threshold was applied to avoid strict filtering, which could eliminate biologically relevant genes, especially those with moderate expression changes. To improve the robustness of the findings, subsequent downstream gene set enrichment analysis (GSEA) was conducted to refine the DEG selection based on pathway-level significance, providing additional biological validation.

### 3.22 Gene Set Enrichment Analysis

The significant DEGs obtained were further analyzed to identify the activated and

enriched cellular pathways in response to *CARD11* overexpression compared to empty vector-transfected cell lines using the absGSEA, as previously described by Hamoudi *et al.* (2010). AGSEA was performed on expression data using around 90,000 annotated cellular pathways obtained from the Broad Institute's database (https://www.gsea-msigdb.org) and custom pathways. Table 3 illustrates the characteristics of the gene sets used from the MSigDB 138

database. The GSEA was carried out separately for all resulting gene sets from the above- mentioned transcriptomic analyses, including CRC patients, CRC cell lines, normal colon cell lines, and BC patients. First, absolute GSEA was performed to identify the significantly enriched pathways among sets related to the three groups: C2 (curated gene sets); C5 (ontology gene sets including molecular function (MF) and biological process (BP)); C6 (oncogenic signature gene sets), and C7 (immunologic signature gene sets). The results of the AGSEA were ranked and selected according to the nominal p-value ($p < 0.05$) as described in past studies (Subramanian, Tamayo et al. 2005, Hamoudi, Appert et al. 2010). The selected significant pathways were further analyzed to identify the differentially enriched genes and the leading-edge genes

in each pathway. A systematic cross-reference of each gene enriched within statistically significant pathways was carried out to further reduce the resulting genes. Finally, the genes with the highest frequency across the multiple significant pathways enriched between the *CARD11* positive and *CARD11* negative samples were identified.

*Table 4: Gene sets used from the MSigDB database and their characteristics*

| **Gene Sets Used** | **Type** |
|---|---|
| C1 | Positional Gene Sets |
| C2 | Curated Gene Sets |
| C3 | Regulatory-Related Gene Sets |
| C4 | Computational Gene Sets |
| C5 | Gene Ontology Gene Sets (Biological Processes, Molecular Functions, and Cellular Components) |
| C6 | Oncogenic Related Gene Sets |
| C7 | Immunology-Related Gene Sets |
| C8 | Cell type Signature Gene Sets |

### 3.23 Functional Enrichment Analysis by Metascape

Functional clustering and pathway analysis of the common DEGs or frequently occurring genes were performed using Metascape (http://metascape.org) based on the guidance of Zhou *et al.* (2019). To validate the pathways identified using GSEA, the frequently occurring genes across all gene sets were subjected to Metascape analysis.

### 3.24 Validation of Genes Related to *CARD11* Overexpression in CRC

Survival analysis was completed by using the Kaplan–Meier Plotter (kmplot.com/analysis/) to create the overall survival (OS) curves for some of the key genes identified after GSEA analysis of *CARD11*– and *CARD11*+ samples for both adenoma and carcinoma. *IL6ST*, *GLI3* genes for adenoma and MAPK8IP2, and *CPEB4* genes for carcinoma were included in the analysis.

### 3.25 Exploration of Immune Cell Characteristics

Cell-Type Identification by Estimating Relative Subsets of RNA Transcripts (CIBERSORTX) (https://cibersort.stanford.edu), created by Newman *et al.* (2015), is a deconvolution algorithm based on RNA-seq data that allows for accurate quantification of the relative levels of immune cells classified according to their types in a complex gene expression mixture. The CIBERSORTX algorithm determines a p-value that indicates the statistical significance of the deconvolution results across all cell subsets and indicates the degree of confidence in the results (Newman *et al.*, 2015). It also uses gene expression signatures consisting of approximately 500 genes. We applied the original CIBERSORTX gene signature file termed LM22, which contains 547 genes and distinguishes 22 human hematopoietic cell phenotypes, including 7 T cell types, naïve and memory B cells, plasma cells, NK cells, and myeloid subsets. Normalized gene expression data of the *CARD11*-transfected and empty vector-transfected samples for each cell line and the *CARD11*– and *CARD11*+ samples for both adenoma and carcinoma were uploaded to the CIBERSORTX web portal. This methodology

was also employed in the adenoma versus carcinoma study.

### 3.26 Methodology Overview

Figure 8 summarizes the project methodology.

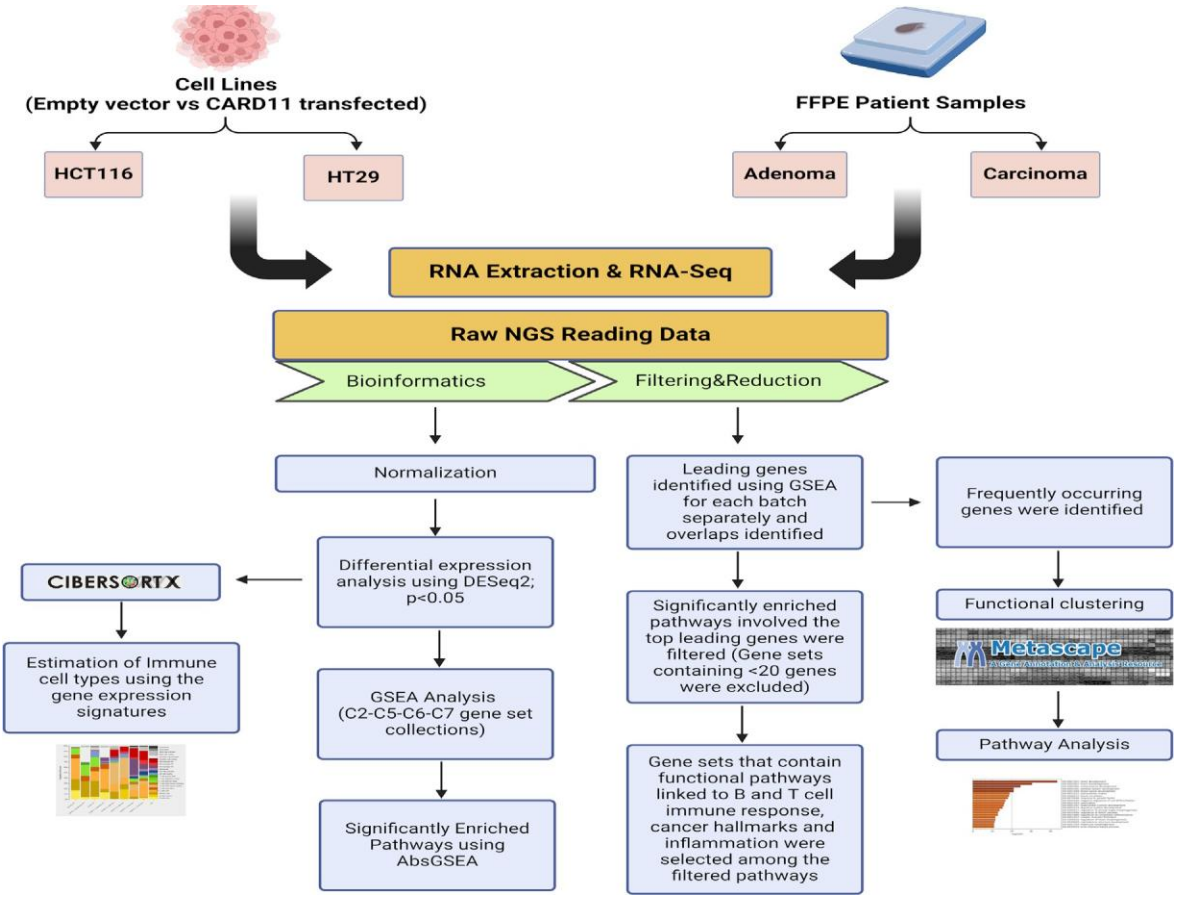


*Figure 8: Flowchart outlining the steps of the bioinformatics approach used to identify differentially expressed genes in CARD11-transfected to empty vector-transfected cell lines and CARD11– to CARD11+ in patient samples. The figure was created using BioRender*

# Chapter IV.

# Results of the *CARD11* Study

## 4.1 Overexpression of *CARD11* in the HCT-116 and HT-29 CRC Cell Lines Shows a Correlation between mRNA and Protein Levels

We aimed to determine if ectopic overexpression of *CARD11* in CRC cell lines induces genome-wide transcriptional changes. Well-differentiated tumors tend to be less aggressive and grow more slowly. Undifferentiated or poorly differentiated cancer cells look and behave very differently from normal cells in the tissue and tend to be more aggressive (Jogi *et al.*, 2012). As part of this study, we used two human colorectal adenocarcinoma cell lines—HCT116 (ATCC® CCL-247™) and HT29 (ATCC® HTB-38™)—to investigate the cellular pathways modulated by CARD11 dysregulation. HCT116 cells are derived from a male patient and exhibit an undifferentiated, epithelial morphology with aggressive growth characteristics. In contrast, HT29 cells, isolated from a female patient, display features of enterocyte-like differentiation under specific conditions and form well-differentiated adenocarcinomas in vivo, suggesting a comparatively less aggressive phenotype.

(ATCC 2024, ATCC 2024)(Yeung *et al.*, 2010). HCT-116 and HT-29 were transiently transfected with either an empty pcDNA3 vector or *CARD11* expression construct. For the HT- 29 cell line, 48 h was shown to be sufficient transfection time, whereas 24 h was enough for the HCT-116 cell line. Successful transfection was confirmed using both RT-qPCR (Figure 9A) and a Western blot (Figure 9B). Compared to the empty vector, *CARD11* expression was 29,193 and 5043 folds higher in *CARD11* transfected HCT-116 and HT-29 cell lines, respectively (Figure 9A). In addition, the Western blot showed clear overexpression of *CARD11* compared to control and empty pCDNA3 transfection in both HCT-116 and HT-29 (Figure 9B). The results indicated that there is a correlation between *CARD11* mRNA and protein levels, confirming similar finding of *CARD11* in clear cell renal cell carcinoma.Tian *et al.*'s (2024)

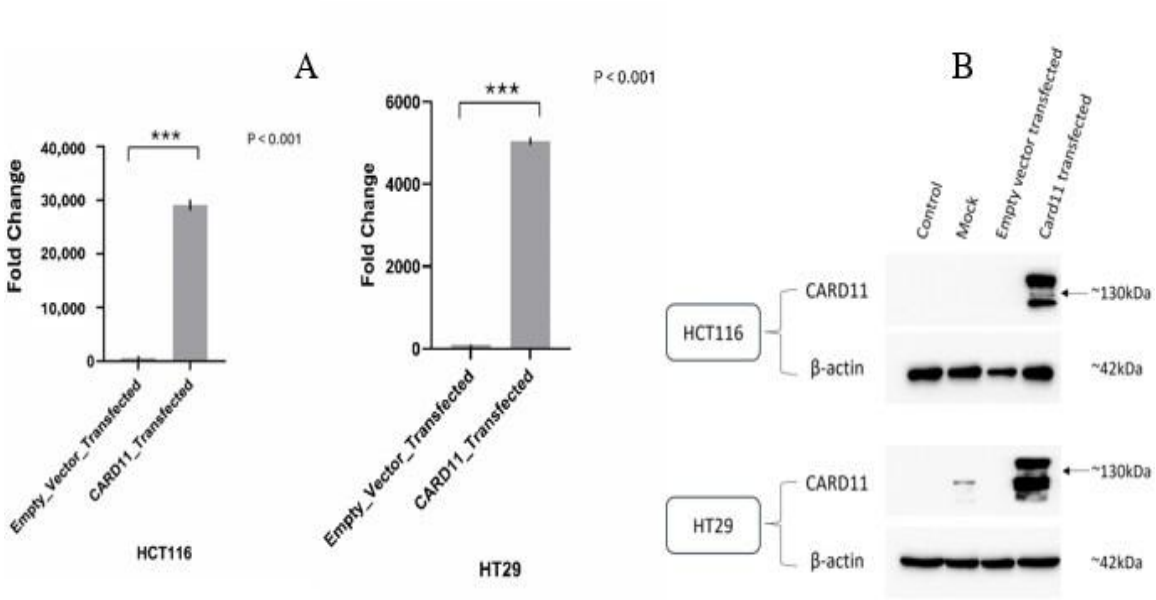


*Figure 9: Validation of successful overexpression of CARD11 in the CRC (HCT-116 and HT-29) cell lines. (A) CARD11 mRNA expression in empty pcDNA3 vector or pcDNA3-CARD11 transfected HCT-116 and HT-29 cells, as determined by qRT-PCR. Data were normalized to the expression of the housekeeping gene and the 18S rRNA gene, and fold expressions were plotted relative to expression in the empty vector-transfected (control). These data represent the mean ± SD of three independent experiments. *** $p < 0.001$. (B) Relative CARD11 protein expression was determined with a Western blot. Blots were probed with anti-β-Actin antibody as control, confirming equal loading across the lanes.*

### *4.2 CARD11* Overexpression Induces NF-κB Activation In Vitro

To determine whether *CARD11* overexpression influences NF-κB, a dual luciferase NF-κB reporter assay was used to test NF-κB activation in *CARD11*-overexpressed HCT-116 and HT-29 CRC cell lines. Results from three biological replicates indicated that endogenous NF-κB activation was not significant in both cell lines. However, the NF-κB pathway significantly increased ($p < 0.001$) with the overexpression of *CARD11* in both cell lines (Figure 10). *CARD11*-mediated activation of NF-κB in HCT-116 and HT-29 cells showed a significant increase of 34.1- and 73.3-fold, respectively.

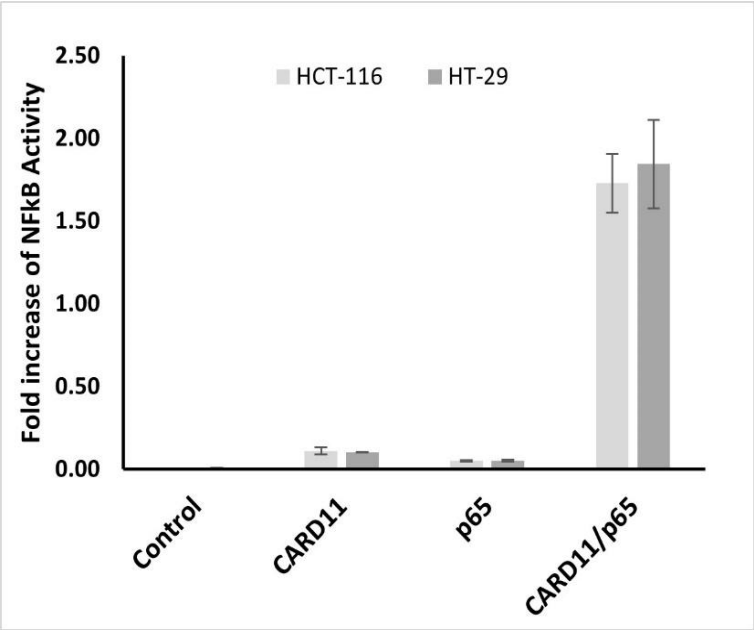


*Figure 10: CARD11 enhances NF-κB activation in HCT-116 and HT-29 cell lines. The cells were co-transfected with NF-κB-luc vector (with NF-κB luciferase reporter gene-p65) or CARD11 plasmid alone or together. LPS induction was undertaken for 6 h. NF-κB activation was measured in triplicate experiments and recorded as a fold increase in vector control*

### 4.3 Overexpression of *CARD11* Induces Distinct Transcriptional Profiles in CRC Cell Lines

As the dual luciferase assay (DLA) showed the potential role of *CARD11* in NF-κB activation, we further investigated the effect of *CARD11* overexpression on the transcriptomic level in both cell lines. RNAs extracted from HCT-116 and HT-29, expressing the empty pcDNA3 vector (control) and the *CARD11*-pcDNA3.1 chimera, were subjected to RNA-seq. As illustrated in Figure 11, PCA showed a clear separation between *CARD11* overexpressing and control samples in HCT-116 and HT-29 cells, confirming the reproducibility of the replicates and the unique transcriptomic profile associated with the overexpression of *CARD11*.

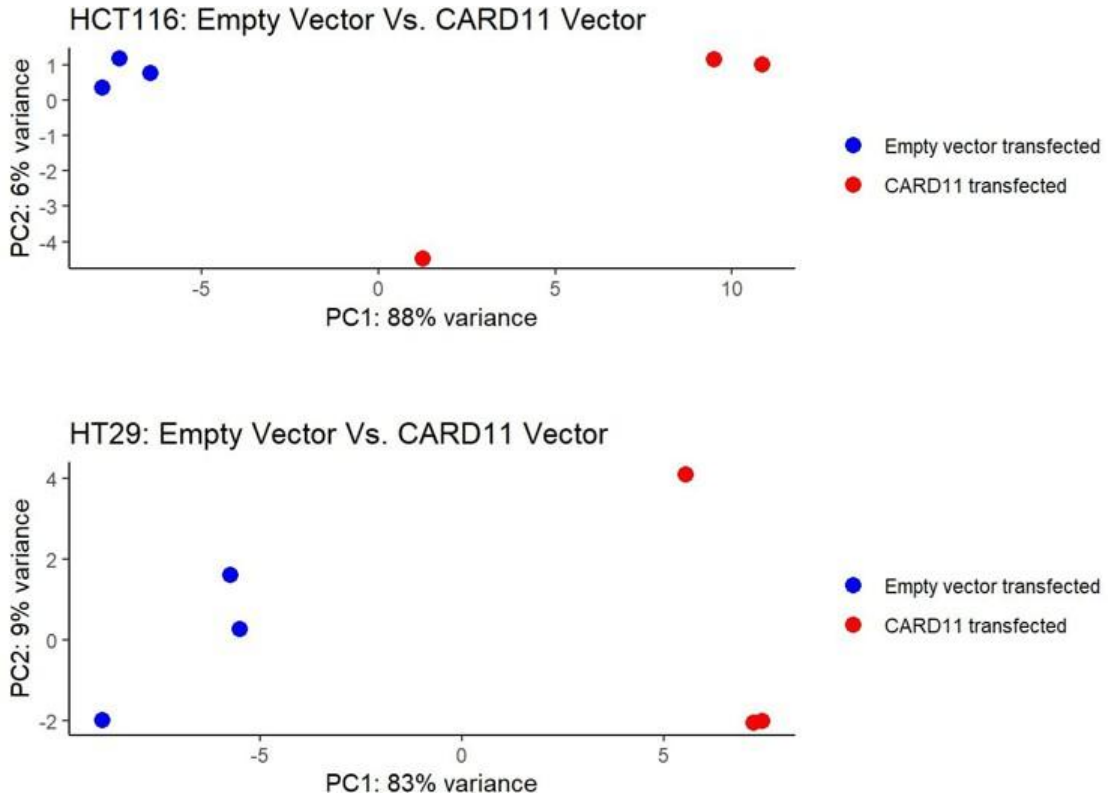


*Figure 11: Principal component analysis (PCA) showed a clear separation between CARD11 overexpressing and control samples in HCT-116*

RNA-seq results, summarized in Figure 12, showed that *CARD11* was significantly differentially expressed between empty vector-transfected (control) and *CARD11*-pcDNA3.1-transfected HCT-116 and HT-29. This finding validates the RNA-seq methodology, showing, as expected, that *CARD11* mRNA is overexpressed in *CARD11*-pcDNA3.1-transfected cell lines.

The differential gene expression analysis showed distinct gene expression profiles amongst *CARD11*-transfected HCT-116 and HT-29 cell lines compared to empty vector-transfected cell lines. Following normalization and filtering, a total of 2995 and 3118 differentially expressed genes (DEGs) were found in *CARD11*-transfected HCT-116 and HT-29 cell lines compared to the control, respectively. The volcano plots of differentially expressed genes are presented in Figure 13.

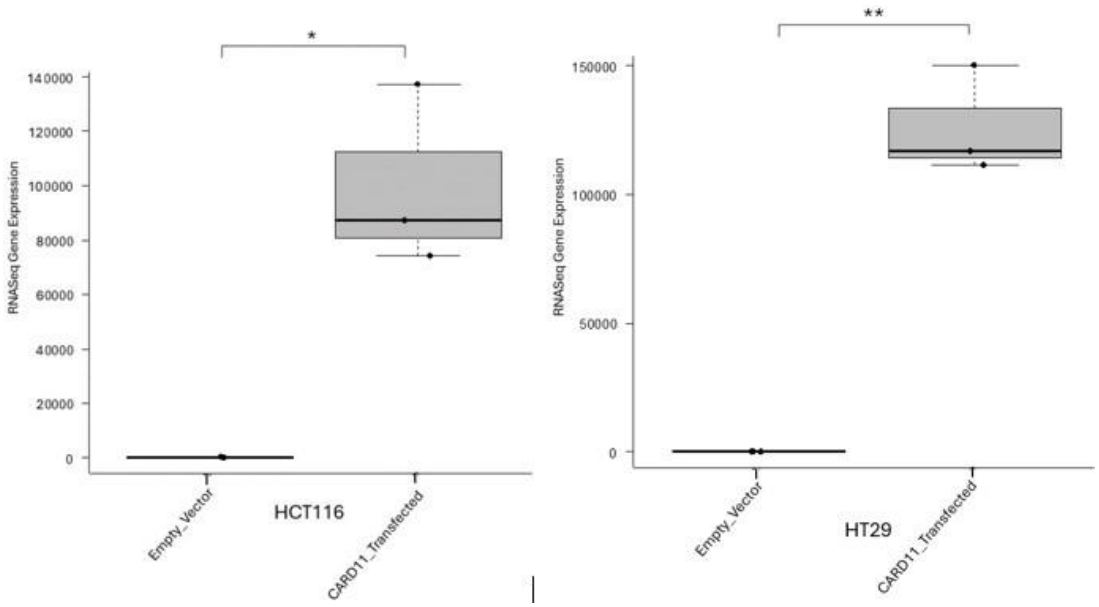


*Figure 12: RNA-seq results showed that CARD11 was significantly differentially expressed between empty vector-transfected (control) and CARD11-pcDNA3.1-transfected HCT-116 and HT-29.*

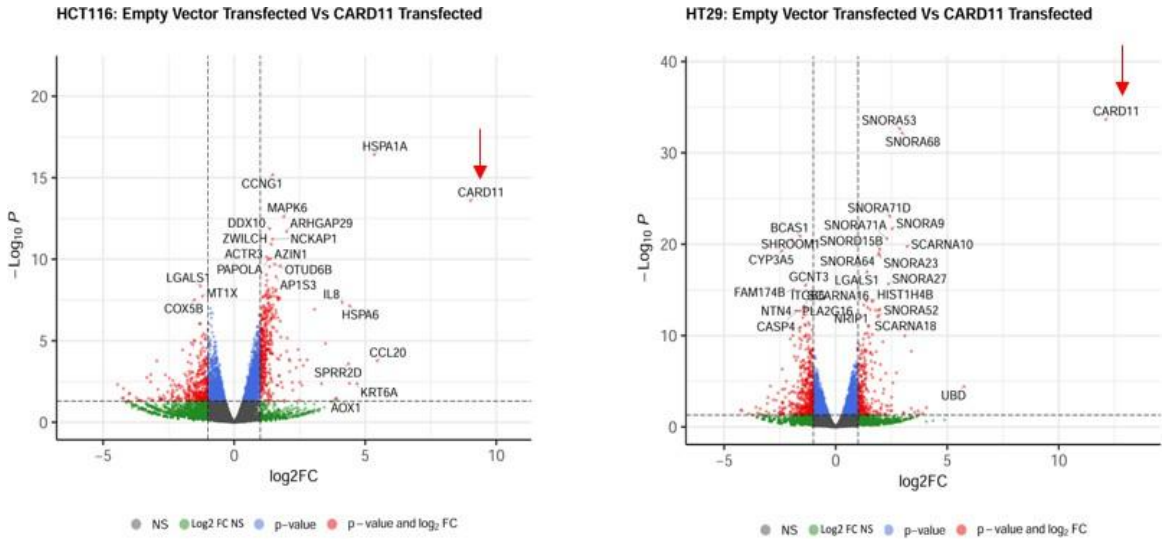


*Figure 13: Volcano plots of differentially expressed genes. Genes that are expressed significantly higher in either empty vector- or CARD11-transfected cell line based on log2-fold change $p < 0.05$ are highlighted by red dots, $p > 0.05$ are highlighted by green dots (Log2FC NS), unchanged transcripts are demarcated as grey (NS). The red arrows indicate that the CARD11 expression is significantly upregulated only in the CARD11-transfected cell lines*

### 4.4 GSEA of DEGs Revealed Distinctive *CARD11*-Mediated Activation of the Tumor Immune Microenvironment and Cancer-Related Cellular Pathways

To identify the activated and significantly enriched pathways in each comparison of *CARD11*-transfected vs. empty vector-transfected for both HCT-116 and HT-29, absGSEA was performed on the gene sets (C2, C5, C6, and C7) covering various pathways related to biological processes, and molecular functions, cancer hallmark, and immune response. The number of significantly enriched pathways derived from absGSEA in *CARD11* overexpressed vs. empty vector for both HCT-116 and HT-29 CRC cell lines are provided in Figure 14 as an upset plot graph. The figure shows a significant increase in the overall activation of pathways in HCT-116, particularly those related to immune responses. The number of enriched pathways in *CARD11*-transfected vs. empty vector-transfected for both cell lines in absGSEA is shown in Figure 14.

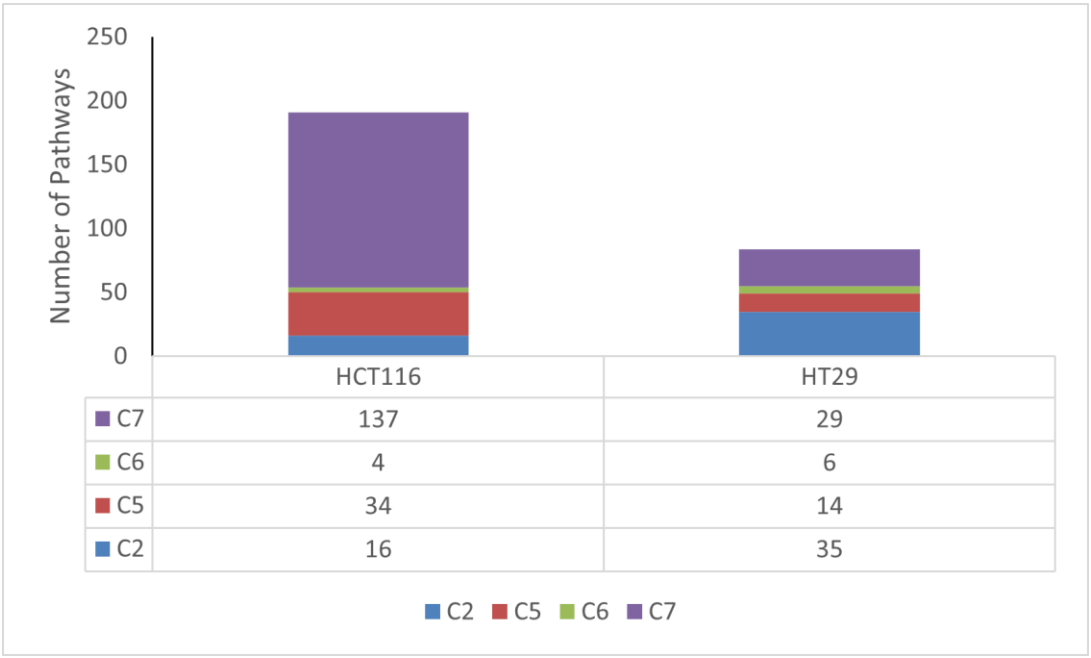


*Figure 14: An upset plot graph of the number of significantly enriched pathways that derived from absGSEA in CARD11 overexpressed vs. empty vector for HCT-116 and HT-29 CRC cell lines.*

Gene frequency was obtained by counting the number of times a gene occurred across all the different pathways. The genes were obtained from the significant number of enriched genes of the significant gene sets. This finding suggests that these genes are highly influential because

of the overexpression of *CARD11*. The leading-edge genes are represented by thehistograms in Figure 15. The top genes based on the gene frequency and significantly activated cellular pathways between *CARD11*- and empty vector-transfected CRC cell lines showed vital genes, including *EP300*, *STAT4, RB1*, and *HDAC2* for HCT-116 and *CXCL1*, *CXCL3*, *CCL22*, and *IL1RN* for HT-29. Among the top enriched genes, three (*HIF1A*, *NFKBIZ*, *DUSP1*) for HCT-116 (Figure 15A) and five (*CXCL1*, *CCL22*, *IL1RN*, *MDK*, *SPP1*) for HT-29 (Figure 15B)

were NF-κB-inducible genes, which is consistent with the dual luciferase assay experiment findings that showed the constitutive activation of NF-κB via *CARD11* expression. Among these five genes in HT-29, three of them (*CXCL1*, *CCL22*, *IL1RN*) were found in the top four of the frequently occurring gene list, indicating that HT-29 probably has more constitutive NF-κB activity than the HCT-116 cell line, again supporting the DLA findings.

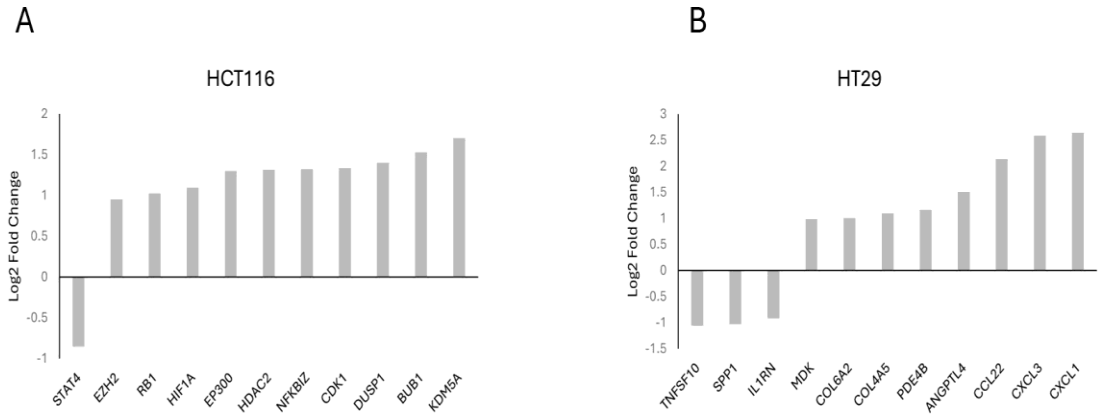


*Figure 15: Histogram of the selected leading-edge genes based on frequency in CARD11-transfected vs. empty vector-transfected HCT-116 (A), HT-29 (B) cell lines.*

### 4.5 Gene Set Enrichment Analysis on CRC Cell Lines Revealed Distinctive *CARD11*-Mediated Activation of Cellular Pathways Related to Cell Cycle, Apoptosis, Chromatin Remodeling, and Chemotaxis

Having identified frequently occurring genes for each group, significant pathways were selected from the list of pathways obtained from the absGSEA based on $p < 0.01$. Then, given that the key focus of the study was to define the putative role of *CARD11* in CRC pathogenesis, we chose gene sets that contained functional pathways especially linked to B- and T-cell immune responses, cancer hallmarks, and inflammation. Among the significant pathways, 40 gene sets for the HCT-116 cell line and 23 gene sets for the HT-29 cell line were selected, which were found to be related to B- and T-cell mediated immunity, cancer hallmarks, and inflammation.

The functional annotation of the top leading-edge genes showed highly significant enrichment of categories related to chromatin organization, cell cycle, and regulation of the apoptotic signaling pathway for the HCT-116 cell line, indicated using red arrows in Figure 17A. Absolute GSEA results revealed that a subset of chromatin modeling genes was over-represented in the *CARD11*-transfected HCT-116 cell line ($p < 0.001$, Figure 16B).

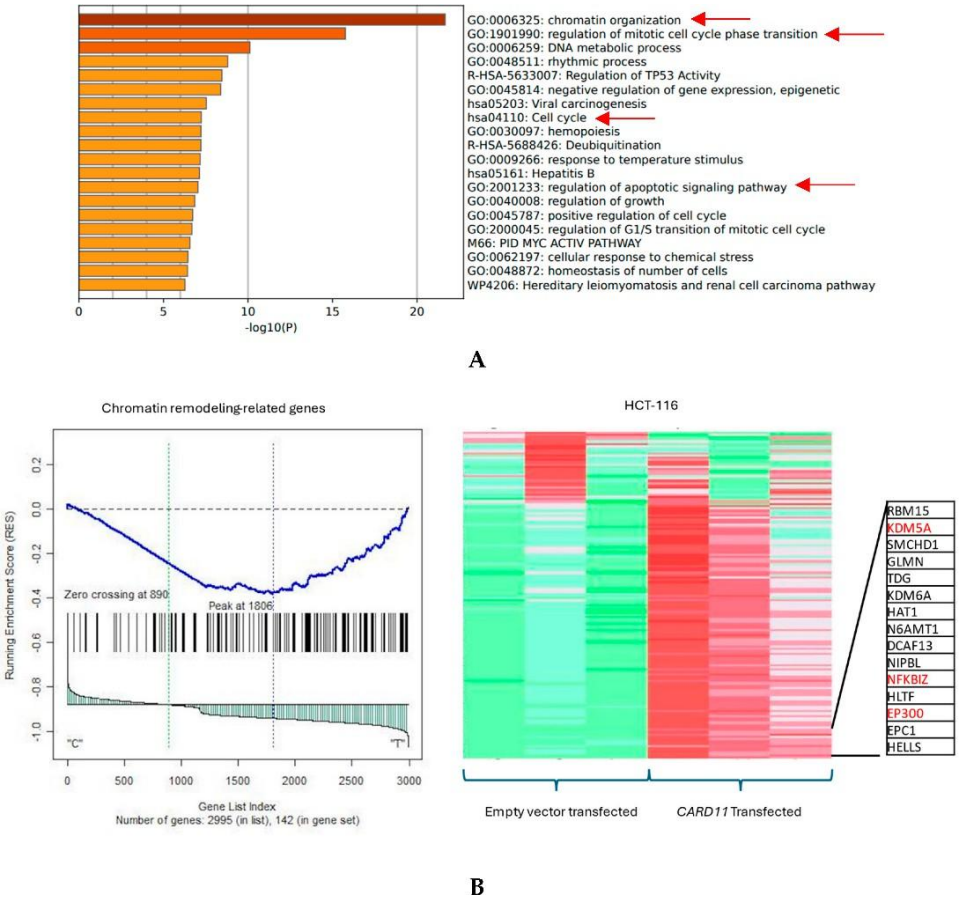


*Figure 16: (A) Significant enrichment pathways based on frequency in CARD11-transfected vs. empty vector-transfected HCT-116 cell line. Red arrows show the interest-enriched pathways in HCT-116. (B) Leading edge analysis showed that 82 core genes accounted for the significant enrichment in the CARD11-transfected HCT-116 cell line ($p < 0.001$). The top 15 leading-edge core genes are shown; the frequently found ones are indicated in red*

The functional annotation of the top leading-edge genes showed significant enrichment of categories related to extracellular matrix organization, chemotaxis, and programmed cell death for the HT-29 cell line (Figure 17A). The expression of a subset of ECM organization genes was over-represented in the *CARD11*-transfected HT-29 cell line, which is a hallmark of cancer (Figure 17B).

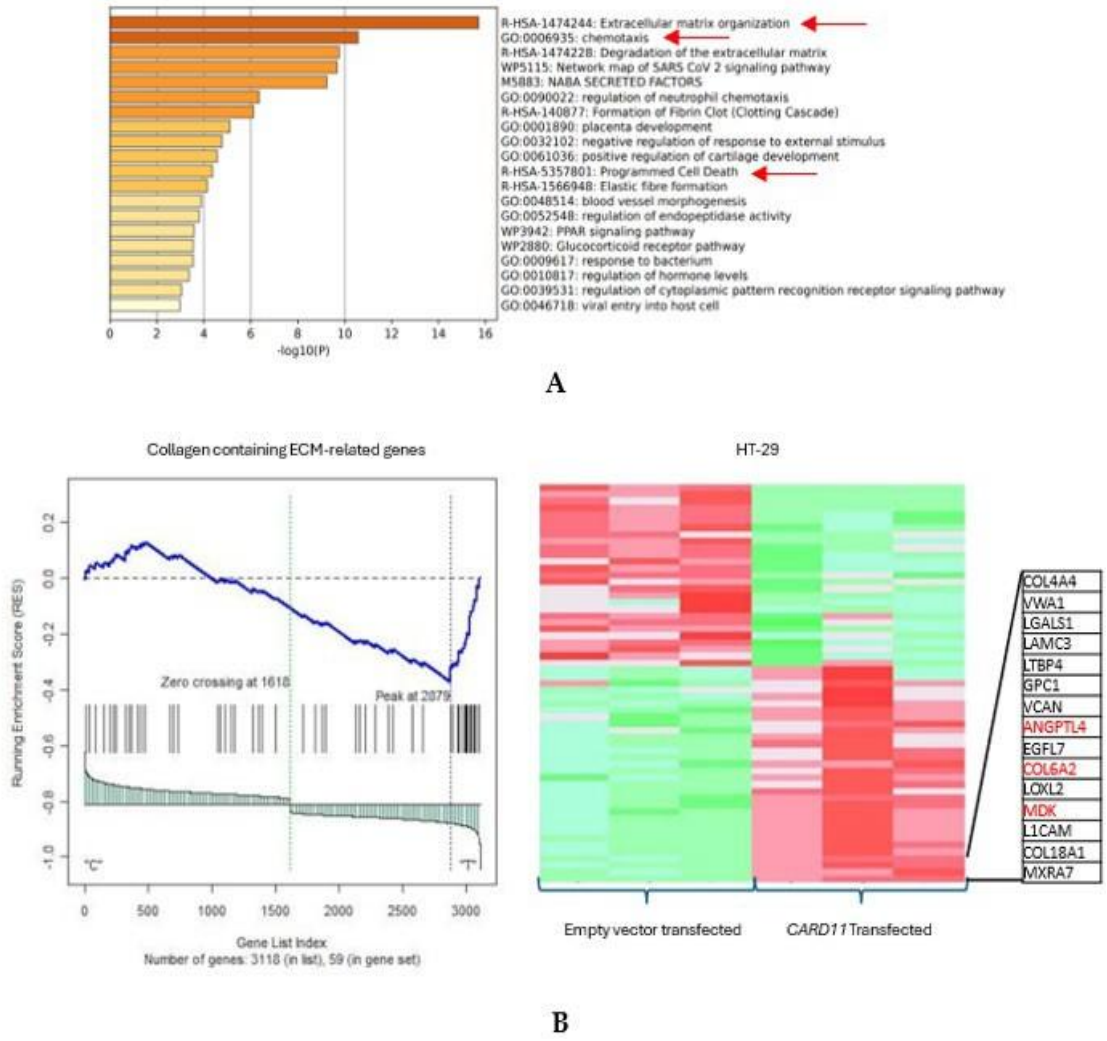


*Figure 17: (A) Significant enrichment pathways based on frequency in a CARD11-transfected vs. empty vector-transfected HT-29 cell line. The red arrows show the significant pathways involved in cancer progression (B). Leading edge analysis showed that 20 core genes accounted for the significant enrichment in the CARD11-transfected HT-29 cell line ($p < 0.001$). The top 15 leading-edge core genes are shown; the frequently found ones are indicated in red.*

#

Results from the GSEA and Metascape (for functional annotations) showed that *CARD11* is involved in regulating cancer-related pathways, including apoptosis, proliferation, cell cycle, and chromatin remodeling in the HCT-116 cell line. However, in the HT-29 cell line, *CARD11* seemed more involved with activating chemotaxis and extra-cellular matrix (ECM) pathways, which are seen in metastatic cancers, suggesting that perhaps HT-29 is possibly more invasive.

### 4.6 Transcriptional Profiling in CRC Patients Based on *CARD11* Differential Expression

We next examined the transcriptional patterns in human formalin-fixed, paraffin-embedded (FFPE) tissue specimens from CRC patients with variable expression levels of *CARD11*, as cell lines exhibit a homogenous system, and a two-dimensional culture might not be a true reflection of an actual tumor mass and its associated TME. To achieve this objective, we included only patients with tubular adenoma and patients with primary CRC (adenocarcinoma) in the study.

After RNA extraction, the whole transcriptome sequencing was conducted for 34 CRC samples. The stratification of patient samples to *CARD11*+ and *CARD11*− was determined by applying a median-centered cutoff (73) on the RNA-Seq data. Samples with values below the median cutoff were considered *CARD11*−, and those above the median cutoff were considered *CARD11*+. Based on the RNA-seq data, from the 34 samples ten adenoma and 13 carcinoma patients showed extreme expression of *CARD11* which were then identified as having either low *CARD11* expression (*CARD11*−) patients or having high *CARD11* expression (*CARD11*+). Among 10 adenoma, four samples were identified as having low *CARD11* expression (*CARD11*−), and six samples were identified as having high *CARD11* expression (*CARD11*+). Conversely, in 13 carcinoma samples, eight were identified as having low *CARD11* expression (*CARD11*−), and five were identified as having high *CARD11* expression (*CARD11*+).

PCA showed a slight admixture between the *CARD11*− and *CARD11*+, mostly likely due to the inherent intra-tumoral heterogeneity for adenoma (Figure 18) and carcinoma

(Figure19) patients' biopsies. In addition, RNA-seq results showed that *CARD11* had a higher trend in *CARD11*− compared to *CARD11*+ adenoma and was significantly differentially expressed in carcinoma patients (Figure 20)

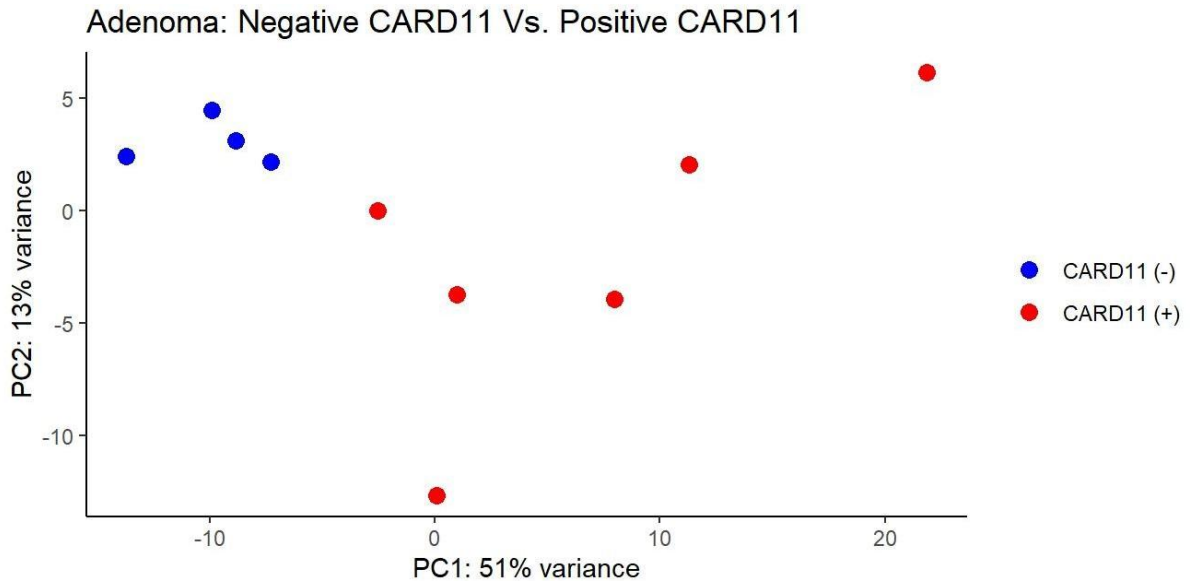


*Figure 18: Principal component analysis (PCA) showed a separation between CARD11+ and CARD11- among Adenoma cohorts.*

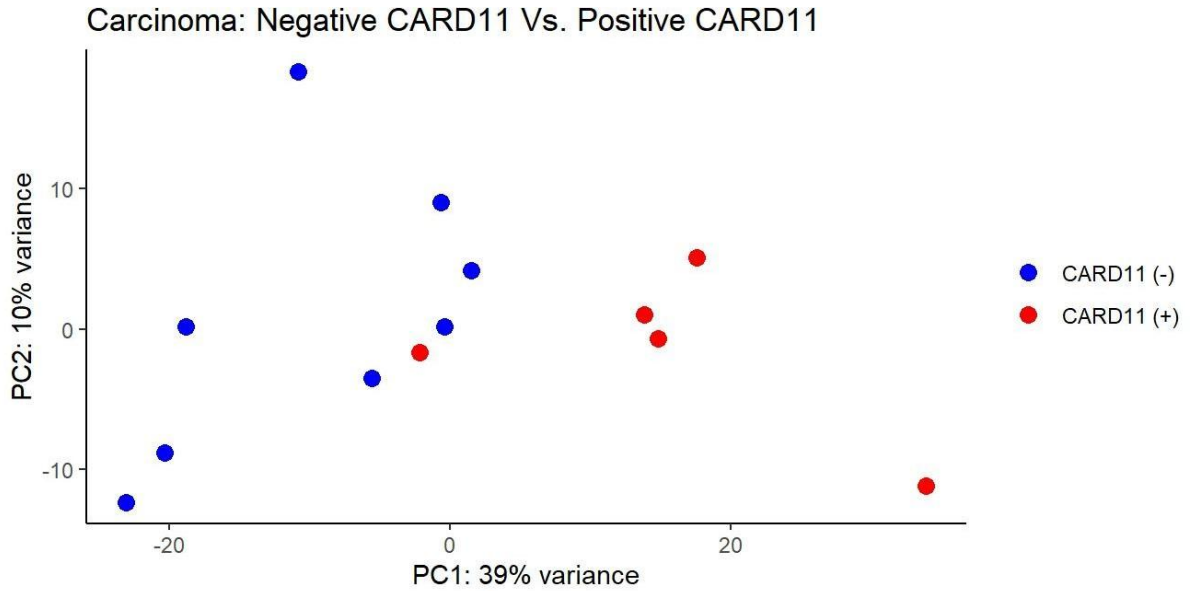


*Figure 19: Principal component analysis (PCA) showed a separation between CARD11+ and CARD11- among Carcinoma cohorts.*

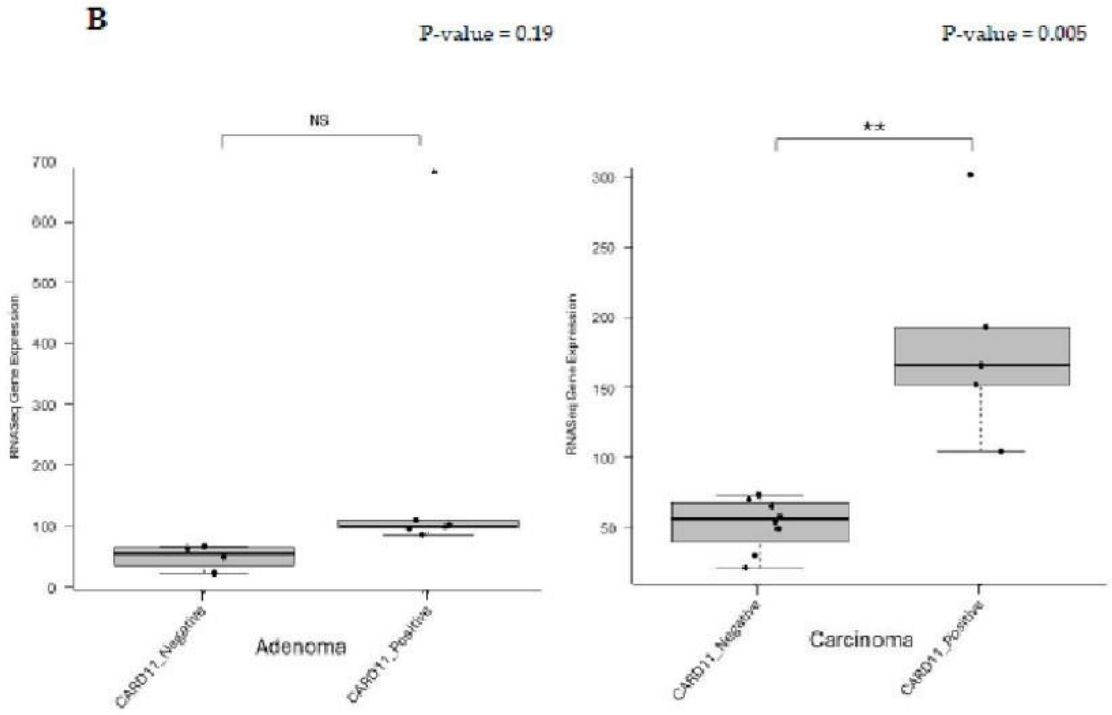


*Figure 20: Boxplots of RNA-seq results showed that CARD11 had a higher trend in CARD11 than CARD11+ adenoma and was significantly differentially expressed in carcinoma patients.*

The differential gene expression analysis showed distinct gene expression profiles between *CARD11*+ patient samples compared to *CARD11*− patient samples. Following normalization and filtering, the DEGs found in adenoma and carcinoma patients for *CARD11*− compared to *CARD11*+ expression were 1132 and 1017, respectively. The most upregulated and downregulated DEGs are also annotated in the volcano plots and based on log2-fold changes of <−1.5 and >1.5 and $p < 0.05$, 521 and 583 genes were significantly differentially expressed in *CARD11*+ adenoma and carcinoma patients, respectively (Figure 21).

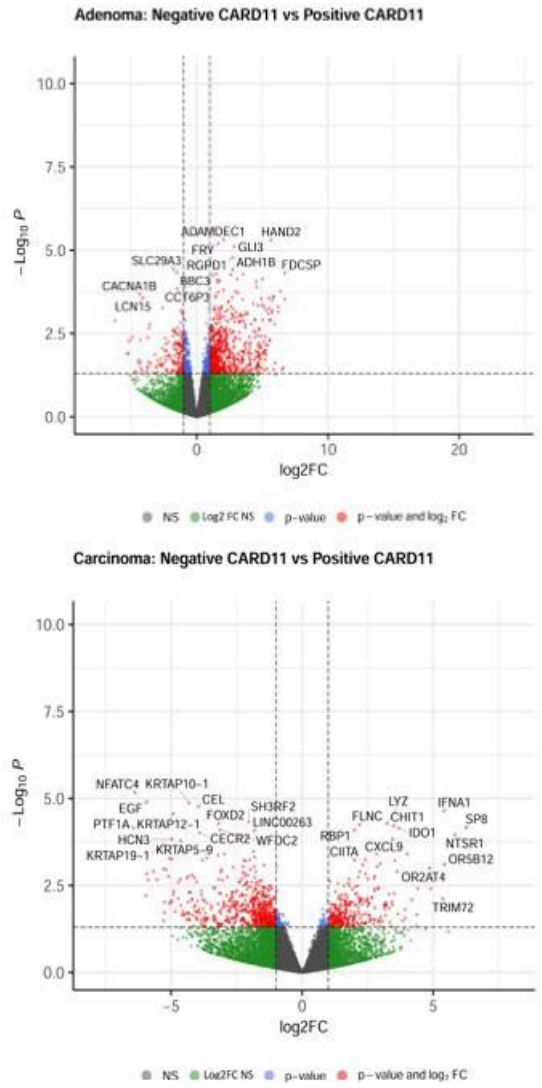


*Figure 21: Volcano plots of differentially expressed genes. Genes that were expressed significantly higher in either CARD11– and CARD11+ patients based on log2 fold change p < 0.05 are highlighted by red dots, p > 0.05 are highlighted by green dots (Log2FC NS), unchanged transcripts are demarcated as grey (NS)*

absGSEA was performed to identify the activated and significantly enriched pathways in each comparison of *CARD11*− vs. *CARD11*+ for both adenoma and carcinoma. The number of significantly enriched pathways derived from absGSEA in *CARD11*− vs. *CARD11*+ CRC patients are provided in Figure 14 as an upset plot graph. The graph showed that adenoma has more immune response activated than carcinoma.

Gene frequency was obtained by counting the number of times a gene occurred across all the different pathways in the cell lines and patients. The genes were obtained from the significant number of enriched genes of the significant gene sets. This finding suggested that

these genes are highly influential because of the overexpression of *CARD11*. The leading-edge genes are represented by the histograms in Figure 22.

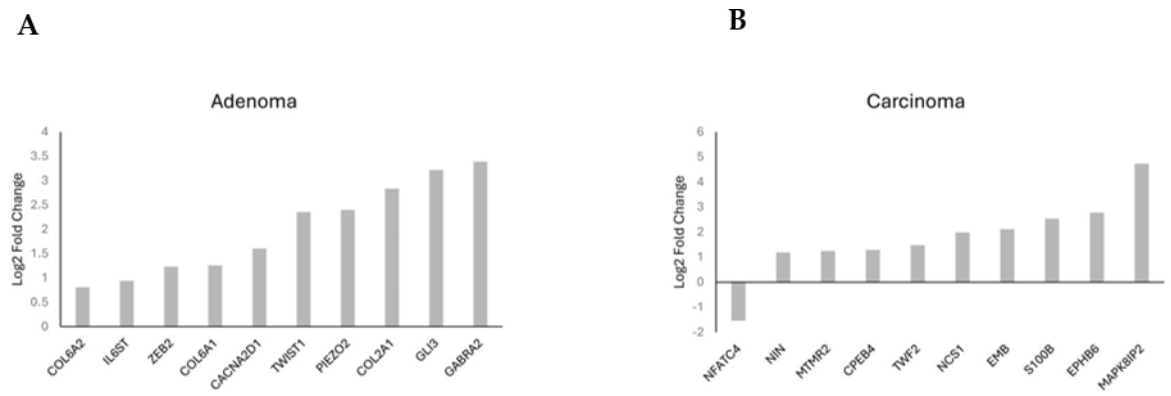


*Figure 22: Histogram of the selected leading-edge genes based on frequency in CARD11− vs. CARD11+ adenoma (A) and carcinoma (B) patient samples*

The detailed list of selected leading genes based on frequency for *CARD11*– vs. *CARD11*+ in adenoma and carcinoma is also provided in Tables 5 and 6.

*Table 5: The selected leading genes based on frequency for CARD11– vs. CARD11+ in adenoma*

| **Gene** | **Frequency** | **Expression direction in *CARD11*+** | **Fold Change** |
|---|---|---|---|
| *IL6ST* | 5 | Upregulated | 1.920 |
| CACNA2D1 | 5 | Upregulated | 3.040 |
| ZEB2 | 5 | Upregulated | 2.350 |
| COL2A1 | 4 | Upregulated | 7.140 |
| COL6A1 | 4 | Upregulated | 2.390 |
| COL6A2 | 4 | Upregulated | 1.750 |
| GABRA2 | 4 | Upregulated | 10.480 |
| GLI3 | 4 | Upregulated | 9.290 |
| PIEZO2 | 4 | Upregulated | 5.270 |
| TWIST1 | 4 | Upregulated | 5.110 |

*Table 6: The selected leading genes based on frequency for CARD11– vs. CARD11+ in carcinoma*

| **Gene** | **Frequency** | **Expression direction in *CARD11*+** | **Fold Change** |
|---|---|---|---|
| MAPK8IP2 | 9 | Upregulated | 26.560 |
| MTMR2 | 9 | Upregulated | 2.370 |
| NIN | 8 | Upregulated | 2.280 |
| *CPEB4* | 8 | Upregulated | 2.440 |
| S100B | 8 | Upregulated | 5.780 |
| *EMB* | 7 | Upregulated | 4.330 |
| *EPHB6* | 7 | Upregulated | 6.880 |
| NCS1 | 7 | Upregulated | 3.970 |
| NFATC4 | 7 | Downregulated | 0.010 |
| TWF2 | 7 | Upregulated | 2.780 |

### 4.7 Gene Set Enrichment Analysis Revealed Transcriptomic Changes Related to Inflammation, Tumor Immune Microenvironment, and Cancer Hallmark Pathways in *CARD11*− Compared to *CARD11*+ Patients

The annotation of the top leading-edge genes showed enrichment of categories related to response to abiotic stimulus, immune response (human papillomavirus infection), and cytokine signaling in the immune system for adenoma patients (Figure 23). Among the significant pathways, ten gene sets for adenoma and 14 gene sets for carcinoma patient samples were selected, which were found to be related to especially B- and T-cell mediated immunity, cancer hallmarks, and inflammation (Tables 7 and 8).

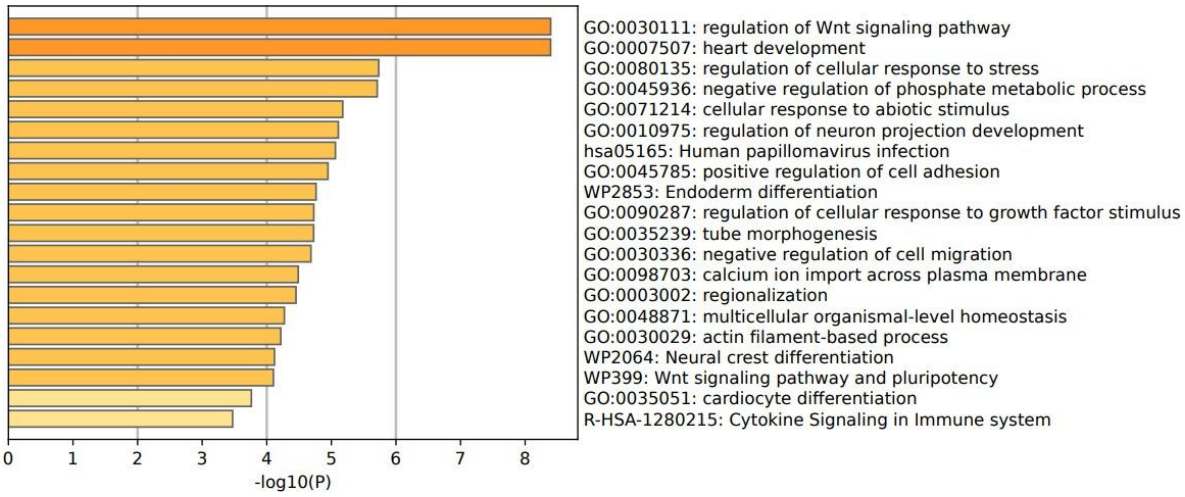


*Figure 23:Significant enrichment pathways based on CARD11− vs. CARD11+ frequency in adenoma*

*Table 7: GSEA of significantly activated pathways in CARD11+ compared to CARD11- adenoma patients*

| **Gene sets** | **Source** | **Size** | **ES** | **NES** | **NOM *p*-value** | **Tag %** | **Gene %** | **Signal** |
|---|---|---|---|---|---|---|---|---|
| **B cell-mediated immunity** | | | | | | | | |
| B cell activation and response | M40863 | 27 | 0.52401 | 1.7566 | 0.007722 | 0.63 | 0.252 | 0.483 |
| Functional activity of B cells | M9311 | 17 | 0.48943 | 1.6479 | 0.04466 | 0.647 | 0.302 | 0.458 |
| **Cancer hallmarks** | | | | | | | | |
| ESC-like gene | M17183 | 23 | 0.4828 | 1.6768 | 0.03143 | 0.652 | 0.302 | 0.465 |

| | | | | | | | | |
|---|---|---|---|---|---|---|---|---|
| expression signature in poorly differentiated aggressive human tumors | | | | | | | | |
| Cervical Carcinoma | M2505 | 31 | 0.4198 | 1.6608 | 0.0001 | 0.484 | 0.232 | 0.382 |
| Breast Cancer | M3062 | 21 | 0.3958 | 1.3845 | 0.04955 | 0.762 | 0.463 | 0.417 |
| **Chromatin and Histon remodeling** | | | | | | | | |
| Chromatin Remodeling and Growth Regulation | M1804 | 26 | 0.51219 | 1.5809 | 0.03239 | 0.577 | 0.223 | 0.459 |
| **Inflammatory response** | | | | | | | | |
| Leukocytes | M5365 | 15 | 0.52232 | 1.407 | 0.04593 | 0.733 | 0.307 | 0.515 |
| Neutrophil | M405 | 15 | 0.581 | 1.7532 | 0.01124 | 0.8 | 0.302 | 0.566 |

| | | | | | | | | |
|---|---|---|---|---|---|---|---|---|
| | | | 6 | | | | | |
| **Immune response** | | | | | | | | |
| Early/innate B and T cell responses | M9996 | 16 | 0.53508 | 1.5632 | 0.04264 | 0.625 | 0.223 | 0.493 |
| **NF-κB related** | | | | | | | | |
| TAK1-deleted splenic B cells | M9924 | 18 | 0.46875 | 1.6035 | 0.02697 | 0.611 | 0.277 | 0.449 |

*Table 8: List of the pathways activated in CARD11+ compared to CARD11- carcinoma patients analyzed using GSEA*

| **Gene sets** | **Source** | **Size** | **ES** | **NES** | **NOM p-value** | **Tag %** | **Gene %** | **Signal** |
|---|---|---|---|---|---|---|---|---|
| **Cellular component morphogenesis** | | | | | | | | |
| Cellular Component Morphogenesis | GO:0032989 | 42 | 0.4934 | 1.763 | 0.001916 | 0.452 | 0.182 | 0.386 |
| Cell Part Morphogenesi | GO:0032990 | 34 | 0.4515 | 1.669 | 0.003745 | 0.412 | 0.182 | 0.349 |

| | | | | | | | | |
|---|---|---|---|---|---|---|---|---|
| s | | | | | | | | |
| Regulation of Membrane Potential | GO:0042391 | 25 | 0.4164 | 1.5111 | 0.01587 | 0.64 | 0.373 | 0.412 |
| Polymeric Cytoskeletal Fiber | GO:0099513 | 38 | 0.4163 | 1.5563 | 0.008944 | 0.658 | 0.398 | 0.411 |
| **Response to abiotic stimulus** | | | | | | | | |
| Response to Abiotic Stimulus | GO:0009628 | 52 | 0.3768 | 1.4403 | 0.04093 | 0.577 | 0.382 | 0.375 |
| Response to Radiation | GO:0009314 | 17 | 0.4927 | 1.5435 | 0.01667 | 0.588 | 0.311 | 0.412 |
| **Cell cycle** | | | | | | | | |
| Histone modifications | M2013 | 19 | 0.4551 | 1.5713 | 0.01744 | 0.316 | 0.0924 | 0.292 |
| Cell cycle arrest | M18120 | 37 | 0.4032 | 1.5949 | 0.03333 | 0.405 | 0.205 | 0.335 |
| **Cancer hallmarks** | | | | | | | | |
| Hypomethylation of Hepatocellula | M16009 | 45 | 0.3555 | 1.4184 | 0.0329 | 0.778 | 0.532 | 0.381 |

| | | | | | | | | |
|---|---|---|---|---|---|---|---|---|
| r carcinoma | | | | | | | | |
| Upregulated genes in Bladder cancer | M6782 | 25 | 0.4562 | 1.5225 | 0.03992 | 0.36 | 0.159 | 0.31 |
| Downregulated genes in HNSCC | M12527 | 16 | 0.4957 | 1.5285 | 0.04066 | 0.438 | 0.211 | 0.351 |
| **T Cell-Mediated Immunity** | | | | | | | | |

The functional annotation of the top leading-edge genes showed significant enrichment of categories related to the adherens junction, developmental cell growth, and cellular response to organic cyclic compounds for carcinoma patients (Figure 24B). In addition to promoting and stabilizing cell-cell adhesion, the adhesion junction regulates the actin cytoskeleton, intracellular signaling, and transcription. In carcinoma patients, the direction of affected pathways was related to cellular component morphogenesis and cell cycle, and an adherens junction-enriched pathway found from Metascape also supports these findings. The adherens junctions (AJs) are essential in epithelial cells. Their dysregulation is an important step in tumor metastasis because they regulate epithelial tissue architecture and integrity. As a crucial part of cancer progression, AJ remodeling plays a key role in tumor cell growth, survival, and dissemination (Newman *et al.*, 2015).

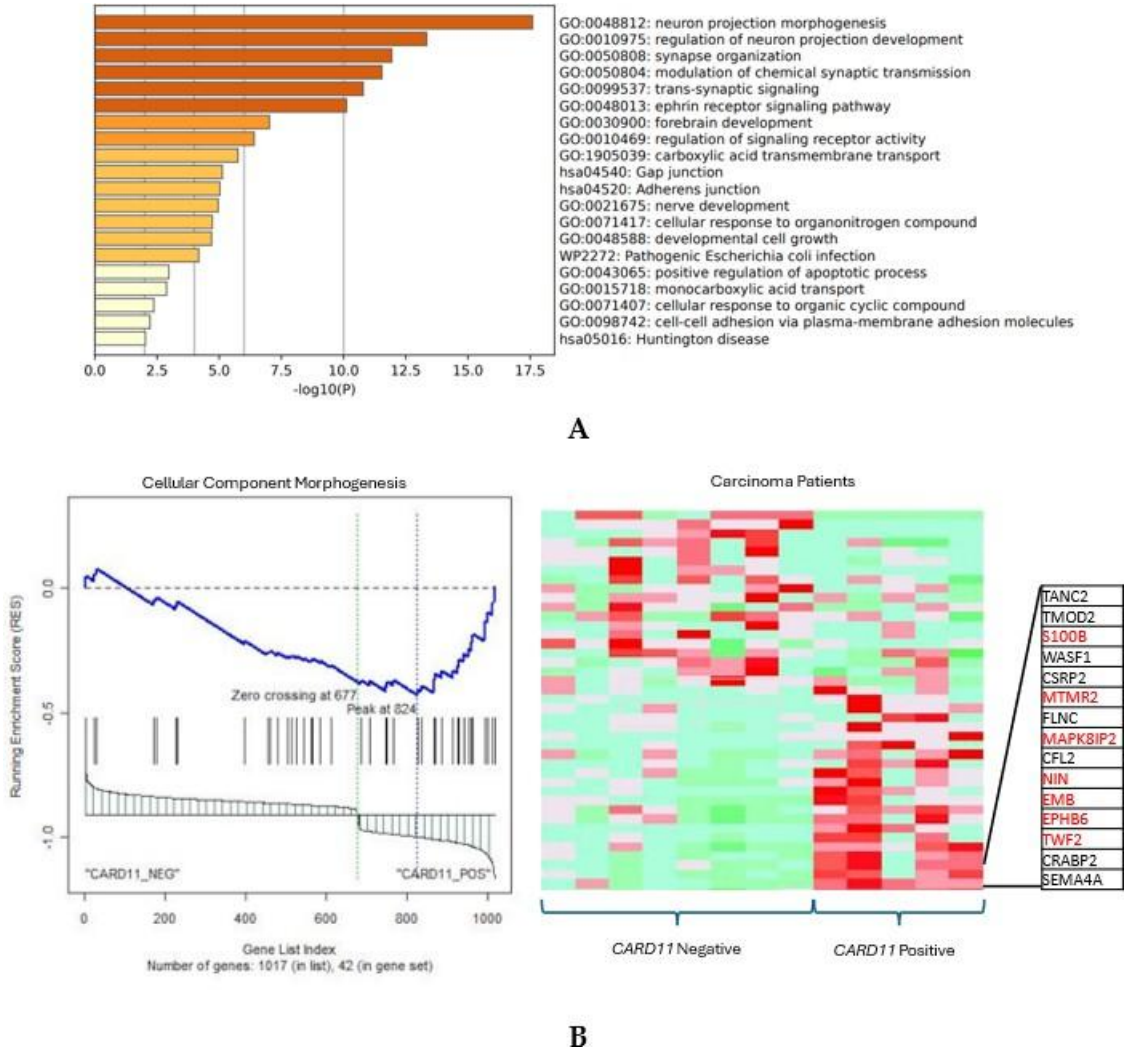


*Figure 24: (A) Significant enrichment pathways based on frequency in CARD11− vs. CARD11+ in carcinoma. (B) Leading edge analysis showed that there was a significant gene enrichment in the cellular component morphogenesis pathway in CARD11-positive carcinoma patients (p = 0.0019). The top 15 leading-edge core genes are shown; the frequently found ones are indicated in red*

### 4.8 Validation of Genes Related to *CARD11* Overexpression in CRC

For the validation of some key genes identified in adenoma (*IL6ST*, GLI3) and carcinoma (MAPK8IP2, *CPEB4*) patients, survival analysis was completed by using the Kaplan–Meier Plotter (Figure 26A–C). As Figure 25 shows, higher levels of *IL6ST*, GLI3, and *MAPK8IP2* were associated with worse overall survival (OS) in CRC patients. A previous study already showed an increase in *CPEB4* protein levels in CRC patient samples using a Western blot analysis (Figure 25). The Western blot data provided direct evidence of elevated *CPEB4* protein in CRC tissues compared to normal counterparts. In the

same study, high *CPEB4* expression was correlated with advanced tumor stage, lymph node metastasis, distant metastasis, and poor prognosis in patients with CRC (Zhong *et al.*, 2015) (Figure 25).

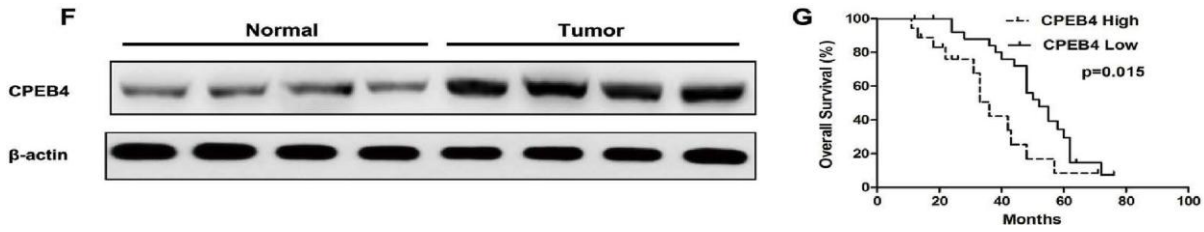


*Figure 25: Western blot (left) and survival plot (right)*

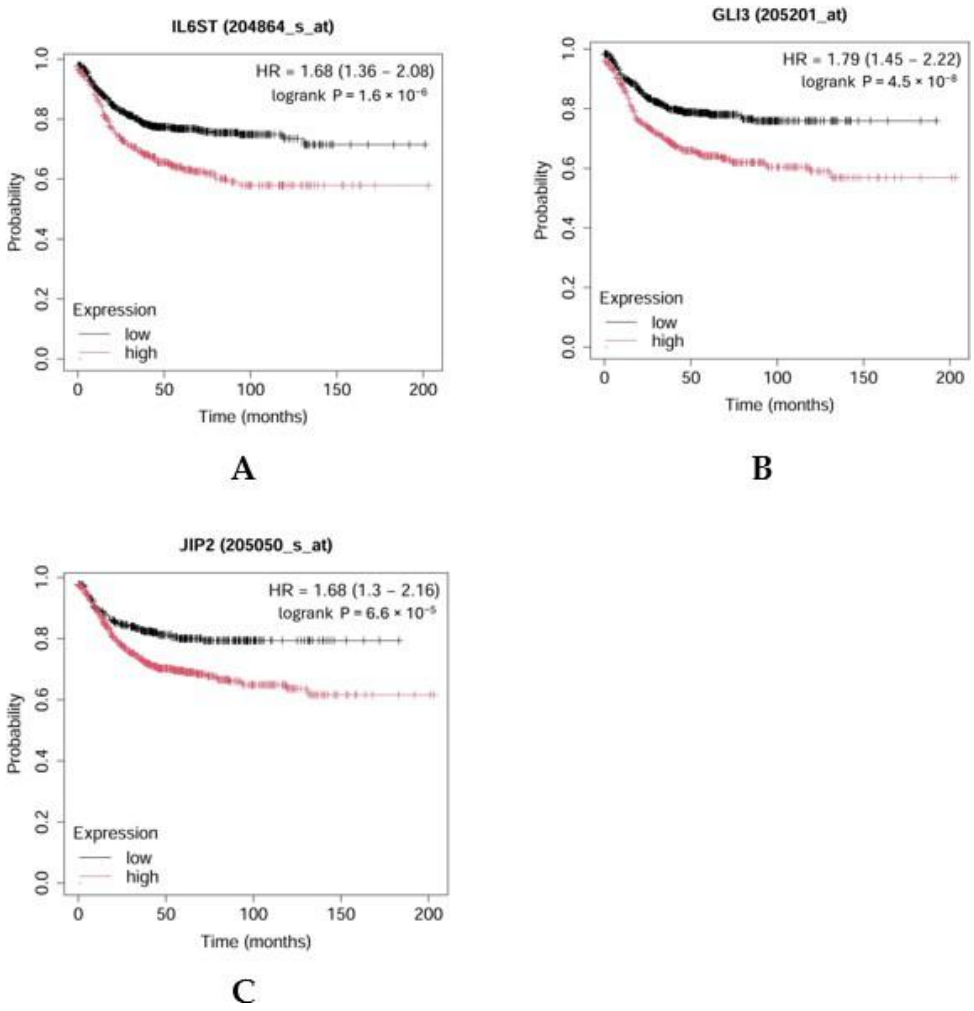


*Figure 26: Kaplan–Meier overall survival plot for CRC patients based on IL6ST (A), GLI3 (B), and MAPK8IP2 (JIP2) (C) expression (https://kmplot).*

### 4.9 Identification of Immune Cell Types in *CARD11* Overexpressed CRC Cell Line and Patients

Investigation of the immune cell distribution profile between the cell lines and patients using CIBERSORTX, which was applied to transcriptomic data of CRC cell lines and patients, showed that *CARD11* expression plays a significant role in modulating various types of immune response related to CRC progression and pathogenesis (Figure 27).

For HCT-116, the results showed a 2.57-fold decrease in CD8 T cells and a 1.4-fold increase in the proportion of plasma B cells, while the proportion of naïve B cells showed a decline in the HCT-116 *CARD11*-transfected cell line, suggesting that plasma cells may play a role in CRC progression. On the other hand, *CARD11*-transfected HT-29 cells results exhibited a 0.21-fold decrease in plasma B cells and a 2.83-fold increase in naive B cells. Moreover, the proportion of the CD8 T cell fraction increased by two-fold, suggesting a possible interplay between B and T cell immune response in CRC pathogenesis.

In CRC patients, the results showed distinct immune cell types with different proportions between *CARD11*− and *CARD11*+ patients in adenoma and carcinoma. Adenoma patients exhibited higher fractions of CD4 memory resting T cells compared to other groups (with a 0.95-fold decrease in *CARD11*+ compared to *CARD11*− adenoma). In comparison, carcinoma cases showed higher fractions of M0-type macrophages (with a 3.33-fold increase in *CARD11*− compared to *CARD11*+ carcinoma) as opposed to other groups. This comparison suggested a more complex interplay between innate and acquired immune response in CRC progression and pathogenesis. The detailed information for the fold changes is provided in Table 9.

*Table 9: The fold changes results from CIBERSORTx*

| **Immune cell type** | **HCT116 FC** | **HT29 FC** | **Adenoma FC** | **Carcinoma FC** |
|---|---|---|---|---|
| B cells naive | 0.235 | 2.829 | 0 | 7.074 |
| B cells memory | 0 | 0 | 1.908 | 0 |
| Plasma cells | 1.461 | 0.207 | 0.660 | 0.300 |
| T cells CD8 | 0.257 | 2.084 | 0.809 | 1.887 |
| T cells CD4 naive | 1.416 | 1.247 | 0 | 0 |
| T cells CD4 memory resting | 0 | 0 | 0.953 | 0.534 |
| T cells CD4 memory activated | 0 | 0 | 0 | 1.088 |
| T cells follicular helper | 1.825 | 0 | 0 | 0.726 |
| NK cells resting | 0 | 0.146 | 1.493 | 25.875 |
| NK cells activated | 0 | 0 | 0 | 1.458 |
| Monocytes | 0.357 | 0.447 | 0.929 | 2.362 |
| Macrophages M0 | 0 | 0.635 | 0.395 | 0.301 |
| Macrophages M1 | 0 | 0 | 13.744 | 3.670 |
| Macrophages M2 | 0 | 0 | 0.716 | 1.067 |
| Dendritic cells resting | 0 | 0 | 0 | 0.137 |
| Dendritic cells activated | 19.150 | 7.861 | 0 | 0 |
| Mast cells activated | 0 | 1.328 | 0.557 | 3.340 |

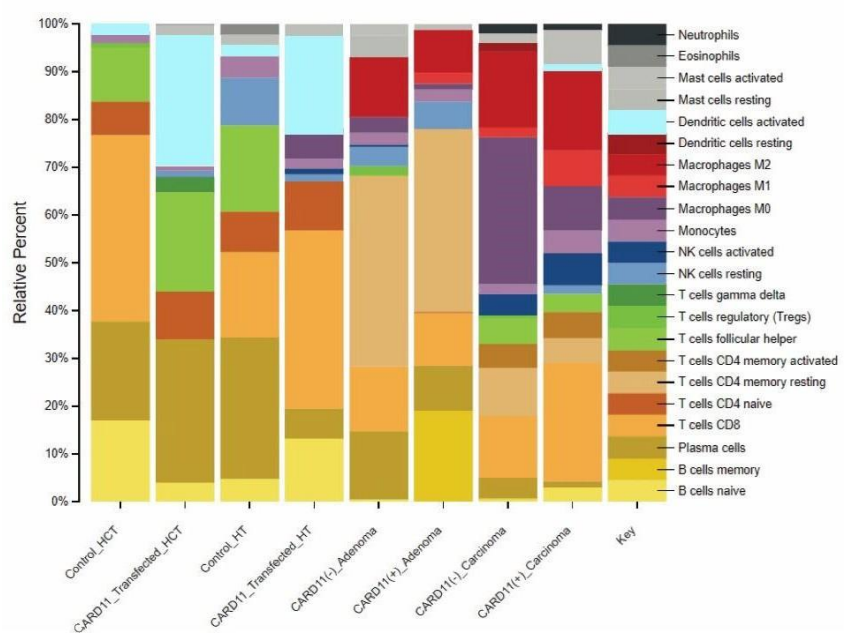


*Figure 27: Comparison of CIBERSORTX immune cell fractions between CARD11-transfected vs. empty vector-transfected for both cell lines, as well as CARD11− versus CARD11+ for both tissue samples*

### 4.10 Immunohistochemistry staining of FFPE samples

Immunohistochemical staining was conducted to characterize CRC patient samples based on a scoring system utilizing visual assessments of intensity and distribution. Immunohistochemical staining for the CARD11 protein reveals distinct patterns across different tumor subtypes.

Adenomas are considered a control for the other two subtypes, and they consistently exhibited moderate to high expression of the CARD11 protein throughout the glandular structures. This suggests a significant role for CARD11 in this benign tumor subtype and its potential involvement in the early stages of tumorigenesis, even in non-invasive lesions.

In adenocarcinomas, the CARD11 protein is highly expressed, characterized by intense and heterogeneous staining within the malignant glandular structures. The variable expression observed in different areas highlights CARD11 role in tumor progression and invasive behavior.

In carcinoma in situ, strong and uniform expression of CARD11 is noted throughout the pre-invasive lesion, indicating that CARD11 could serve as a marker for early malignant transformation before stromal invasion occurs.

These findings emphasize the differential expression of CARD11 across various stages of tumor development and its potential role in tumorigenesis.

A)

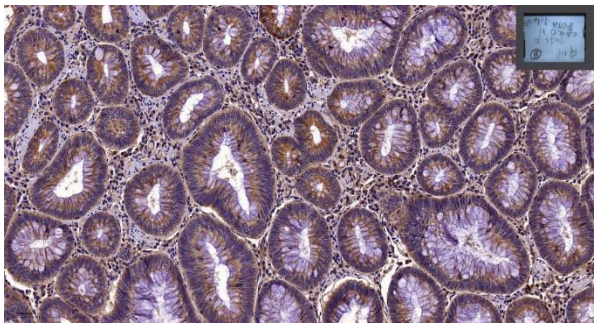

B)

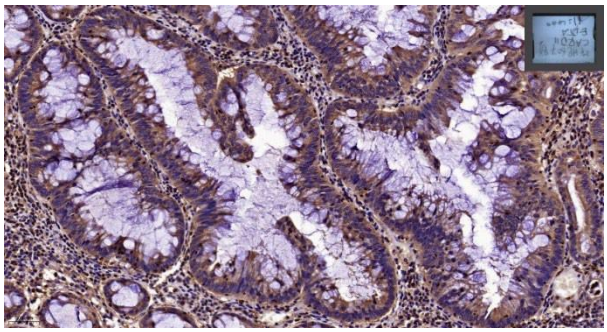

C)

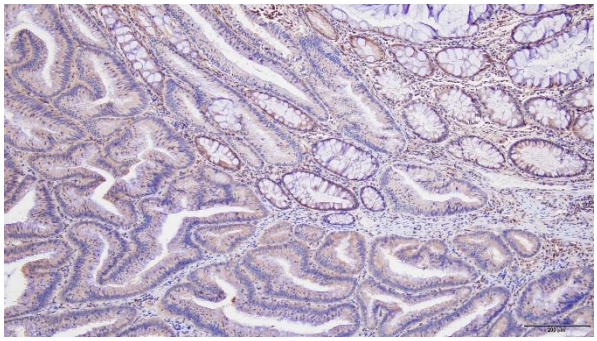

*Figure 28. IHC of CRC FFPEs from various stages based CARD11 expression*
A) Adenoma. B) Adenocarcinoma. C) Carcinoma in situ (magnification 20x).

# Chapter V.

## Results for Biomarker Discovery Using FFPE Tissue Samples

### 5.1 Introduction

The second phase of the study aimed to identify the biomarkers that distinguish various stages of CRC. In this study, we analyzed a cohort of CRC patients, comprising ten adenomas, eleven adenocarcinomas, and eight carcinomas in situ (CIS) which were included based on the clear separation on PCA plots.

Principal component analysis (PCA) for the RNASeq data showed a clear separation between Adenoma and Adenocarcinoma (figure 29A). In contrast, Adenoma and CIS samples showed overlapping profiles (figure 29B), indicating the need for further investigation to identify DEGs. Transcriptomic analysis identified distinct expression profiles between Adenoma and Adenocarcinoma patient samples, resulting in a total of 6,739 significant DEGs (figure 29C). Of these, 1,261 DEGs were upregulated (Log2FC > 2), while 433 DEGs were downregulated (Log2FC <- 2) in Adenocarcinoma.

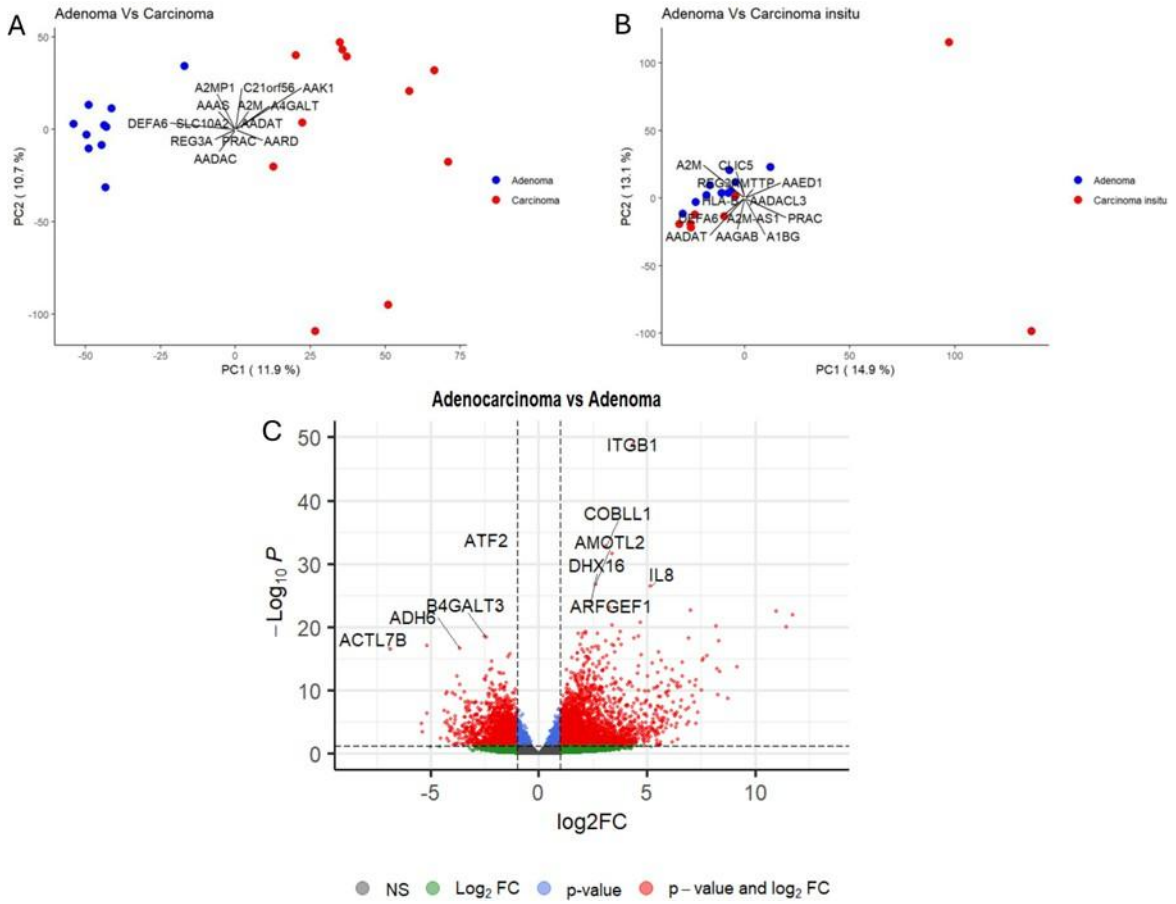


*Figure 29: Principle Component Analysis (PCA) and Volcano Plot of DEGs. (A) PCA plot showing the separation between adenoma and carcinoma patient samples. Based on the top principal components. Each point represents a sample, with adenoma samples in blue and carcinoma samples in red. (B) PCA plot displaying the separation between adenoma and carcinoma in situ (CIS) samples. Adenoma in blue and CIS in red. (C) Volcano plot of DEGs between adenoma and adenocarcinoma samples. Genes significantly up- or downregulated (log2FC, $p < 0.05$) in Adenocarcinoma patients are shown in red*

### 5.2 Gene-set Enrichment Analysis of Differentially Expressed Genes Highlights Distinct Molecular Signatures between Adenoma and Adenocarcinoma

absGSEA and Standard GSEA were conducted to identify significantly enriched pathways in Adenocarcinoma samples, utilizing the MSigDB database that encompass diverse gene sets from the C1 to C8 collections. Particular emphasis was placed on the C5, as they offer detailed insights into molecular, and biological aspects to the study. Using *p*-value threshold of <0.05 and an FDR of <0.25, 99 significant pathways from C5 were identified. The enriched pathways essentially demonstrate diverse biological processes and molecular functions involving signal transduction,

transcription regulation, catalytic activity, and molecular binding. After identifying the significant pathways, gene frequency within these significant pathways were analyzed to assess

their level of association and relevance to different stages of CRC. Table 10 presents the top 20 selected genes from C5 gene sets, ranked from highest to lowest based on their frequency. The log2 fold change values are oriented towards Adenocarcinoma, indicating differences in expression in this condition. Genes with higher frequency are likely to play critical roles in pathways enriched for Adenocarcinoma, highlighting their potential importance in the disease's progression and biological process.

***Table 10:*** *Top 20 genes from C5 gene set based on their frequencies for each of the cohort groups A, B, and C.*

| **A** | **Adenoma Compared to Carcinoma insitu** | | |
|---|---|---|---|
| **Gene** | **Frequency** | ***P-value*** | **Log2FC** |
| *APOBR* | 8 | 0.0006 | -1.9 |
| *ARL5B* | 8 | 0.0458 | 1.0 |
| *BLNK* | 8 | 0.0049 | -1.6 |
| *CD93* | 8 | 0.0008 | -1.6 |
| *CHAD* | 8 | 0.0040 | -3.1 |
| *COL4A5* | 8 | 0.0150 | -1.7 |
| *COQ9* | 8 | 0.0013 | -1.5 |
| *CPPED1* | 8 | 0.0005 | -1.9 |
| *FBXL19* | 8 | 0.0024 | -1.4 |
| *FLT3LG* | 8 | 0.0205 | -2.5 |
| *FOXJ3* | 8 | 0.0044 | -1.1 |
| *HAGH* | 8 | 0.0026 | -1.4 |
| *HHLA2* | 8 | 0.0233 | -2.1 |
| *ISG20* | 8 | 0.0042 | -1.6 |
| *LGALS4* | 8 | 0.0123 | -1.8 |
| *MAOA* | 8 | 0.0010 | -1.9 |
| *MFAP4* | 8 | 0.0149 | -2.2 |

| | | | |
|---|---|---|---|
| *MPC1* | 8 | 0.0085 | -1.3 |
| *MUC4* | 8 | 0.0002 | -2.7 |
| *MXD3* | 8 | 0.0152 | -2.0 |

| **B** | **Adenoma Compared to Adenocarcinoma** | | |
|---|---|---|---|
| **Gene** | **Frequency** | ***P-value*** | **Log2FC** |
| *SIRT6* | 15 | 0.0039 | -1.6 |
| *ARRB1* | 13 | 2.79x10-05 | -2.5 |
| *TADA2A* | 13 | 3.72x10-5 | -2.2 |
| *ATF2* | 12 | 7.03x10-9 | -3.5 |
| *CTBP2* | 12 | 0.0002 | -1.5 |
| *CTBP1* | 11 | 1.33x10-5 | -1.6 |
| *KAT2A* | 11 | 9.57x10-5 | -2.3 |
| *KAT5* | 11 | 0.0007 | -1.4 |
| *KAT8* | 11 | 0.0002 | -1.6 |
| *SIRT2* | 11 | 0.0018 | -1.7 |
| *CAMK2G* | 10 | 7.57x10-5 | -1.7 |
| *HIPK2* | 10 | 9.90x10-5 | -1.6 |
| *ITPR3* | 10 | 2.49x10-6 | -1.7 |
| *P2RX4* | 10 | 2.15x10-6 | -1.8 |
| *PPARA* | 10 | 9.59x10-5 | -1.5 |
| *PTK2B* | 10 | 0.001213967 | -1.978752198 |
| *SIRT7* | 10 | 0.000518649 | -1.956905616 |
| *TPCN2* | 10 | 6.09819E-05 | -1.75 |
| *TRPM6* | 10 | 0.04737162 | -2.4 |
| *AARS2* | 9 | 0.000290527 | -2.24 |

| **C** | **Carcinoma insitu Compared to Aenocarcinoma** | | |
|---|---|---|---|
| **Gene** | **Frequency** | ***P-value*** | **Log2FC** |
| *COL1A2* | 4 | 0.0064 | 3.6 |
| *COL1A1* | 3 | 0.0115 | 3.5 |
| *MMP14* | 3 | 0.0384 | 1.3 |
| *ALOX5* | 2 | 0.0262 | -1.4 |

| | | | |
|---|---|---|---|
| *COL12A1* | 2 | 0.0161 | 1.8 |
| *COL14A1* | 2 | 0.0356 | 2.3 |
| *COL15A1* | 2 | 0.0220 | 2.5 |
| *COL18A1* | 2 | 0.0174 | 1.7 |
| *COL3A1* | 2 | 0.0165 | 3.6 |
| *COL4A1* | 2 | 0.0186 | 1.9 |
| *COL4A2* | 2 | 0.0151 | 2.1 |
| *COL5A1* | 2 | 0.0176 | 2.0 |
| *COL5A2* | 2 | 0.0117 | 2.9 |
| *COL6A1* | 2 | 0.0196 | 1.6 |
| *COL6A2* | 2 | 0.0304 | 2.1 |
| *COL7A1* | 2 | 0.0146 | 2.2 |
| *COL9A2* | 2 | 0.0467 | -2.6 |
| *GREM1* | 2 | 0.0306 | 2.3 |
| *ISG15* | 2 | 0.0360 | 2.3 |
| *PTN* | 2 | 0.0321 | -1.2 |

### 5.3. Gene-set Enrichment Analysis on Patient Samples Revealed Distinctive Tumor Stage-Mediated Activation of Transcriptional Co-Regulatory Mechanisms, Protein Kinase Functional Pathways and Cellular Metabolic Processes.

The transcriptional co-regulatory mechanisms pathway was identified as enriched in the Adenocarcinoma cohorts; with DEGs including *CEBPZ, MED10, and PAWR* (Figure 30A). *SIRT6, ARRB1, TADA2A, CTBP1, and CTBP2* are genes identified based on the top 20 frequently occurring genes are therefore upregulated in Adenoma samples. Additionally, the protein kinase functional pathways was selected, and it exhibited downregulation of *OBSCN, ERN1, ERN2,* and *CAM2KG* genes in the Adenocarcinoma cohorts (Figure 30B), and these genes are part of the top 20 frequently occurring genes. Furthermore, the direction of affected pathways was correlated with phosphorylation and the regulation of transferase activity pathways inferred from Metascape analysis (Figure 29C). Dysregulation of these pathways is pivotal in CRC cell proliferation and

tumorigenesis (Ahmad et al., 2021; Ren et al., 2023; Wang et al., 2023). Distinct gene expression profiles are observed between Adenoma and Adenocarcinoma samples. *ARRB1, CTBP1*, and *CTBP2* exhibited notable upregulation in Adenoma (Figure 31A), whereas *COL1A2, CEBPZ, MED10*, and *PAWR* genes exhibited significant upregulation in Carcinoma (Figure 31B). Figure 32 illustrates the Log2FC of the selected biomarkers ranked in descending order. These findings substantiate the reliability of the RNA-sequencing methodology.

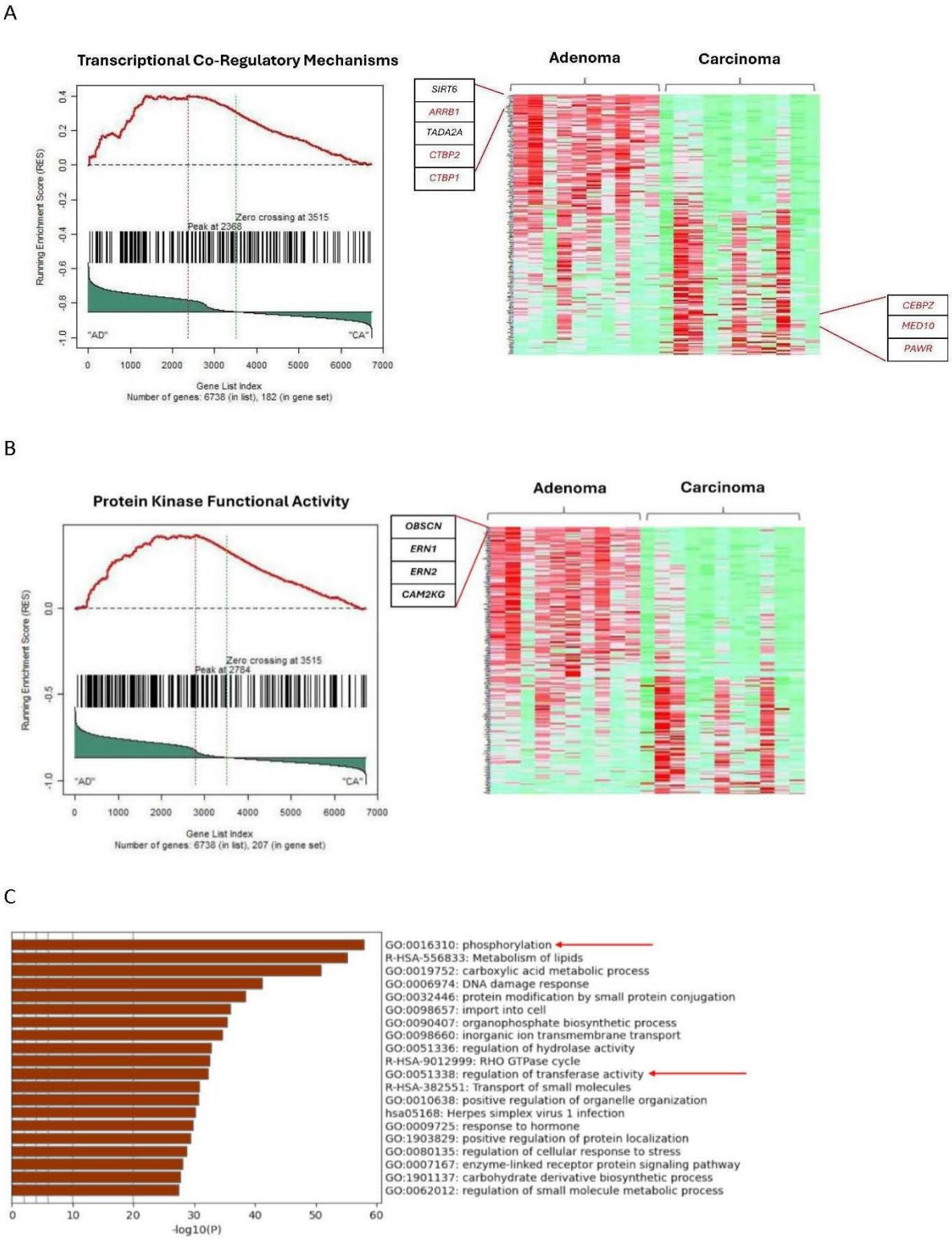


*Figure 30: Significant enriched pathways based on gene frequency obtained from Adenoma vs Carcinoma. A) Transcriptional coregulatory Mechanism: this pathway includes genes from the top 20 gene frequency analysis such as: SIRT6, ARRB1, TADA2A, CTBP2, CTBP1 (all downregulated in CRC). B) Protein Kinase: this pathway includes genes such as: OBSCN, ERN1, ERN2, CAMK2G (all downregulated in CRC). C) Enriched pathways obtained from Metascape*

A

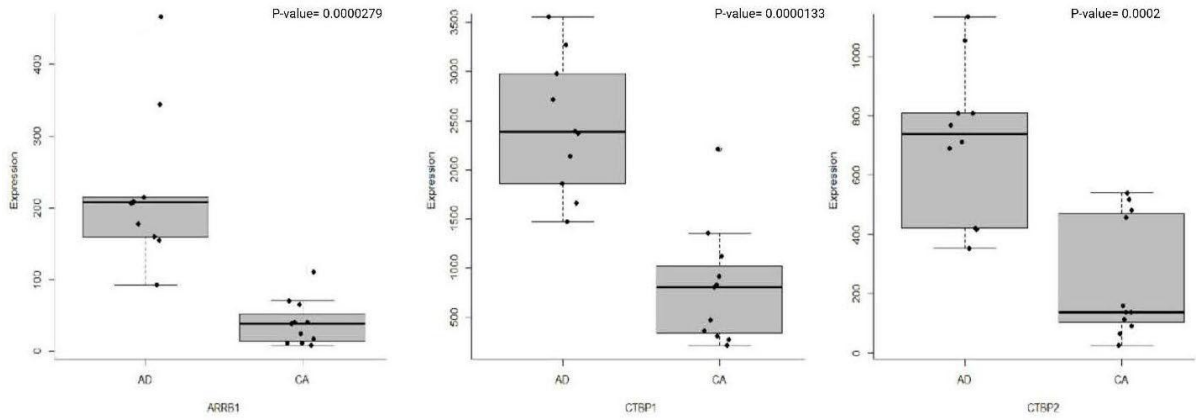


B

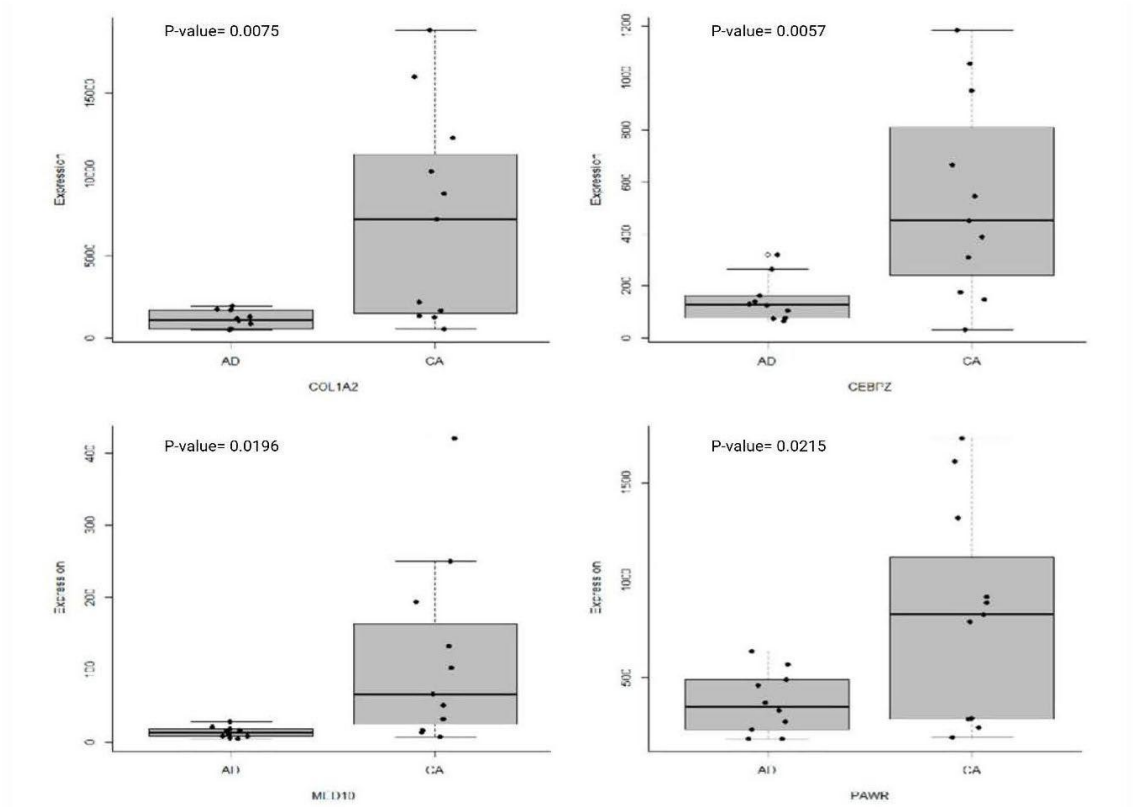


*Figure 31: DEGs presented as boxplots revealed distinct differential expression profiles among adenoma and adenocarcinoma. ARRB1, CTBP1, and CTBP2 genes exhibited significant upregulation in Adenoma (A), while COL1A2, CEBPZ, MED10, and PAWR genes exhibited significant upregulation in Carcinoma (B). These findings validate the RNA-seq methodology, demonstrating that CRC biomarkers undergo differential expression across various stages. AD: adenoma, CA: adenocarcinoma*

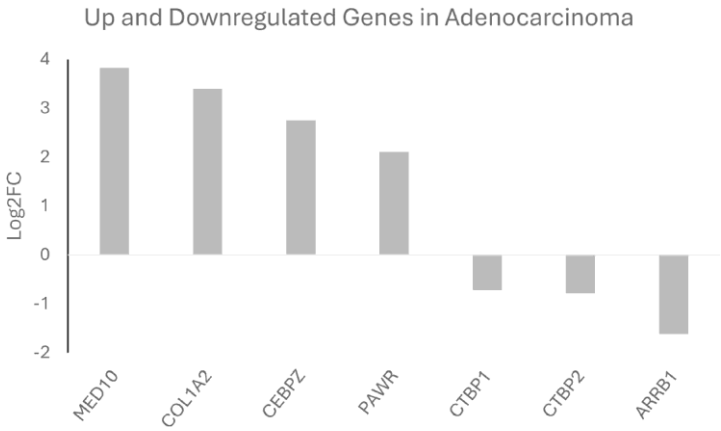


*Figure 32: The figure represents the Log2FC of the selected biomarkers. Ranked by highest to lowest Log2FC value*

### 5.4. Differential gene expression analysis in Tumor, Normal, and Metastatic

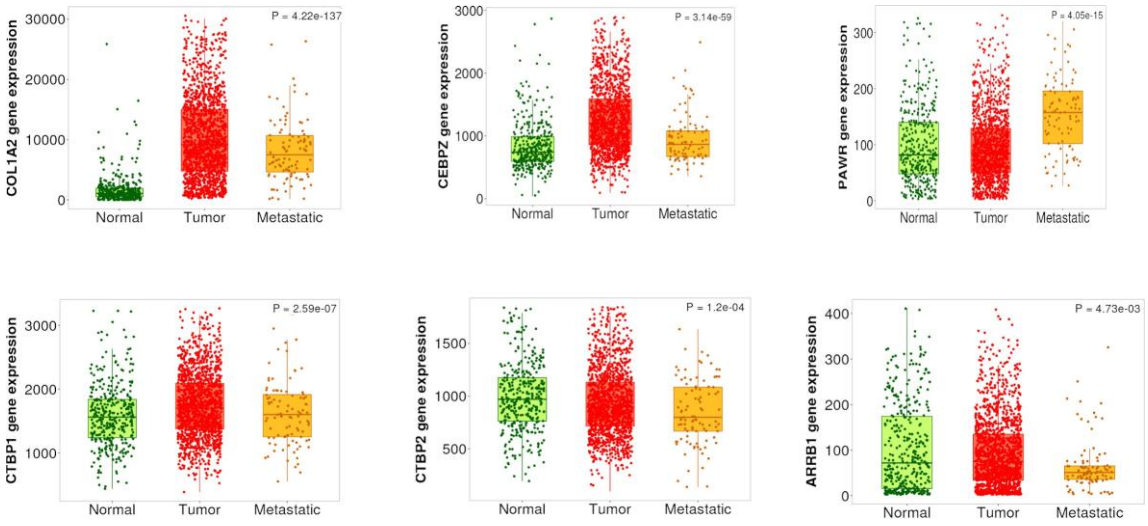


*Figure 33: The figure indicates that the expression levels of these genes are significantly different across the three conditions, collectively showing higher expression in tumor and metastatic state compared to normal state, except for ARRB1 which showed lower expression in metastatic state. Images obtained from TNMplot.*

The box plots captured in Figure 33 reveal significant differences in gene expression levels of the biomarkers across Normal, Tumor, and Metastatic conditions. Notably, tumor and metastatic samples generally exhibit higher or altered expression compared to normal tissues, underscoring the role of these biomarkers in cancer progression and metastasis. Collectively,

the biomarkers exhibited higher expression in the tumor and metastatic states compared to the normal state, with the exception of ARRB1, which exhibited similar expression in both normal and tumor states. This finding highlights the potential utility of these biomarkers in distinguishing between cancer stages and aiding in understanding of molecular changes associated with CRC.

### 5.5. Identification of Immune Cell Types in different stages of CRC patients

In CRC patients, the results showed distinct immune cell types with different proportions between Adenoma, CIS, and Adenocarcinoma. The highest fractions of immune cells observed in Adenoma compared to CIS and Adenocarcinoma were from Macrophages (23%), followed by T cells CD4 Naïve (18%), and B cells memory (17%) and these results align with previous findings (Kuwahara et al., 2019; Shimabukuro-Vornhagen et al., 2014; Soncin et al., 2018). While dendritic cells resting and macrophages M1 were fully depleted compared to CIS and adenocarcinoma. For CIS, the highest fractions of immune cells observed were from B cells Naïve (17%), and the elevation of this specific immune cell could be attributed to the progressive state that transitioned from adenoma, as previously observed (Zhang et al., 2023), followed by T cells follicular helper (Tfh) (6%), then T cells gamma delta (γδ Tcells) (4%). This finding suggests a favorable development of the anti-tumor immune response and may potentially interact with B cells, mediating the humoral immune response (Corsale et al, 2023; Rezende et al., 2018). While mast cells activated reveal they are completely depleted compared to adenoma and adenocarcinoma. In Adenocarcinoma samples, the highest fractions were observed from the T cells CD4 memory resting (21%), followed by Macrophages M0 (14%), T cell regulatory (8%), then T cells CD4 memory activated (7%) compared to adenoma and CIS as observed previously (Du et al., 2024; Li et al., 2022; MacLeod et al, 2009; Masle-Farquhar et al., 2023). Figure 34 illustrates the CIBERSORTX immune cell fractions

between Adenoma, CIS, and Adenocarcinoma samples, while Table 11 presents the immune cell fractions presented as percentages.

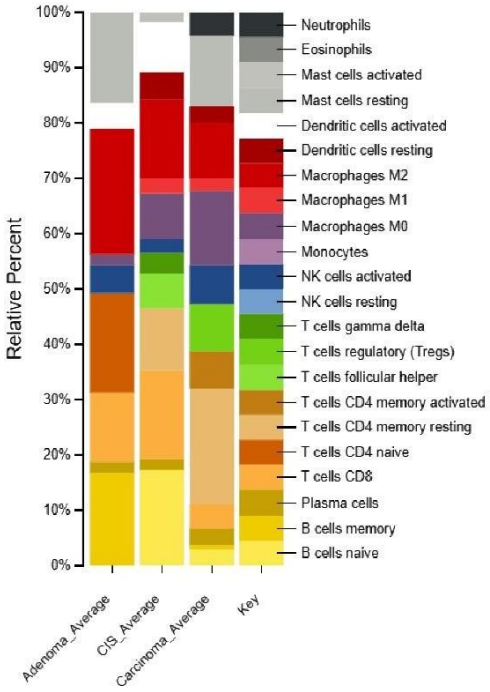


*Figure 34: Comparison of CIBERSORTX immune cell fractions between Adenoma, CIS, and Adenocarcinoma samples.*

*Table 11: Immune cell fractions presented as percentages among different CRC subtypes from CIBERSORTx*

| Immune Cells | Adenoma (%) | CIS (%) | Carcinoma (%) |
|---|---|---|---|
| B cells memory | 17 | 0 | 1 |
| T cells CD4 naive | 18 | 0 | 0 |
| Macrophages M2 | 23 | 14 | 10 |
| B cells naive | 0 | 17 | 3 |
| T cells follicular helper | 0 | 6 | 0 |
| T cells gamma delta | 0 | 4 | 0 |
| Mast cells activated | 0 | 3 | 0 |
| T cells CD4 memory resting | 0 | 11 | 21 |
| T cells CD4 memory activated | 0 | 0 | 7 |
| T cells regulatory (Tregs) | 0 | 0 | 8 |
| Macrophages M0 | 2 | 8 | 14 |
| Neutrophils | 0 | 0 | 4 |
| Plasma cells | 2 | 2 | 3 |
| T cells CD8 | 12 | 16 | 4 |
| NK cells resting | 0 | 0 | 0 |
| NK cells activated | 5 | 2 | 7 |
| Monocytes | 0 | 0 | 0 |
| Macrophages M1 | 0 | 3 | 2 |
| Dendritic cells resting | 0 | 5 | 3 |
| Dendritic cells activated | 4 | 9 | 0 |
| Mast cells resting | 17 | 0 | 13 |
| Eosinophils | 0 | 0 | 0 |

# Chapter VI.

# Discussion

## 6.1 CARD11 Study

The study showed that in CRC, the overexpression of *CARD11* leads to dysregulation in NF-κB. This process subsequently activates many cellular pathways and genes related to the modulation of tumor immune microenvironment and cancer-related pathways. This scenario may impact on the discovery of putative early diagnostic and prognostic biomarkers and may help identify downstream therapeutic targets for CRC.

As part of this study, two colorectal carcinoma cell lines—HCT-116 and HT-29—were used to investigate CARD11-mediated molecular mechanisms in CRC. According to ATCC, HCT-116 is derived from a male patient with colorectal carcinoma and exhibits aggressive behavior with metastatic potential, making it suitable for modeling advanced-stage CRC(ATCC 2024). In contrast, HT-29, established from a primary tumor of a female patient, represents a less invasive phenotype and is commonly used to model early-stage disease(ATCC 2024). These intrinsic differences likely influence how each cell line responds to CARD11 overexpression and the activation of immune and cancer-related pathways.Using dual luciferase NF-κB reporter assays, this project demonstrated that the overexpression of CARD11 significantly affected NF-κB activation in both the HCT-116 and HT-29 CRC cell lines. Notably, CARD11 overexpression in HT-29 cells resulted in a greater level of NF-κB activation compared to HCT-116. However, in both cell lines, CARD11 expression consistently exhibited an additive effect on NF-κB activation. Furthermore, many of the leading edge genes identified among the top ten are known to be inducible by NF-κB. Collectively, the findings from the bioinformatics analysis and the dual luciferase assays suggest that CARD11 overexpression plays a crucial role in NF-κB activation in CRC. These results corroborate prior studies that described the various mechanisms by which CARD11 activates NF-κB, including its role as a scaffold protein that integrates signals from B-cell and

T-cell antigen receptors. This process leads to a conformational change that activates downstream signaling pathways, including the recruitment of BCL10 and MALT1 complexes (Bedsaul, Carter et al. 2018). Consequently, this initiates NF-κB activation via stimulation of the IKK complex, which phosphorylates IκB proteins. This phosphorylation leads to their degradation, ultimately releasing NF-κB dimers (Barnabei, Laplantine et al. 2021).

As the DLA showed the potential role of *CARD11* in NF-κB activation, we further investigated the effect of *CARD11* overexpression on the transcriptomic level in both cell lines. The analysis showed there were relatively more genes upregulated in HCT- 116 compared to the HT-29 cell line, indicating that *CARD11* overexpression has a more pronounced effect on the HCT-116. While HT-29 maintained a more stable expression pattern, HCT-116 showed significant activation of pathways related to immune responses.

CARD11 overexpression in HCT-116 was associated with promoted cell growth, tissue remodeling, and immune response. Notably, genes such as EP300, HIF1A, and DUSP1 were co-expressed, all of which also appeared elevated in CARD11+ adenoma patients, particularly in those exhibiting heightened immune microenvironment markers, such as IL6ST and collagen family members.

In the HCT-116 cell line, functional annotation of the top leading-edge genes associated with CARD11 overexpression revealed significant enrichment in pathways related to chromatin organization, cell cycle regulation, and apoptotic signaling. Among the frequently altered genes, EP300 emerged as a notable regulator. EP300 encodes a histone acetyltransferase that modulates chromatin structure and transcriptional activity, and has been implicated in the progression of multiple cancers, including bladder cancer (Meng *et al.*, 2021) and colorectal cancer (CRC). In CRC, EP300 influences the expression of pro- and anti-apoptotic genes such as BAX and BCL2, linking it to tumor cell survival and patient prognosis(Kowalczyk *et al.*, 2017). Additionally, STAT4, another gene enriched in the CARD11-overexpressing group, has been reported to promote CRC invasiveness. High

STAT4 expression is associated with increased tumor aggressiveness, whereas its inhibition leads to reduced proliferation and invasion (Cheng *et al.*, 2015). Furthermore, the expression of key cell cycle regulators—including RB1, CDK1, and EZH2—was also positively correlated with CARD11 overexpression. These findings suggest that CARD11 may contribute to CRC pathogenesis by modulating transcriptional regulators, chromatin structure, and cell cycle progression, further supporting its role as a driver of aggressive tumor behavior.

Interestingly, *CARD11* was co-expressed with IκB-ζ (*NFKBIZ*), one of the inhibitors in NF-κB signaling. Dysregulation of IκB-ζ disrupts the regulation of the canonical NF-κB pathway, leading to abnormal activation of various NF-κB target genes, including MAPK, E2F, and CDK1, among others. Therefore, modifications in the IκB-ζ expression may contribute to the improper control of cell cycle and survival pathways in CRC. Further exploration of how *CARD11* influences this process is necessary to fully understand the implications of CRC.

Additionally, a few genes, such as HDAC2 and *KDM5A*, related to chromatin remodeling were co-expressed with *CARD11*. *KDM5A* facilitates the recruitment of chromatin remodeling complexes to specific genomic loci, enabling gene expression changes in response to various cellular signals, including DNA damage (Gong *et al.*, 2017). In addition, *KDM5A* also regulates B cell proliferation and differentiation, essential for developing antibody-secreting plasma cells and memory B cells. Studies have shown that *KDM5A* can influence B cell differentiation in germinal centers, affecting specific IgG antibody production in response to antigens (Qu *et al.*, 2023), which may explain the increase in plasma B cells observed in the CIBERSORTX analysis.

The functional annotation of the top leading-edge genes showed significant enrichment of categories related to extracellular matrix organization, chemotaxis, and programmed cell death for the HT-29 cell line. As solid cancer progress, the ECM undergoes significant changes

in composition and function, which enable cancer cells to grow and spread. In most tumor tissues, ECM remodeling is characterized by increased collagen synthesis, which explains why we find more collagen-related genes in frequency analysis (Sangaletti *et al.*, 2017).

In HT-29 cells, CARD11 overexpression activated chemotaxis and ECM organization pathways. This was reflected in the upregulation of genes such as IL1RN, CXCL1, SPP1, and CCL22—key players in invasiveness, consistent with patterns observed in CARD11+ carcinoma patients. These patients also exhibited increased expression of MAPK8IP2, EMB, and CPEB4.

The top two frequently occurring genes in the *CARD11*-transfected HT-29 cell line were *CXCL1* and *CXCL3* chemokines. *CXCL1* promotes tumor progression by enhancing cell growth, motility, invasion, angiogenesis, and metastasis, making it a critical factor in the aggressive behavior of cancer cells across different types of cancer. *CXCL1* has been implicated in various cancers, including triple-negative breast cancer (Banerjee *et al.*, 2023). It is also shown that *CXCL1* promotes colon cancer development through the activation of NF-κB/P300 (Zhuo *et al.*, 2022). *CXCL3* has also been linked to attracting natural killer (NK) cells, T helper 1 (Th1) cells, monocytes, and CD8+ T cells, which are crucial in the immune response against tumors, which confirms our findings (Cheng *et al.*, 2023). *CCL22* was the other frequently occurring gene identified in the HT-29 cell line. Both *CXCL1* and *CXCL3* genes, along with *CCL22*, are involved in the chemotaxis of tumor cells and stromal cells within the surrounding microenvironment, which is essential in tumor dissemination during progression and metastasis. *CCL22* has been shown to regulate chemo-taxis and to be involved in the recruitment of T cells and other immune cells in breast, ovarian, and gastric cancers and leukemia (Roussos *et al.*, 2011).

As cell lines exhibit a homogenous system, and a two-dimensional culture might not be a true reflection of an actual tumor mass and tumor microenvironment, we next examined the transcriptional patterns in human FFPE tissue specimens from CRC patients with variable

expression levels of *CARD11*. For patients, *CARD11* overexpression was associated with different transcriptomics profiles at various stages of CRC.

Adenoma patients showed enrichment in pathways related to inflammation, immune response, and TIME. One gene co-expressed with *CARD11* was the IL-6 Receptor Subunit Beta (*IL6ST*), associated with IL6. Interestingly, IL6 modulates the TIME to facilitate metastatic colonization of CRC cells (Toyoshima *et al.*, 2019). Moreover, *IL6ST* affects the JAK/STAT pathway in CRC (Yue *et al.*, 2020). Other frequently enriched genes in adenoma include collagen family members, such as COL6A1, COL6A2, and COL6A3. These genes play crucial roles in cancer development and prognosis through their interactions with the tumor microenvironment and immune responses. Previous studies have shown that collagen proteins are increased in CRC patients (Kehlet *et al.*, 2016). Other genes related to the CRC progression through invasion, such as *GLI3* (Shen *et al.*, 2021), and proliferation, such as PIE-ZO2 (Shang *et al.*, 2023), were also identified.

CRC patients predominantly showed genes related to cancer hallmark pathways. *MAPK8IP2* is associated with the MAP kinase pathway, a common cancer pathway, and encodes the JNK interacting protein 2 or JIP2. In CRC patients in this study, MAPK8IP2promoted tumor progression, similar to its role in prostate cancer (Zeng *et al.*, 2022). The MAP kinase pathway can be activated through NF-κB dysregulation in some cancers (Hamoudi *et al.*, 2010), suggesting a similar interplay in CRC. MTMR2 promotes invasion and metastasis of gastric cancer via inactivating IFNγ/STAT1 signaling (Jiang *et al.*, 2019) and modulates TIME by fostering the progression of NK/T cell lymphoma by targeting JAK1 (Wang *et al.*, 2020). *EPHB6* is an ephrin-B receptor, where its overexpression promotes CRC and modulates the tumor immune microenvironment of primary colorectal adenocarcinomas metastasizing to the liver or lungs (Kim *et al.*, 2021). *CPEB4* is involved in the regulation of intestinal inflammation resolution and CRC development. *CPEB4* is overexpressed in inflammatory cells in patients with IBD and CRC, favoring tumor

development (Sibilio *et al.*, 2022). S100B is involved in the regulation of cell cycle progression and differentiation. It was found to be overexpressed in the liver metastases of CRC patients (Moravkova *et al.*, 2016).

In-silico validation of overall survival with the key genes and the literature findings support our data from the patients. The *IL6ST* is a critical component in the IL-6/STAT3 signaling pathway, which is known to promote CRC malignancy. Continuous activation of STAT3 by IL-6 signaling is linked to aggressive tumor behavior and poor patient prognosis in CRC (Heichler *et al.*, 2020). Based on our findings, aside from the *IL6ST* gene, CRC transition markers, such as GLI3, are also expressed at elevated levels. Studies utilizing data from The Cancer Genome Atlas (TCGA) and Gene Expression Omnibus (GEO) have shown that patients with elevated *GLI3* expression experience poorer survival outcomes compared to those with lower levels of *GLI3* (Shen *et al.*, 2021).

Kaplan–Meier's overall survival plot for CRC patients based on *MAPK8IP2* expression revealed a significant decrease ($p < 0.001$) in survival for colorectal patients with a higher expression of MAPK8IP2. Studies indicate that the suppression of *CPEB4* expression can enhance apoptosis and decrease cellular

proliferation in colon cancer cells. These reports suggest that *CPEB4* may help maintain the survival and proliferative capacity of metastatic CRC cells, thereby contributing to their invasive potential. In one of the studies, high *CPEB4* expression was correlated with advanced tumor stage, lymph node metastasis, distant metastasis, and poor prognosis in patients with CRC (Zhong *et al.*, 2015). It has also been shown that *CPEB4* is highly expressed in the peripheral blood of CRC patients as well (Chang *et al.*, 2014).

Investigation of the immune cell distribution profile between the cell lines and patients was performed by applying CIBERSORTX to the transcriptomic data. The results identified differences in immune cell types in *CARD11* overexpressed HCT-116 compared to the empty vector, suggesting modulation of TIME related to the progression of CRC. The analysis showed

that B cell infiltration of primary CRC was characterized by an accumulation of terminally differentiated memory B cells or plasma cells. This observation suggested a specific immune response against the tumor (Shimabukuro-Vornhagen *et al.*, 2014), most likely through the dysregulation of NF-κB as the NF-κB pathway is essential for generating a complete and diverse B cell pool, with different B cell subsets showing varying degrees of dependence on NF-κB signaling for survival and development (Roy *et al.*, 2023). In addition, CD8 T cells were depleted with *CARD11* overexpression, which can be a sign of immune suppression and may lead to cancer progression.

In the current study, the results showed an increase in the proportion of the NK resting cells in *CARD11*-transfected HCT-116 compared to the control. One of the studies deconvolving immune cells from bulk transcriptomes of 521 human CRCs found that NK cells are present in colorectal tumors. However, most of these cells in CRC adopt a "resting", non-activated state, which supports our finding. It must be noted that the increase in the resting NK cells of the HT-29 cell line is not significant, which implies that the HT-29 cell line is still capable of balancing itself, unlike the HCT-116 cell line, which became increasingly aggressive and uncontrollable as a result of *CARD11* transfection (Dean *et al.*, 2024).

CIBERSORTX analysis for the HT-29 cell line showed that *CARD11* overexpression led to a significant increase in CD8 T cells, indicating that the cell line is still intact and attempting to combat cancer cells by infiltrating CD8 T cells to the TIME. The presence of elevated CD8+ T cells in the tumor microenvironment has been linked to a favorable prognosis in cancer (Maimela *et al.*, 2019). GSEA results for HT-29 revealed enrichment in genes involved in the upregulation of transcripts related to T cell function, consistent with the increased number of CD8 T cells identified in this study. However, in the HCT-116 control, a fraction of CD8 T cells already existed but was depleted in *CARD11* overexpressed HCT-116. Therefore, the two CRC cell lines were affected by *CARD11* overexpression in different ways. In CRC patients, the results showed distinct immune cell types with different

proportions between *CARD11*– and *CARD11*+ patients in adenoma and carcinoma. Adenoma patients exhibited higher fractions of CD4 memory resting T cells compared to other groups, whereas carcinoma cases showed higher fractions of M0-type macrophages as opposed to other groups. These findings suggest a more complex interplay between innate and acquired immune responses in CRC progression and pathogenesis. Moreover, there seemed to be a difference in the distribution profile of immune cells between different cell lines and patients, supporting the conclusion in this study that obtaining different GSEA results is as expected.

Taken together, the results showed the involvement of *CARD11* overexpression in CRC pathogenesis via the dysregulation of the NF-κB pathway. The loss of tight control of the NF-κB pathway leads to a shift in the cellular response related to cell cycle, proliferation, and apoptosis, which are critical pathways in CRC, as well as modulation in the tumor immune microenvironment associated with CRC. This conclusion is inferred from the presence of different types of immune responses in various stages of CRC.

The immuno-staining confirmed that the cells exhibited positive expression of the CARD11 receptor. Generally, the staining was distributed over larger areas in the adenocarcinomas than in situ or carcinoma. However, CARD11 staining was found in some samples but absent in others, and its intensity and distribution also varied mainly due to intra-tumoural heterogeneity. This variability suggests that CARD11 may serve as an early biomarker for CRC in some of the CRC cases, but at the same time, it also indicates that additional biomarkers may exist to map CRC progression.

### 6.2 Adenocarcinoma vs Adenoma CRC Study

Three stages of CRC, Adenoma, Carcinoma in situ, and Adenocarcinoma, were covered in this study. Adenoma is a non-cancerous (benign) tumor originates from glandular epithelium of the colon and is considered as early marker for CRC and can be classified further into three main different types based on histological features, Tubular adenoma which is the most common type with a tubular structure, Tubulovillous adenoma which have both tubular

and villous features and have higher risk for cancer progression, and villous adenoma, the least common form but having significant risk of malignancy(Pan et al., 2023).

Carcinoma in-situ refers to a localized form of cancer where abnormal cells growth is present but has not spread to surrounding tissues. CIS can be defined as non-invasive limited to the mucosa, not deeper layers, progression potential which could turn invasive if untreated, and detection which is usually detected during colonoscopy and has no symptoms (Tian et al., 2021).

On the other hand, Adenocarcinoma is a malignant form of CRC that arises from glandular epithelial cells and is characterized by invasive behavior, metastasizes to the surroundings, and has different stages ranging from localized to advanced (Sawicki et al., 2021). Since all of the various stages of CRC could share similar symptoms such as bowel habits changes, abdominal pain, weight loss, and rectal bleeding (Holtedahl et al., 2021), there is still a need for the identification of molecular key markers for a better prognosis and therapeutic strategies. The objective of the research is to investigate potential biomarkers to facilitate better differentiation between the different stages of CRCThe study showed there are differences in biomarkers with the distinct CRC stages. For adenoma samples, the following biomarkers, *CTBP1* and *ARRB1* genes, were identified: *CTBP1* gene was previously reported to be associated with an Adenomatous polyposis coli (*APC*) tumour suppressor, indicating a role in suppressing Wnt target gene expression. Specifically in CRC, *APC* mutations that involve the *CTBP-APC* interaction lead to a dysfunctional Wnt signaling, driving cancer development (Hamada & Bienz, 2004; Sierra et al, 2006), whereas *ARRB1* gene Transcriptional Regulation which interacts with the transcription factor NF-κB, playing a role in regulating the expression of genes involved in immune responses and inflammation, hence associated with cancer progression. It can regulate cell proliferation, migration, and invasion, often through its effects on *GPCR* signaling and downstream pathways such as the *MAPK*/*ERK* and *PI3K*/*AKT* pathways, it can be context- dependent, as it may act as either a

promoter or suppressor of tumor growth depending on the specific signaling context and cancer type (Rosanò & Bagnato, 2016).

On the other hand, the *COL1A2*, *CEBPZ*, *MED10*, and *PAWR* genes were identified as biomarkers in adenocarcinoma samples. *COL1A2* gene (collagen type I alpha 3 chain) is a key component in ECM and may indicate its role in tumor progression and tumor microenvironment. The *COL1A2* expression was significantly upregulated in Adenocarcinoma (*p*-value: 0.0075). This was also highlighted by (Yuan et al., 2023) Yuan *et. al* , suggesting a disadvantageous prognosis, and there was evidence that *COL1A2* is positively corelated with immune infiltration. Moreover, it was reported that *COL1A2* is a potential biomarker for detecting adenocarcinoma (Jin et al., 2022; Mortezapour et al., 2023). The Enhancer Binding Protein Zeta (*CEBPZ*) is a cellular protein that responds to environmental stimuli. It functions as a DNA-binding transcriptional activator, specifically mediating the heat-shock protein 70 (*HSP70*) promoter. *CEBPZ* is also involved in hematopoietic differentiation. Notably, this gene positively correlated with potential prognostic value as a CRC biomarker, as determined by the Human Protein Atlas (Proteinatlas). The *MED10* gene is a component of the Mediator complex and functions as a coactivator for DNA-binding transcription factors that facilitate RNA polymerase II activation. Research has established a correlation between aberrant expression of the *MED10* gene and advanced tumor stages, as well as diminished survival outcomes in bladder urothelial carcinoma patients (Wu et al., 2021). Lastly, the *PAWR* gene, as an antitumor suppressor gene, exhibits antitumor activity by inducing the apoptosis of uncontrolled cell growth through intracellular and extracellular mechanisms. Specifically, it induces apoptosis through the Fas-mediated pathway and binds to glucose-regulated protein 78 (*GRP78*), activating the extrinsic apoptotic pathway. Furthermore, higher expression of this gene has been associated with improved survival outcomes in various cancers, including prostate, ovarian, and bladder cancers (Cheratta et al., 2021; Tan et al., 2020; Yang et al., 2021).

# Chapter VII.

# Conclusion

## 7.1 Conclusion and Recommendations

This thesis explored the molecular mechanisms underlying colorectal cancer (CRC) progression, integrating two complementary studies: one focused on the effects of CARD11 overexpression in CRC, and the other on genes and pathways changes across distinct stages of CRC development.

The study demonstrated that in CRC, CARD11 overexpression results in the dysregulation of the NF-κB pathway, which subsequently activates various cellular pathways and genes involved in the modulating the immune microenvironment and promoting cancer progression. Whole transcriptome RNAseq analysis revealed CARD11's crucial role in promoting cell growth and tissue remodeling in the HCT-116 CRC cell line, and in activating chemotaxis and extracellular matrix (ECM) organization in the HT-29 cell line. Key genes associated with CARD11 overexpression included EP300, KDM5A, HIF1A, NFKBIZ, and DUSP1 in HCT-116, and IL1RN, MDK, SPP1, and various chemokines—CXCL1, CXCL3, and CCL22—in HT-29.

In CRC patients, CARD11+ adenoma cases exhibited elevated expression of IL6ST, GLI3, and PIEZO2, as well as members of the collagen gene family. In contrast, CARD11+ carcinoma cases exhibited a dramatic upregulation of MAPK8IP2, MTMR2, EMB, EPHB6, and CPEB4, reflecting the progression-linked activation of cancer hallmarks. The results showed that CARD11 overexpression contributes to the progression of CRC through modulation of various tumor immune microenvironment pathways and activation of cancer pathways via the dysregulation of NF-κB.

Complementing this, transcriptomic profiling across progressive stages of CRC adenoma, carcinoma in situ (CIS), and adenocarcinoma identified candidate biomarkers specific to each stage. CIS was characterized by significant enrichment in apoptotic signaling and Wnt pathways, whereas adenocarcinoma was associated with the activation of transcriptional co-regulatory mechanisms and ECM remodeling. Biomarkers validated via RT-qPCR included ARRB1 for adenoma, COL4A5 and RPS3A for CIS, and COL1A2 and MED10 for adenocarcinoma.

Taken together, these findings offer a comprehensive understanding of CRC pathogenesis, revealing how CARD11 influences immune modulation and cancer-related signaling, and highlighting stage-specific molecular targets. While further validation in independent cohorts is necessary, the current work lays a strong foundation for future translational research in CRC diagnosis, prognosis, and targeted therapy.

**7.2 Limitations of the Study**

There are a few limitations to this study. While using CIBERSORTx to predict the immune cell environment is based on in silico analysis, it only provides insights into the possibility of tumor cells secreting or behaving like immune cells through their transcriptome profile. Moreover, the transcriptomic analysis in CRC cell lines was conducted post-transient transfection in HCT-116 and HT-29. It is possible that short-term transfection in CRC cell lines will result in transcriptomic changes that are distinct from those observed in cell lines evolved under selective pressure for *CARD11* overexpression. The results from this study warrant further work to investigate some of the molecular mechanisms of *CARD11* in CRC, which could be conducted using 3D organoid models. Despite these limitations, the following two points ensured the experiments' validity: (a) the analysis involved *CARD11*– and *CARD11*+ CRC patient samples, which is a better in vivo model with a more intact tumor immune microenvironment than the homogenous CRC cell line, 3D organoid, and in vivo mouse models; and (b) two cell lines from different stages of CRC were used to investigate the effect of

*CARD11* overexpression on CRC.

### 7.3 Future Work

Despite the relatively limited sample size and lack of validation in a broader population, the results indicate that transcriptional profiling can be a valuable method for identifying biomarkers involved in the pathogenesis of $CARD11^{+}$ and $CARD11^{-}$ colorectal cancer (CRC). Additional research could be conducted across diverse population cohorts to understand better the role of CARD11 in CRC initiation and progression.

Future work focuses on several key directions to expand upon these findings:

- Utilizing 3D organoid models to experimentally test the functional roles of the identified genes in CRC pathogenesis, offering a physiologically relevant platform for mechanistic studies.
- Identifying potential binding partners for CARD11 in CRC to uncover novel protein–protein interactions that may contribute to tumor development and immune modulation.
- Exploring shared molecular pathways between inflammatory bowel disease (IBD) and CRC, which may reveal overlapping mechanisms and therapeutic targets linking chronic inflammation to carcinogenesis.
- Conducting functional characterizations of the identified genes using various biological assays, including those assessing immune response, apoptosis, and cellular proliferation, to determine their mechanistic contributions to CRC progression.

These approaches could provide deeper insights into the molecular landscape of CRC and reinforce the potential of CARD11 as both a biomarker and a therapeutic target.

## References


Ahmad, R., Singh, J. K., Wunnava, A., Al-Obeed, O., Abdulla, M., & Srivastava, S. K. (2021). Emerging trends in colorectal cancer: Dysregulated signaling pathways (Review). *Int J Mol Med, 47*(3). doi:10.3892/ijmm.2021.4847

Ahmed, D., Eide, P. W., Eilertsen, I. A., Danielsen, S. A., Eknæs, M., Hektoen, M., Lind, G. E., & Lothe, R. A. (2013). *Epigenetic and genetic features of 24 colon cancer cell lines. Oncogenesis, 2*(9), e71-e71. https://doi.org/10.1038/oncsis.2013.35

Alzaabi, A. (2022). Colorectal Cancer in the Arab World. In (pp. 363-379). Springer Singapore. https://doi.org/10.1007/978-981-16-7945-2_23

Attar, L., Trabulsi, N., Maghrabi, A. A., & Nassif, M. (2018). Adenocarcinoma of the Colon Disguised as Abdominal Wall Abscess: Case Report and Review of the Literature. *Case Reports in Surgery*, 2018, 1-6. https://doi.org/10.1155/2018/1974627

Banerjee, S. M., Acedo, P., El Sheikh, S., Harati, R., Meecham, A., Williams, N. R., ... & Hamoudi, R. (2023). Combination of verteporfin-photodynamic therapy with 5-aza-2'-deoxycytidine enhances the anti-tumour immune response in triple-negative breast cancer. *Frontiers in Immunology*, *14*, 1188087. https://doi.org/10.3389/fimmu.2023.1188087.

Baojun, D. Y., Zhao; Jun, Bai; Jianhua, Wang; Xianglong, Duan; Xiaohui, Luo; Rong Zhang; Yansong, Pu; Mingqing, Kou; Jianyuan, Lei; and Shangzhen, Yang. (2022). Chapter 1 Colorectal Cancer: An Overview. In M.-D. Jose (Ed.), *Gastrointestinal Cancers*. Exon Publications. https://www.ncbi.nlm.nih.gov/books/NBK586003/#Ch1-cit0012

Bauer, V. P., & Papaconstantinou, H. T. (2008). Management of serrated adenomas and hyperplastic polyps. *Clinics in Colon and Rectal Surgery, 21*(04), 273-279. https://doi.org/10.1055/s-0028-1089942

Bedsaul, J. R., Carter, N. M., Deibel, K. E., Hutcherson, S. M., Jones, T. A., Wang, Z., ... & Pomerantz, J. L. (2018). Mechanisms of regulated and dysregulated *CARD11* signaling in adaptive immunity and disease. *Frontiers in Immunology*, *9*, 2105. https://doi.org/10.3389/fimmu.2018.02105.

Berg, K. C. G., Eide, P. W., Eilertsen, I. A., Johannessen, B., Bruun, J., Danielsen, S. A., Bjørnslett, M., Meza-Zepeda, L. A., Eknæs, M., Lind, G. E., Myklebost, O., Skotheim, R. I., Sveen, A., & Lothe, R. A. (2017). Multi-omics of 34 colorectal cancer cell lines - a resource for biomedical studies. *Molecular Cancer, 16*(1). https://doi.org/10.1186/s12943-017-0691-y

Bresalier, R. S., Grady, W. M., Markowitz, S. D., Nielsen, H. J., Batra, S. K., & Lampe, P. D. (2020). Biomarkers for Early Detection of Colorectal Cancer: The Early Detection Research Network, a Framework for Clinical Translation. *Cancer Epidemiology Biomarkers & Prevention, 29*(12), 2431-2440. https://doi.org/10.1158/1055-9965.epi-20-0234

Bu, R., Bavi, P., Abubaker, J., Jehan, Z., Al-Haqawi, W., Ajarim, D., Al-Dayel, F., Uddin, S., & Al-Kuraya, K. S. (2012). Role of nuclear factor-κB regulators TNFAIP3 and *CARD11* in Middle Eastern diffuse large B-cell lymphoma. *Leukemia & Lymphoma, 53*(10), 1971-1977. https://doi.org/10.3109/10428194.2012.668286

Chang, Y. T., Huang, C. S., Yao, C. T., Su, S. L., Terng, H. J., Chou, H. L., ... & Chu, C. M. (2014). Gene expression profile of peripheral blood in colorectal cancer. *World journal of gastroenterology: WJG*, *20*(39), 14463. https://doi.org/10.3748/wjg.v20.i39.14463.

Chardalias, L., Papaconstantinou, I., Gklavas, A., Politou, M., & Theodosopoulos, T. (2023). Iron Deficiency Anemia in Colorectal Cancer Patients: Is Preoperative Intravenous Iron Infusion Indicated? A Narrative Review of the Literature. *Cancer Diagnosis & Prognosis, 3*(2), 163-168. https://doi.org/10.21873/cdp.10196

Chen, X., Ma, Z., Yi, Z., Wu, E., Shang, Z., Tuo, B., ... & Liu, X. (2024). The effects of metabolism on the immune microenvironment in colorectal cancer. *Cell Death Discovery*, *10*(1), 118. https://doi.org/10.1038/s41420-024-01865-z.

Cheng, J. M., Yao, M. R., Zhu, Q., Wu, X. Y., Zhou, J., Tan, W. L., & Zhan, S. H. (2015). Silencing of stat4 gene inhibits cell proliferation and invasion of colorectal cancer cells. *Journal of Biological Regulators and Homeostatic Agents*, *29*(1), 85-92.

Cheng, Y., Yang, X., Liang, L., Xin, H., Dong, X., Li, W., ... & Wang, W. (2023). Elevated expression of *CXCL3* in colon cancer promotes malignant behaviors of tumor cells in an ERK-dependent manner. *BMC cancer*, *23*(1), 1162. https://doi.org/10.21203/rs.3.rs-2551584/v1.

Christian, F., Smith, E. L., & Carmody, R. J. (2016). The regulation of NF-κB subunits by phosphorylation. *Cells*, *5*(1), 12. https://doi.org/10.3390/cells5010012.

Colling, R., Wang, L. M., & Soilleux, E. (2016). Automated PCR detection of BRAF mutations in colorectal adenocarcinoma: a diagnostic test accuracy study. *Journal of Clinical Pathology*, *69*(5), 398-402. https://doi.org/10.1136/jclinpath-2015-203345

Colussi, D., Brandi, G., Bazzoli, F., & Ricciardiello, L. (2013). Molecular Pathways Involved in Colorectal Cancer: Implications for Disease Behavior and Prevention. International *Journal of Molecular Sciences, 14*(8), 16365-16385. https://doi.org/10.3390/ijms140816365

Corsale, A. M., Di Simone, M., Lo Presti, E., Dieli, F., & Meraviglia, S. (2023). gammadelta T cells and their clinical application in colon cancer. *Front Immunol, 14*, 1098847. doi:10.3389/fimmu.2023.1098847

Davis, R. E., Brown, K. D., Siebenlist, U., & Staudt, L. M. (2001). Constitutive nuclear factor κB activity is required for survival of activated B cell-like diffuse large B cell

lymphoma cells. *The Journal of Experimental Medicine*, *194*(12), 1861-1874. https://doi.org/10.1084/jem.194.12.1861.

Dean, I., Lee, C. Y., Tuong, Z. K., Li, Z., Tibbitt, C. A., Willis, C., ... & Withers, D. R. (2024). Rapid functional impairment of natural killer cells following tumor entry limits anti-tumor immunity. *Nature Communications*, *15*(1), 683. https://doi.org/10.1038/s41467-024-44789-z.

Dobre, M., Trandafir, B., Milanesi, E., Salvi, A., Ioana, Vasilescu, C., Niculae, A. M., Herlea, V., Hinescu, M. E., & Constantinescu, G. (2022). Molecular profile of the <scp>NF-κB</scp> signalling pathway in human colorectal cancer. *Journal of Cellular and Molecular Medicine, 26*(24), 5966-5975. https://doi.org/10.1111/jcmm.17545

Dong, G., Chanudet, E., Zeng, N., Appert, A., Chen, Y.-W., Au, W.-Y., Hamoudi, R. A., Watkins, A. J., Ye, H., Liu, H., Gao, Z., Chuang, S.-S., Srivastava, G., & Du, M.-Q. (2011). 20, ABIN-1/2, and *CARD11* Mutations and Their Prognostic Value in Gastrointestinal Diffuse Large B-Cell Lymphoma. *Clinical Cancer Research, 17*(6), 1440-1451. https://doi.org/10.1158/1078-0432.ccr-10-1859

Dorjbal, B., Stinson, J. R., Ma, C. A., Weinreich, M. A., Miraghazadeh, B., Hartberger, J. M., ... & Snow, A. L. (2019). Hypomorphic caspase activation and recruitment domain 11 (*CARD11*) mutations associated with diverse immunologic phenotypes with or without atopic disease. *Journal of Allergy and Clinical Immunology*, *143*(4), 1482-1495. https://doi.org/10.1016/j.jaci.2018.08.013.

Dorrington, Michael G., and Iain DC Fraser. "NF-κB signaling in macrophages: dynamics, crosstalk, and signal integration." *Frontiers in Immunology* 10 (2019): 705. https://doi.org/10.3389/fimmu.2019.00705.

Du, W., Quan, X., Wang, C., Song, Q., Mou, J., & Pei, D. (2024). Regulation of tumor metastasis and CD8+ T cells infiltration by circRNF216/miR-576-5p/ZC3H12C axis in

colorectal cancer. *Cellular & Molecular Biology Letters, 29*(1), 19. doi:10.1186/s11658-024-00539-z

Evrard, Tachon, Randrian, Karayan, T., & Tougeron. (2019). Microsatellite Instability: Diagnosis, Heterogeneity, Discordance, and Clinical Impact in Colorectal Cancer. *Cancers, 11*(10), 1567. https://doi.org/10.3390/cancers11101567

Fleming, M., Ravula, S., Tatishchev, S. F., & Wang, H. L. (2012). Colorectal carcinoma: Pathologic aspects. *J Gastrointest Oncol, 3*(3), 153-173. https://doi.org/10.3978/j.issn.2078-6891.2012.030

Ghatak, S., Mehrabi, S. F., Mehdawi, L. M., Satapathy, S. R., & Sjölander, A. (2022). Identification of a Novel Five-Gene Signature as a Prognostic and Diagnostic Biomarker in Colorectal Cancers. *International Journal of Molecular Sciences, 23*(2), 793. https://doi.org/10.3390/ijms23020793

Gibney, G. T., Messina, J. L., Fedorenko, I. V., Sondak, V. K., & Smalley, K. S. (2013). Paradoxical oncogenesis—the long-term effects of BRAF inhibition in melanoma. *Nature Reviews Clinical Oncology, 10*(7), 390-399. https://doi.org/10.1038/nrclinonc.2013.83

Gong, F., Clouaire, T., Aguirrebengoa, M., Legube, G., & Miller, K. M. (2017). Histone demethylase *KDM5A* regulates the ZMYND8–NuRD chromatin remodeler to promote DNA repair. *Journal of Cell Biology*, *216*(7), 1959-1974. https://doi.org/10.1083/jcb.201611135.

Gonzalez-Pons, M., & Cruz-Correa, M. (2015). Colorectal Cancer Biomarkers: Where Are We Now? *BioMed Research International*, 2015, 1-14. https://doi.org/10.1155/2015/149014

Gorroño-Etxebarria, I., Aguirre, U., Sanchez, S., González, N., Escobar, A., Zabalza, I., Quintana, J. M., Vivanco, M. D., Waxman, J., & Kypta, R. M. (2019). Wnt-11 as a

Potential Prognostic Biomarker and Therapeutic Target in Colorectal Cancer. *Cancers, 11*(7), 908. https://doi.org/10.3390/cancers11070908

Grigorean, V. T., Erchid, A., Coman, I. S., & Liţescu, M. (2023). Colorectal Cancer—The "Parent" of Low Bowel Obstruction. *Medicina, 59*(5), 875. https://doi.org/10.3390/medicina59050875

Hamoudi, R. A., Appert, A., Ye, H., Ruskone-Fourmestraux, A., Streubel, B., Chott, A., ... & Du, M. Q. (2010). Differential expression of NF-κB target genes in MALT lymphoma with and without chromosome translocation: insights into molecular mechanism. *Leukemia*, *24*(8), 1487-1497. https://doi.org/10.1038/leu.2010.118.

Hanahan, D., & Weinberg, R. A. (2011). Hallmarks of cancer: the next generation. *Cell*, *144*(5), 646-674. http://dx.doi.org/10.1016/j.cell.2011.02.013

Hassanzadeh, P. (2011). Colorectal cancer and NF-κB signaling pathway. *Gastroenterology and Hepatology From Bed to Bench*, *4*(3), 127.

Heichler, C., Scheibe, K., Schmied, A., Geppert, C. I., Schmid, B., Wirtz, S., ... & Neufert, C. (2020). STAT3 activation through IL-6/IL-11 in cancer-associated fibroblasts promotes colorectal tumour development and correlates with poor prognosis. *Gut*, *69*(7), 1269-1282. https://doi.org/10.1136/gutjnl-2019-319200.

Holtedahl, K., Borgquist, L., Donker, G. A., Buntinx, F., Weller, D., Campbell, C., . . . Parajuli, R. (2021). Symptoms and signs of colorectal cancer, with differences between proximal and distal colon cancer: a prospective cohort study of diagnostic accuracy in primary care. *BMC Family Practice, 22*(1), 148. doi:10.1186/s12875-021-01452-6

IJspeert, J. E., Vermeulen, L., Meijer, G. A., & Dekker, E. (2015). Serrated neoplasia—role in colorectal carcinogenesis and clinical implications. *Nature Reviews Gastroenterology & Hepatology, 12*(7), 401-409. https://doi.org/10.1038/nrgastro.2015.73

Jiang, L., Liu, J. Y., Shi, Y., Tang, B., He, T., Liu, J. J., ... & Yu, P. W. (2019). MTMR2 promotes invasion and metastasis of gastric cancer via inactivating IFNγ/STAT1 signaling. *Journal of Experimental & Clinical Cancer Research*, *38*, 1-16. https://doi.org/10.1186/s13046-019-1186-z.

Jögi, A., Vaapil, M., Johansson, M., & Påhlman, S. (2012). Cancer cell differentiation heterogeneity and aggressive behavior in solid tumors. *Upsala Journal of Medical Sciences*, *117*(2), 217-224. https://doi.org/10.3109/03009734.2012.659294.

Jogi, A.; Vaapil, M.; Johansson, M.; Pahlman, S. Cancer cell differentiation heterogeneity and aggressive behavior in solid tumors. *Ups. J. Med. Sci.* **2012**, *117*, 217–224. https://doi.org/10.3109/03009734.2012.659294

Kanwar, S. S., Yu, Y., Nautiyal, J., Patel, B. B., & Majumdar, A. P. (2010). The Wnt/β-catenin pathway regulates growth and maintenance of colonospheres. *Molecular Cancer, 9*(1), 212. https://doi.org/10.1186/1476-4598-9-212

Kasprzak, A. (2021). The Role of tumor microenvironment cells in colorectal cancer (CRC) cachexia. *International Journal of Molecular Sciences, 22*(4), 1565. https://doi.org/10.3390/ijms22041565

Kehlet, S. N., Sanz-Pamplona, R., Brix, S., Leeming, D. J., Karsdal, M. A., & Moreno, V. (2016). Excessive collagen turnover products are released during colorectal cancer progression and elevated in serum from metastatic colorectal cancer patients. *Scientific reports*, *6*(1), 30599. https://doi.org/10.1038/srep30599.

Khorrami, S., Zavaran Hosseini, A., Mowla, S. J., & Malekzadeh, R. (2015). Verification of ALDH activity as a biomarker in colon cancer stem cells-derived HT-29 cell line. Iranian *Journal of Cancer Prevention, 8*(5). https://doi.org/10.17795/ijcp-3446

Kim, J. C., Ha, Y. J., Park, I. J., Kim, C. W., Yoon, Y. S., Lee, J. L., ... & Kim, Y. S. (2021). Tumor immune microenvironment of primary colorectal adenocarcinomas

metastasizing to the liver or lungs. *Journal of Surgical Oncology*, *124*(7), 1136-1145. https://doi.org/10.1002/jso.26631.

Kowalczyk, A. E., Krazinski, B. E., Godlewski, J., Kiewisz, J., Kwiatkowski, P., Sliwinska-Jewsiewicka, A., ... & Kmiec, Z. (2017). Expression of the *EP300*, TP53 and BAX genes in colorectal cancer: Correlations with clinicopathological parameters and survival. *Oncology Reports*, *38*(1), 201-210. https://doi.org/10.3892/or.2017.5687.

Kuipers, E. J., Grady, W. M., Lieberman, D., Seufferlein, T., Sung, J. J., Boelens, P. G., Van De Velde, C. J. H., & Watanabe, T. (2015). Colorectal cancer. *Nature Reviews Disease Primers, 1*(1), 15065. https://doi.org/10.1038/nrdp.2015.65

Kuwahara, T., Hazama, S., Suzuki, N., Yoshida, S., Tomochika, S., Nakagami, Y., . . . Nagano, H. (2019). Intratumoural-infiltrating CD4 + and FOXP3 + T cells as strong positive predictive markers for the prognosis of resectable colorectal cancer. *British Journal of Cancer, 121*(8), 659-665. doi:10.1038/s41416-019-0559-6

La Vecchia, S., & Sebastián, C. (2020). Metabolic pathways regulating colorectal cancer initiation and progression. *Seminars in Cell & Developmental Biology, 98*, 63-70. https://doi.org/10.1016/j.semcdb.2019.05.018

Lenz, G., Davis, R. E., Ngo, V. N., Lam, L., George, T. C., Wright, G. W., ... & Staudt, L. M. (2008). Oncogenic *CARD11* mutations in human diffuse large B cell lymphoma. *Science*, *319*(5870), 1676-1679. *Science, 319(*5870), 1676-1679. https://doi.org/10.1126/science.1153629

Lewandowska, A., Rudzki, G., Lewandowski, T., Stryjkowska-Gora, A., & Rudzki, S. (2022). Risk factors for the diagnosis of colorectal cancer. *Cancer control*, *29*, 10732748211056692. https://doi.org/10.1177/10732748211056692.

Li, H. (2012). Exploring single-sample SNP and INDEL calling with whole-genome de novo assembly. *Bioinformatics*, *28*(14), 1838-1844. https://doi.org/10.1093/bioinformatics/bts280.

Li, Y., Chen, Z., Han, J., Ma, X., Zheng, X., & Chen, J. (2022). Functional and Therapeutic Significance of Tumor-Associated Macrophages in Colorectal Cancer. *Front Oncol, 12*, 781233. doi:10.3389/fonc.2022.781233

Link, A., Balaguer, F., Shen, Y., Nagasaka, T., Lozano, J. J., Boland, C. R., & Goel, A. (2010). Fecal MicroRNAs as novel biomarkers for colon cancer screening. *Cancer Epidemiology, Biomarkers & Prevention, 19*(7), 1766-1774. https://doi.org/10.1158/1055-9965.epi-10-0027

Liu, X., Zhang, G., Li, S., Liu, Y., Ma, K., & Wang, L. (2024). Identification of gut microbes-related molecular subtypes and their biomarkers in colorectal cancer. *Aging (Albany NY)*, *16*(3), 2249. https://doi.org/10.18632/aging.205480

Liu, Y., Sethi, N. S., Hinoue, T., Schneider, B. G., Cherniack, A. D., Sanchez-Vega, F., & Meyerson, M. (2018). Comparative molecular analysis of gastrointestinal adenocarcinomas. *Cancer Cell, 33*(4), 721-735. https://doi.org/10.1016/j.ccell.2018.03.010

Loktionov, A. (2020). Biomarkers for detecting colorectal cancer non-invasively: DNA, RNA or proteins? *World Journal of Gastrointestinal Oncology, 12*(2), 124-148. https://doi.org/10.4251/wjgo.v12.i2.124

Love, M. I., Huber, W., & Anders, S. (2014). Moderated estimation of fold change and dispersion for RNA-seq data with DESeq2. *Genome Biology*, *15*, 1-21. https://doi.org/10.1186/s13059-014-0550-8.

Lu, H. Y., Sharma, M., Sharma, A. A., Lacson, A., Szpurko, A., Luider, J., & Turvey, S. E. (2021). Mechanistic understanding of the combined immunodeficiency in complete

human *CARD11* deficiency. *Journal of Allergy and Clinical Immunology*, *148*(6), 1559-1574. https://doi.org/10.1016/j.jaci.2021.04.006

MacLeod, M. K., Clambey, E. T., Kappler, J. W., & Marrack, P. (2009). CD4 memory T cells: what are they and what can they do? *Semin Immunol, 21*(2), 53-61. doi:10.1016/j.smim.2009.02.006

Maimela, N. R., Liu, S., & Zhang, Y. (2019). Fates of CD8+ T cells in tumor microenvironment. *Computational and structural biotechnology journal*, *17*, 1-13. https://doi.org/10.1016/j.csbj.2018.11.004.

Marcuello, M., Vymetalkova, V., Neves, R. P., Duran-Sanchon, S., Vedeld, H. M., Tham, E., ... & Gironella, M. (2019). Circulating biomarkers for early detection and clinical management of colorectal cancer. *Molecular Aspects of Medicine*, *69*, 107-122. https://doi.org/10.1016/j.mam.2019.06.002

Martin, M., Sun, M., Motolani, A., & Lu, T. (2021). The pivotal player: components of NF-κB pathway as promising biomarkers in colorectal cancer. *International Journal of Molecular Sciences*, *22*(14), 7429. https://doi.org/10.3390/ijms22147429.

Masle-Farquhar, E., Jeelall, Y., White, J., Bier, J., Deenick, E. K., Brink, R., . . . Goodnow, C. C. (2023). CARD11 gain-of-function mutation drives cell-autonomous accumulation of PD-1(+) ICOS(high) activated T cells, T-follicular, T-regulatory and T-follicular regulatory cells. *Front Immunol, 14*, 1095257. doi:10.3389/fimmu.2023.1095257

McGuire, M. H., Dasari, S. K., Yao, H., Wen, Y., Mangala, L. S., Bayraktar, E., ... & Sood, A. K. (2021). Gene body methylation of the lymphocyte-specific gene *CARD11* results in its overexpression and regulates cancer mTOR signaling. *Molecular Cancer Research*, *19*(11), 1917-1928. https://doi.org/10.1158/1541-7786.mcr-20-0753

Mehran Taherian, Saran Lotfollahzadeh ., Parnaz Daneshpajouhnejad, and Komal Arora. (2023). *Tubular adenoma*. StatPearls [Internet]. https://www.ncbi.nlm.nih.gov/books/NBK553180/

Meklin, J., Syrjänen, K., & Eskelinen, M. (2020). Fecal occult blood tests in colorectal cancer screening: Systematic Review and meta-analysis of traditional and new-generation fecal immunochemical tests. *Anticancer Research, 40*(7), 3591-3604. https://doi.org/10.21873/anticanres.14349

Meng, J., Lu, X., Zhou, Y., Zhang, M., Ge, Q., Zhou, J., ... & Liang, C. (2021). Tumor immune microenvironment-based classifications of bladder cancer for enhancing the response rate of immunotherapy. *Molecular Therapy-Oncolytics*, *20*, 410-421. https://doi.org/10.1016/j.omto.2021.02.001.

Moravkova, P., Kohoutova, D., Rejchrt, S., Cyrany, J., & Bures, J. (2016). Role of S100 proteins in colorectal carcinogenesis. *Gastroenterology research and practice*, *2016*(1), 2632703. https://doi.org/10.1155/2016/2632703.

Murphy, N., Moreno, V., Hughes, D. J., Vodicka, L., Vodicka, P., Aglago, E. K., Gunter, M. J., & Jenab, M. (2019). Lifestyle and dietary environmental factors in colorectal cancer susceptibility. *Molecular Aspects of Medicine, 69*, 2-9. https://doi.org/10.1016/j.mam.2019.06.005

Newman, A. M., Liu, C. L., Green, M. R., Gentles, A. J., Feng, W., Xu, Y., .... & Alizadeh, A. A. (2015). Robust enumeration of cell subsets from tissue expression profiles. *Nature Methods*, *12*(5), 453-457. https://doi.org/10.1038/nmeth.3337.

Ng, L., Wan, T. M. H., Man, J. H. W., Chow, A. K. M., Iyer, D., Chen, G.,..... & Law, W. L. (2017). Identification of serum miR-139-3p as a non-invasive biomarker for colorectal cancer. *Oncotarget*, *8*(16), 27393. https://doi.org/10.18632/oncotarget.16171

Nguyen, L. H., Goel, A., & Chung, D. C. (2020). Pathways of Colorectal Carcinogenesis. *Gastroenterology, 158*(2), 291-302. https://doi.org/10.1053/j.gastro.2019.08.059

Ning, Z., Cox, A. J., & Mullikin, J. C. (2001). SSAHA: a fast search method for large DNA databases. *Genome Research*, *11*(10), 1725-1729. https://doi.org/10.1101/gr.194201.

Pan, P., Li, J., Wang, B., Tan, X., Yin, H., Han, Y., . . . Tian, G. (2023). Molecular characterization of colorectal adenoma and colorectal cancer via integrated genomic transcriptomic analysis. *Frontiers in Oncology, 13*. doi:10.3389/fonc.2023.1067849

Pino, M. S., & Chung, D. C. (2010). The chromosomal instability pathway in colon cancer. *Gastroenterology, 138*(6), 2059-2072.

Qu, L., Yin, T., Zhao, Y., Lv, W., Liu, Z., Chen, C., ... & Dong, H. (2023). Histone demethylases in the regulation of immunity and inflammation. *Cell Death Discovery*, *9*(1), 188. https://doi.org/10.1038/s41420-023-01489-9.

Rawla, P., Sunkara, T., & Barsouk, A. (2019). Epidemiology of colorectal cancer: incidence, mortality, survival, and risk factors. *Gastroenterology Review, 14*(2), 89-103. https://doi.org/10.5114/pg.2018.81072

Ren, L., Meng, L., Gao, J., Lu, M., Guo, C., Li, Y., . . . Ye, Y. (2023). PHB2 promotes colorectal cancer cell proliferation and tumorigenesis through NDUFS1-mediated oxidative phosphorylation. *Cell Death & Disease, 14*(1), 44. doi:10.1038/s41419-023-05575-9

Rezende, R. M., Lanser, A. J., Rubino, S., Kuhn, C., Skillin, N., Moreira, T. G., . . . Weiner, H. L. (2018). γδ T cells control humoral immune response by inducing T follicular helper cell differentiation. *Nat Commun, 9*(1), 3151. doi:10.1038/s41467-018-05487-9

Ritchie, M. E., Phipson, B., Wu, D. I., Hu, Y., Law, C. W., Shi, W., & Smyth, G. K. (2015). limma powers differential expression analyses for RNA-sequencing and microarray studies. *Nucleic Acids Research*, *43*(7), e47-e47. https://doi.org/10.1093/nar/gkv007.

Roussos, E. T., Condeelis, J. S., & Patsialou, A. (2011). Chemotaxis in cancer. *Nature Reviews Cancer*, *11*(8), 573-587. https://doi.org/10.1038/nrc3078.

Roy, K., Chakraborty, M., Kumar, A., Manna, A. K., & Roy, N. S. (2023). The NFκB signaling system in the generation of B-cell subsets: from germinal center B cells to memory B cells and plasma cells. *Frontiers in Immunology*, *14*, 1185597. https://doi.org/10.3389/fimmu.2023.1185597.

Rubio, C. A., & Delinassios, J. G. (2010). Invasive carcinomas may arise in colorectal adenomas with high-grade dysplasia and with carcinoma in situ. I*nt J Clin Exp Med, 3*(1), 41-47.

Sangaletti, S., Chiodoni, C., Tripodo, C., & Colombo, M. P. (2017). The good and bad of targeting cancer-associated extracellular matrix. *Current opinion in pharmacology*, *35*, 75-82. https://doi.org/10.1016/j.coph.2017.06.003.

Sawicki, T., Ruszkowska, M., Danielewicz, A., Niedźwiedzka, E., Arłukowicz, T., & Przybyłowicz, K. E. (2021). A Review of Colorectal Cancer in Terms of Epidemiology, Risk Factors, Development, Symptoms and Diagnosis. *Cancers, 13*(9), 2025. Retrieved from https://www.mdpi.com/2072-6694/13/9/2025

Shang, H., Xu, A., Yan, H., Xu, D., Zhang, J., & Fang, X. (2023). *PIEZO2* promotes cell proliferation and metastasis in colon carcinoma through the SLIT2/ROBO1/VEGFC pathway. *Advances in Clinical and Experimental Medicine*, *32*(7), 763-776. https://doi.org/10.17219/acem/157515.

Shen, M., Zhang, Z., & Wang, P. (2021). *GLI3* promotes invasion and predicts poor prognosis in colorectal cancer. *BioMed Research International*, *2021*(1), 8889986. https://doi.org/10.1155/2021/8889986.

Shi, X., Xia, S., Chu, Y., Yang, N., Zheng, J., Chen, Q., Fen, Z., Jiang, Y., Fang, S., & Lin, J. (2021). *CARD11* is a prognostic biomarker and correlated with immune infiltrates in uveal melanoma. *PLOS ONE, 16*(8), e0255293. https://doi.org/10.1371/journal.pone.0255293

Shimabukuro-Vornhagen, A., Schlößer, H. A., Gryschok, L., Malcher, J., Wennhold, K., Garcia-Marquez, M., ... & von Bergwelt-Baildon, M. S. (2014). Characterization of tumor-associated B-cell subsets in patients with colorectal cancer. *Oncotarget*, *5*(13), 4651. https://doi.org/10.18632/oncotarget.1701.

Shimabukuro-Vornhagen, A., Schlößer, H. A., Gryschok, L., Malcher, J., Wennhold, K., Garcia-Marquez, M., . . . von Bergwelt-Baildon, M. S. (2014). Characterization of tumor-associated B-cell subsets in patients with colorectal cancer. *Oncotarget, 5*(13), 4651-4664. doi:10.18632/oncotarget.1701

Sibilio, A., Suñer, C., Fernández-Alfara, M., Martín, J., Berenguer, A., Calon, A., ... & Méndez, R. (2022). Immune translational control by *CPEB4* regulates intestinal inflammation resolution and colorectal cancer development. *Iscience*, *25*(2). https://doi.org/10.1016/j.isci.2022.103790.

Siegel, R. L., Wagle, N. S., Cercek, A., Smith, R. A., & Jemal, A. (2023). Colorectal cancer statistics, 2023. *CA: A Cancer Journal for Clinicians*, *73*(3), 233-254. https://doi.org/10.3322/caac.21772

Slattery, M. L., Mullany, L. E., Sakoda, L., Samowitz, W. S., Wolff, R. K., Stevens, J. R., & Herrick, J. S. (2018). The NF-κB signalling pathway in colorectal cancer: associations between dysregulated gene and miRNA expression. Journal of Cancer Research and *Clinical Oncology, 144*(2), 269-283. https://doi.org/10.1007/s00432-017-2548-6

Smith, T. F., Waterman, M. S., & Fitch, W. M. (1981). Comparative biosequence metrics. *Journal of Molecular Evolution*, *18*, 38-46. https://doi.org/10.1007/bf01733210.

Soncin, I., Sheng, J., Chen, Q., Foo, S., Duan, K., Lum, J., Ruedl, C. (2018). The tumour microenvironment creates a niche for the self-renewal of tumour-promoting

macrophages in colon adenoma. *Nature Communications, 9*(1), 582. doi:10.1038/s41467-018-02834-8

Staudt, L. M. (2010). Oncogenic activation of NF-κB. *Cold Spring Harbor Perspectives in Biology*, *2*(6), a000109. https://doi.org/10.1101/cshperspect.a000109.

Tanaka, T., Tanaka, M., Tanaka, T., & Ishigamori, R. (2010). Biomarkers for Colorectal Cancer. *International Journal of Molecular Sciences, 11*(9), 3209-3225. https://doi.org/10.3390/ijms11093209

Thomsen, M., Skovlund, E., Sorbye, H., Bolstad, N., Nustad, K. J., Glimelius, B., ... & Guren, T. K. (2018). Prognostic role of carcinoembryonic antigen and carbohydrate antigen 19-9 in metastatic colorectal cancer: a BRAF-mutant subset with high CA 19-9 level and poor outcome. *British Journal of Cancer*, *118*(12), 1609-1616. https://doi.org/10.1038/s41416-018-0115-9

Tian, K., Chen, H., Wang, Q., Jiang, F., Feng, C., Li, T., Pu, X., Tang, Y., & Liu, J. (2024). *CARD11* serves as a therapeutic biomarker for the drug therapies of ccRCC. *BIOCELL, 48*(5), 817-834. https://doi.org/10.32604/biocell.2024.048737

Tian, Y., Kharazmi, E., Brenner, H., Xu, X., Sundquist, K., Sundquist, J., & Fallah, M. (2021). Importance of Family History of Colorectal Carcinoma In Situ Versus Invasive Colorectal Cancer: A Nationwide Cohort Study. *Journal of the National Comprehensive Cancer Network, 19*(11), 1252-1257. doi:10.6004/jnccn.2021.7004

Toyoshima, Y., Kitamura, H., Xiang, H., Ohno, Y., Homma, S., Kawamura, H., ... & Taketomi, A. (2019). IL6 modulates the immune status of the tumor microenvironment to facilitate metastatic colonization of colorectal cancer cells. *Cancer Immunology Research*, *7*(12), 1944-1957. https://doi.org/10.1158/2326-6066.Cir-18-0766.

Turvey, S. E., Durandy, A., Fischer, A., Fung, S. Y., Geha, R. S., Gewies, A., ... & Warnatz, K. (2014). The *CARD11*-BCL10-MALT1 (CBM) signalosome complex: stepping into

the limelight of human primary immunodeficiency. *Journal of Allergy and Clinical Immunology*, *134*(2), 276-284. https://doi.org/10.1016/j.jaci.2014.06.015.

Valle, L. (2014). Genetic predisposition to colorectal cancer: Where we stand and future perspectives. *World Journal of Gastroenterology, 20*(29), 9828. https://doi.org/10.3748/wjg.v20.i29.9828

Wang, C., Gan, L., Gao, Z., Shen, Z., Jiang, K., & Ye, Y. (2023). Young adults with colon cancer: clinical features and surgical outcomes. *BMC Gastroenterology*, *23*(1), 192. https://doi.org/10.1186/s12876-023-02770-y.

Wang, H., Zheng, H., Cao, X., Meng, P., Liu, J., Zuo, H., . . . Wang, Z. (2023). Association between serum gamma-glutamyl transferase and advanced colorectal adenoma among inpatients: a case-control study. *Front Oncol, 13*, 1188017. doi:10.3389/fonc.2023.1188017

Wang, J., He, A. L., Zhang, W. G., Cao, X. M., Chen, Y. X., Liu, J., ... & Ma, X. R. (2020). MTMR2 promotes the progression of NK/T cell lymphoma by targeting JAK1. *European Review for Medical & Pharmacological Sciences*, *24*(15). https://doi.org/10.26355/eurrev_202008_22489.

Wei, Z., Zhang, Y., Chen, J., Hu, Y., Jia, P., Wang, X., Zhao, Q., Deng, Y., Li, N., Zang, Y., Qin, J., Wang, X., & Lu, W. (2019). Pathogenic *CARD11* mutations affect B cell development and differentiation through a noncanonical pathway. Science *Immunology, 4*(41), eaaw5618. https://doi.org/10.1126/sciimmunol.aaw5618

Weinberg, B. A., & Marshall, J. L. (2019). Colon cancer in young adults: trends and their implications. *Current Oncology Reports*, *21*, 1-7. https://doi.org/10.1007/s11912-019-0756-8

World Health Organization (2024). *Estimated number of deaths from 2022 to 2045, Both sexes, age [0-85+]: Colorectum*.

https://gco.iarc.fr/tomorrow/en/dataviz/bars?years=2045&populations=903_904_905_908_909_935&types=1&cancers=41

Xia, L., Tan, S., Zhou, Y., Lin, J., Wang, H., Oyang, L., ... & Liao, Q. (2018). Role of the NFκB-signaling pathway in cancer. *Onco Targets Ther 11: 2063–2073*. https://doi.org/10.2147/ott.s161109

Xia, Y., Shen, S., & Verma, I. M. (2014). NF-κB, an Active Player in Human Cancers. *Cancer Immunology Research, 2*(9), 823-830. https://doi.org/10.1158/2326-6066.cir-14-0112

Ye, P., Cai, P., Xie, J., & Wei, Y. (2021). The diagnostic accuracy of digital PCR, ARMS and NGS for detecting KRAS mutation in cell-free DNA of patients with colorectal cancer: A systematic review and meta-analysis. *PLOS ONE, 16*(3), e0248775. https://doi.org/10.1371/journal.pone.0248775

Yeung, T. M., Gandhi, S. C., Wilding, J. L., Muschel, R., & Bodmer, W. F. (2010). Cancer stem cells from colorectal cancer-derived cell lines. *Proceedings of the National Academy of Sciences*, *107*(8), 3722-3727. https://doi.org/10.1073/pnas.0915135107.

Yue, Y., Zhang, Q., Wu, S., Wang, S., Cui, C., Yu, M., & Sun, Z. (2020). Identification of key genes involved in JAK/STAT pathway in colorectal cancer. *Molecular Immunology*, *128*, 287-297. https://doi.org/10.1016/j.molimm.2020.10.007.

Yutian, S. A., Lin; Weimin, Ding; Hui, Meng; Peng, Luo; and Jian, Zhang. (2021). *CARD11* alteration as a candidate biomarker of skin cutaneous melanoma treated with immune checkpoint blockade. *Am J Transl Res, 13*, 256-300.

Zeng, Z., He, W., Jiang, Y., Jiang, H., Cheng, X., Deng, W., ... & Wang, G. (2022). *MAPK8IP2* is a potential prognostic biomarker and promote tumor progression in prostate cancer. *BMC Cancer*, *22*(1), 1162. https://doi.org/10.1186/s12885-022-10259-2.

Zhang, E., Ding, C., Li, S., Zhou, X., Aikemu, B., Fan, X., . . . Yang, X. (2023). Roles and mechanisms of tumour-infiltrating B cells in human cancer: a new force in immunotherapy. *Biomarker Research, 11*(1), 28. doi:10.1186/s40364-023-00460-1

Zhong, X., Xiao, Y., Chen, C., Wei, X., Hu, C., Ling, X., & Liu, X. (2015). MicroRNA-203-mediated posttranscriptional deregulation of *CPEB4* contributes to colorectal cancer progression. *Biochemical and Biophysical Research Communications*, *466*(2), 206-213. https://doi.org/10.1016/j.bbrc.2015.09.008.

Zhou, Y., Zhou, B., Pache, L., Chang, M., Khodabakhshi, A. H., Tanaseichuk, O., ... & Chanda, S. K. (2019). Metascape provides a biologist-oriented resource for the analysis of systems-level datasets. *Nature Communications*, *10*(1), 1523. https://doi.org/10.1038/s41467-019-09234-6.

Zhu, M., Huang, Z., Zhu, D., Zhou, X., Shan, X., Qi, L. W., & Liu, P. (2017). A panel of microRNA signature in serum for colorectal cancer diagnosis. *Oncotarget*, *8*(10), 17081. https://doi.org/10.18632/oncotarget.15059

Zhuo, C., Ruan, Q., Zhao, X., Shen, Y., & Lin, R. (2022). *CXCL1* promotes colon cancer progression through activation of NF-κB/P300 signaling pathway. *Biology direct*, *17*(1), 34. https://doi.org/10.1186/s13062-022-00348-4.

Zong, L., Abe, M., Ji, J., Zhu, W.-G., & Yu, D. (2016). Tracking the correlation between CpG island methylator phenotype and other molecular features and clinicopathological features in human colorectal cancers: A systematic review and meta-analysis. *Clinical and Translational Gastroenterology, 7*(3), e151. https://doi.org/10.1038/ctg.2016.14

Ahmad, R., Singh, J. K., Wunnava, A., Al-Obeed, O., Abdulla, M., & Srivastava, S. K. (2021). Emerging trends in colorectal cancer: Dysregulated signaling pathways (Review). Int J Mol Med, 47(3). doi:10.3892/ijmm.2021.4847

Barnabei, L., Laplantine, E., Mbongo, W., Rieux-Laucat, F., & Weil, R. (2021). NF-κB: At the Borders of Autoimmunity and Inflammation. Frontiers in Immunology, 12. doi:10.3389/fimmu.2021.716469

Burgos-Molina, A. M., Téllez Santana, T., Redondo, M., & Bravo Romero, M. J. (2024). The Crucial Role of Inflammation and the Immune System in Colorectal Cancer Carcinogenesis: A Comprehensive Perspective. International Journal of Molecular Sciences, 25(11), 6188. Retrieved from https://www.mdpi.com/1422-0067/25/11/6188

Cheratta, A. R., Thayyullathil, F., Pallichankandy, S., Subburayan, K., Alakkal, A., & Galadari, S. (2021). Prostate apoptosis response-4 and tumor suppression: it's not just about apoptosis anymore. Cell Death & Disease, 12(1), 47. doi:10.1038/s41419-020-03292- 1

Hamada, F., & Bienz, M. (2004). The APC tumor suppressor binds to C-terminal binding protein to divert nuclear beta-catenin from TCF. Dev Cell, 7(5), 677-685. doi:10.1016/j.devcel.2004.08.022

Jin, J. J., Zheng, T., Xu, X. X., Zheng, L., Li, F. Y., Li, X. X., & Zhou, L. (2022).

Comprehensive analysis of the differential expression and prognostic value of COL1A2 in colon adenocarcinoma. Aging (Albany NY), 14(18), 7390-7407. doi:10.18632/aging.204261

Mortezapour, M., Tapak, L., Bahreini, F., Najafi, R., & Afshar, S. (2023). Identification of key genes in colorectal cancer diagnosis by weighted gene co-expression network

analysis. Computers in Biology and Medicine,157, 106779. doi:https://doi.org/10.1016/j.compbiomed.2023.106779

Proteinatlas. CEBPZ. Proteinatlas. Retrieved from https://www.proteinatlas.org/ENSG00000115816-CEBPZ/cancer

Ren, L., Meng, L., Gao, J., Lu, M., Guo, C., Li, Y., . . . Ye, Y. (2023). PHB2 promotes colorectal cancer cell proliferation and tumorigenesis through NDUFS1-mediated oxidative phosphorylation. Cell Death & Disease, 14(1), 44. doi:10.1038/s41419-023- 05575-9

Rosanò, L., & Bagnato, A. (2016). β-arrestin1 at the cross-road of endothelin-1 signaling in cancer. Journal of Experimental & Clinical Cancer Research, 35(1),121. doi:10.1186/s13046-016-0401-4

Sierra, J., Yoshida, T., Joazeiro, C. A., & Jones, K. A. (2006). The APC tumor suppressor counteracts beta-catenin activation and H3K4 methylation at Wnt target genes. Genes Dev, 20(5), 586-600. doi:10.1101/gad.1385806

Tan, J., Tao, K., Zheng, X., Liu, D., Ma, D., & Gao, Q. (2020). Expression of PAWR predicts prognosis of ovarian cancer. Cancer Cell International, 20(1), 598. doi:10.1186/s12935-020-01704-y

Wang, H., Zheng, H., Cao, X., Meng, P., Liu, J., Zuo, H., Wang, Z. (2023). Association between serum gamma-glutamyl transferase and advanced colorectal adenoma among inpatients: a case-control study. Front Oncol, 13, 1188017. doi:10.3389/fonc.2023.1188017

Wu, C. C., Wang, Y. H., Hu, S. W., Wu, W. L., Yeh, C. T., & Bamodu, O. A. (2021). MED10

Drives the Oncogenicity and Refractory Phenotype of Bladder Urothelial Carcinoma

Through the Upregulation of hsa-miR-590. Front Oncol, 11, 744937. doi:10.3389/fonc.2021.744937

Xia, Y., Shen, S., & Verma, I. M. (2014). NF-κB, an active player in human cancers. Cancer Immunol Res, 2(9), 823-830. doi:10.1158/2326-6066.Cir-14-0112

Yang, K., Shen, J., Tan, F. Q., Zheng, X. Y., & Xie, L. P. (2021). Antitumor Activity of Small Activating RNAs Induced PAWR Gene Activation in Human Bladder Cancer Cells. Int J Med Sci, 18(13), 3039-3049. doi:10.7150/ijms.60399

Yuan, X., He, Y., & Wang, W. (2023). ceRNA network-regulated COL1A2 high expression correlates with poor prognosis and immune infiltration in colon adenocarcinoma. Scientific Reports, 13(1), 16932. doi:10.1038/s41598-023-43507-x

Ahmed, D., P. W. Eide, I. A. Eilertsen, S. A. Danielsen, M. Eknaes, M. Hektoen, G. E. Lind and R. A. Lothe (2013). "Epigenetic and genetic features of 24 colon cancer cell lines." Oncogenesis 2(9): e71.

ATCC (2024). "HCT 116." ATCC.

ATCC (2024). "HT-29." ATCC.

Banias, L., I. Jung, R. Chiciudean and S. Gurzu (2022). "From Dukes-MAC Staging System to Molecular Classification: Evolving Concepts in Colorectal Cancer." International Journal of Molecular Sciences 23(16): 9455.

Baojun Duan, Y. Z., Jun Bai, Jianhua Wang, Xianglong Duan, Xiaohui Luo, Rong Zhang, Yansong Pu, Mingqing Kou, Jianyuan Lei, and Shangzhen Yang. (2022). Chapter 1, Colorectal Cancer: An Overview, Gastrointestinal Cancers.

Barnabei, L., E. Laplantine, W. Mbongo, F. Rieux-Laucat and R. Weil (2021). "NF-κB: At the Borders of Autoimmunity and Inflammation." Frontiers in Immunology Volume 12 - 2021.

Bedsaul, J. R., N. M. Carter, K. E. Deibel, S. M. Hutcherson, T. A. Jones, Z. Wang, C. Yang,

Y.-K. Yang and J. L. Pomerantz (2018). "Mechanisms of Regulated and Dysregulated CARD11 Signaling in Adaptive Immunity and Disease." Frontiers in Immunology Volume 9 - 2018.

Bortz, J. H. and H. Friedrich-Nel (2023). The Adenoma-Carcinoma Sequence, Management, and Treatment of Colon Cancer. CT Colonography for Radiographers: A Guide to Performance and Image Interpretation. J. H. Bortz, A. Ramlaul and L. Munro. Cham, Springer International Publishing: 209-220.

Colling, R., L. M. Wang and E. Soilleux (2016). "Automated PCR detection of <em>BRAF</em> mutations in colorectal adenocarcinoma: a diagnostic test accuracy study." Journal of Clinical Pathology 69(5): 398.

Evrard, C., G. Tachon, V. Randrian, L. Karayan-Tapon and D. Tougeron (2019). "Microsatellite Instability: Diagnosis, Heterogeneity, Discordance, and Clinical Impact in Colorectal Cancer." Cancers (Basel) 11(10).

Fo, Y., X. Kang, Y. Tang and L. Zhao (2023). "Analysis of clinical diagnosis and treatment of intestinal volvulus." BMC Gastroenterology 23(1): 93.

Gao, P., K. Zhou, W. Su, J. Yu and P. Zhou (2023). "Endoscopic management of colorectal polyps." Gastroenterology Report 11.

Gonzalez-Pons, M. and M. Cruz-Correa (2015). "Colorectal Cancer Biomarkers: Where Are We Now?" BioMed research international 2015: 149014.

Gulinac, M., N. Mileva, D. Miteva, T. Velikova and D. Dikov (2024). "Primary Signet-Ring-Cell Carcinoma in the Colorectum: A Case-Based Literature Review." Gastroenterology Insights 15(3): 632-646.

Hamoudi, R. A., A. Appert, H. Ye, A. Ruskone-Fourmestraux, B. Streubel, A. Chott, M. Raderer, L. Gong, I. Wlodarska, C. De Wolf-Peeters, K. A. MacLennan, L. de Leval, P. G. Isaacson and M. Q. Du (2010). "Differential expression of NF-kappaB target genes in MALT lymphoma with and without chromosome translocation: insights into

molecular mechanism." Leukemia 24(8): 1487-1497.

Ilhan, Y., O. Y. Balcik, H. G. Guzel, A. H. Onder, B. Demir, M. N. Baser, I. Karadag, M. F. Ozbay, T. B. Genc, S. Uzuntas, O. Poyrazoglu, I. Beypinar, Y. Ergun and B. Ozturk (2025). "Novel tumor marker index combining carcinoembryonic antigen and carbohydrate antigen 19-9: New prognostic factor for metastatic colorectal cancer." World J Gastrointest Oncol 17(5): 104341.

Jang, W. J., S. K. Jung, T. T. L. Vo and C. H. Jeong (2019). "Anticancer activity of paroxetine in human colon cancer cells: Involvement of MET and ERBB3." J Cell Mol Med 23(2): 1106-1115.

Jimenez, B., R. Mirnezami, J. Kinross, O. Cloarec, H. C. Keun, E. Holmes, R. D. Goldin, P. Ziprin, A. Darzi and J. K. Nicholson (2013). "1H HR-MAS NMR spectroscopy of tumor-induced local metabolic "field-effects" enables colorectal cancer staging and prognostication." J Proteome Res 12(2): 959-968.

Kawasaki, K., T. Torisu, T. Nagahata, M. Esaki, K. Kurahara, M. Eizuka, Y. Tanaka, M. Fujiwara, S. Kawatoko, Y. Oshiro, S. Yamada, K. Ikegami, S. Fujioka, Y. Fuyuno, Y. Matsuno, J. Umeno, T. Moriyama, T. Kitazono, T. Sugai and T. Matsumoto (2021). "Role of barium enema examination for the diagnosis of submucosal invasion depth in T1 colorectal cancers." Cancer Imaging 21(1): 66.

Kobayashi, T., M. Ishida, H. Miki, N. Yamamoto, T. Harino, T. Yagyu, S. Hori, M. Hatta, Y. Hashimoto, M. Kotsuka, M. Yamasaki, K. Inoue, Y. Hirose and M. Sekimoto (2024). "Prognostic scoring system based on indicators reflecting the tumor glandular differentiation and microenvironment for patients with colorectal cancer." Scientific Reports 14(1): 14188.

Lang, B. M., J. Kuipers, B. Misselwitz and N. Beerenwinkel (2020). "Predicting colorectal cancer risk from adenoma detection via a two-type branching process model." PLOS Computational Biology 16(2): e1007552.

Lenz, G., R. E. Davis, V. N. Ngo, L. Lam, T. C. George, G. W. Wright, S. S. Dave, H. Zhao, W. Xu, A. Rosenwald, G. Ott, H. K. Muller-Hermelink, R. D. Gascoyne, J. M. Connors, L. M. Rimsza, E. Campo, E. S. Jaffe, J. Delabie, E. B. Smeland, R. I. Fisher, W. C. Chan and L. M. Staudt (2008). "Oncogenic CARD11 mutations in human diffuse large B cell lymphoma." Science (New York, N.Y.) 319(5870): 1676-1679.

Livak, K. J. and T. D. Schmittgen (2001). "Analysis of Relative Gene Expression Data Using Real-Time Quantitative PCR and the 2−ΔΔCT Method." Methods 25(4): 402-408.

Loktionov, A. (2020). "Biomarkers for detecting colorectal cancer non-invasively: DNA, RNA or proteins?" World J Gastrointest Oncol 12(2): 124-148.

Lu, H. Y., M. Sharma, A. A. Sharma, A. Lacson, A. Szpurko, J. Luider, P. Dharmani-Khan, A. Shameli, P. A. Bell, G. M. T. Guilcher, V. A. Lewis, M. R. Vasquez, S. Desai, L. McGonigle, L. Murguia-Favela, N. A. M. Wright, C. Sergi, E. Wine, C. M. Overall, S. Suresh and S. E. Turvey (2021). "Mechanistic understanding of the combined immunodeficiency in complete human CARD11 deficiency." Journal of Allergy and Clinical Immunology 148(6): 1559-1574.e1513.

Maconi, G. (2014). Mesenteric Lymphadenopathy. Ultrasound of the Gastrointestinal Tract. G. Maconi and G. Bianchi Porro. Berlin, Heidelberg, Springer Berlin Heidelberg: 29-36.

Mostafa, H., W. Mousa, M. Houseni and B. Dessouky (2021). "Role of positron emission tomography/computed tomography for the staging of primary colorectal cancers." Menoufia Medical Journal 34(1).

Nakagawa, T., D. Tachibana, K. Kitada, Y. Kurihara, H. Terada, M. Koyama, Y. Sakae, Y. Morotomi, S. Nomura and M. Saito (2015) "A case of fetal intestinal volvulus without malrotation causing severe anemia." Japanese clinical medicine 6, 1-3 DOI: 10.4137/jcm.s20760.

Ng, L., T. M. Wan, J. H. Man, A. K. Chow, D. Iyer, G. Chen, T. C. Yau, O. S. Lo, D. C. Foo,

J. T. Poon, W. K. Leung, R. W. Pang and W. L. Law (2017). "Identification of serum miR-139-3p as a non-invasive biomarker for colorectal cancer." Oncotarget 8(16): 27393-27400.

Si, Y., A. Lin, W. Ding, H. Meng, P. Luo and J. Zhang (2021) "CARD11 alteration as a candidate biomarker of skin cutaneous melanoma treated with immune checkpoint blockade." American journal of translational research 13, 286-300.

Society, A. C. (2024). "Colorectal Cancer Stages." American Cancer Society.

Song, X., J. Li, J. Zhu, Y.-F. Kong, Y.-H. Zhou, Z.-K. Wang and J. Zhang (2024). "Predictors of early colorectal cancer metastasis to lymph nodes: providing rationale for therapy decisions." Frontiers in Oncology Volume 14 - 2024.

Subramanian, A., P. Tamayo, V. K. Mootha, S. Mukherjee, B. L. Ebert, M. A. Gillette, A. Paulovich, S. L. Pomeroy, T. R. Golub, E. S. Lander and J. P. Mesirov (2005). "Gene set enrichment analysis: a knowledge-based approach for interpreting genome-wide expression profiles." Proc Natl Acad Sci U S A 102(43): 15545-15550.

TIAN, K., H. CHEN, Q. WANG, F. JIANG, C. FENG, T. LI, X. PU, Y. TANG and J. LIU (2024). "CARD11 serves as a therapeutic biomarker for the drug therapies of ccRCC." BIOCELL 48(5): 817--834.

UK, C. R. (2024). "Stages, types and grades of bowel cancer." CANCER RESEARCH UK.

Wei, Z., Y. Zhang, J. Chen, Y. Hu, P. Jia, X. Wang, Q. Zhao, Y. Deng, N. Li, Y. Zang, J. Qin, X. Wang and W. Lu (2019). "Pathogenic CARD11 mutations affect B cell development and differentiation through a noncanonical pathway." Science immunology 4(41): eaaw5618.